

Materials Reliability Program: PWR Internals Material Aging Degradation Mechanism Screening and Threshold Values (MRP-175)

1012081

Topical Report, December 2005

Non-proprietary Version for NRC
(Proprietary Version was submitted to NRC
under Affidavit)

EPRI Project Manager
H.T. Tang

DISCLAIMER OF WARRANTIES AND LIMITATION OF LIABILITIES

THIS DOCUMENT WAS PREPARED BY THE ORGANIZATION(S) NAMED BELOW AS AN ACCOUNT OF WORK SPONSORED OR COSPONSORED BY THE ELECTRIC POWER RESEARCH INSTITUTE, INC. (EPRI). NEITHER EPRI, ANY MEMBER OF EPRI, ANY COSPONSOR, THE ORGANIZATION(S) BELOW, NOR ANY PERSON ACTING ON BEHALF OF ANY OF THEM:

(A) MAKES ANY WARRANTY OR REPRESENTATION WHATSOEVER, EXPRESS OR IMPLIED, (I) WITH RESPECT TO THE USE OF ANY INFORMATION, APPARATUS, METHOD, PROCESS, OR SIMILAR ITEM DISCLOSED IN THIS DOCUMENT, INCLUDING MERCHANTABILITY AND FITNESS FOR A PARTICULAR PURPOSE, OR (II) THAT SUCH USE DOES NOT INFRINGE ON OR INTERFERE WITH PRIVATELY OWNED RIGHTS, INCLUDING ANY PARTY'S INTELLECTUAL PROPERTY, OR (III) THAT THIS DOCUMENT IS SUITABLE TO ANY PARTICULAR USER'S CIRCUMSTANCE; OR

(B) ASSUMES RESPONSIBILITY FOR ANY DAMAGES OR OTHER LIABILITY WHATSOEVER (INCLUDING ANY CONSEQUENTIAL DAMAGES, EVEN IF EPRI OR ANY EPRI REPRESENTATIVE HAS BEEN ADVISED OF THE POSSIBILITY OF SUCH DAMAGES) RESULTING FROM YOUR SELECTION OR USE OF THIS DOCUMENT OR ANY INFORMATION, APPARATUS, METHOD, PROCESS, OR SIMILAR ITEM DISCLOSED IN THIS DOCUMENT.

ORGANIZATION(S) THAT PREPARED THIS DOCUMENT

Framatome ANP, Inc.

NOTE

For further information about EPRI, call the EPRI Customer Assistance Center at 800.313.3774 or e-mail askepri@epri.com.

Electric Power Research Institute and EPRI are registered service marks of the Electric Power Research Institute, Inc.

Copyright © 2005 Electric Power Research Institute, Inc. All rights reserved.

CITATIONS

This report was prepared by

Framatome ANP, Inc.
3315 Old Forest Road
P.O. Box 10935
Lynchburg, VA 24506-0935

Principal Investigator
S. Fyfitch

Contributors
H. Xu
K. Moore
R. Gurdal

This report describes research sponsored by the Electric Power Research Institute (EPRI).

The report is a corporate document that should be cited in the literature in the following manner:

Materials Reliability Program: PWR Internals Material Aging Degradation Mechanism Screening and Threshold Values (MRP-175). EPRI, Palo Alto, CA: 2005. 1012081.

REPORT SUMMARY

This report provides screening criteria and their technical bases for age-related degradation evaluation of Pressurized Water Reactor (PWR) internals component items. It is a key element in an overall strategy that uses knowledge of internals design, materials, and material properties and applies screening methodologies for known age-related degradation mechanisms to manage the effects of aging in PWR internals.

Background

The framework for implementation of an aging management program for PWR internals components and using inspections and flaw tolerance evaluations to manage degradation issues has been developed and is documented in MRP-134 and MRP-153. The important elements of this framework are:

- Screening, categorizing, and ranking PWR internals components for susceptibility and significance to the age-related degradation mechanisms
- Performing functionality analyses and safety assessment of PWR internals components to define a safe and cost-effective aging management in-service inspection and evaluation method and strategy

This report describes screening criteria and the associated technical bases for categorization and ranking of aged PWR internals components.

Objectives

To establish technically sound age-related degradation mechanism screening criteria for management of aging effects in PWR internals.

Approach

The principal investigators reviewed in detail the potential and observed age-related degradation mechanisms and effects in PWR internals due to aging, such as irradiation-assisted stress corrosion cracking (IASCC), irradiation embrittlement, void swelling, stress relaxation, and fatigue. Based on available data and results, the investigators defined degradation threshold values where possible and developed screening parameters and criteria for degradation screening.

Results

The report provides screening criteria for PWR internals materials for each age-related degradation mechanism considered: Stress Corrosion Cracking, Irradiation-Assisted Stress Corrosion Cracking, Wear, Fatigue, Thermal Aging Embrittlement, Irradiation Embrittlement, Void Swelling, and Stress Relaxation/Irradiation Creep. For each age-related degradation

mechanism, a screening criteria table displays material types; parameters such as stress, fluence, temperature, stress, and ferrite content; and screening values. The screening criteria provide a basis to either screen in or screen out a component item. For the screened in component items, additional steps will be taken such as engineering judgment, bounding analysis, and functionality, and/or safety evaluation for further categorization as per the MRP-134 outlined strategy for appropriate inspection considerations.

EPRI Perspective

The EPRI MRP Reactor Internals Issue Task Group (RI-ITG) has been conducting studies to develop technical bases to support aging management of PWR internals, with a particular attention to utility License Renewal commitments. This *Aging Degradation Mechanism Screening and Threshold Values* report is the second of a three-part document series on an overall strategy for managing the effects of aging in PWR internals. The first document in the series, *Materials Reliability Program: Framework and Strategies for Managing Aging Effects in PWR Internals (MRP-134)* (EPRI report 1008203, June 2005), focuses on the overall framework and strategy. The third document, *Materials Reliability Program: Inspection and Flaw Evaluation Strategies for Managing Aging Effects in PWR Internals (MRP-153)* (EPRI report 1012082, December 2005), details inspection and flaw evaluation methodologies.

Currently, based on the strategies and the screening criteria developed, the RI-ITG focuses on performing screening and functionality and safety evaluation of the effects of age-related degradation in PWR internals components. In parallel, hot cell testing to quantify aged/irradiated materials behavior and performance is continuing. These studies and results together with the three-part document series on aging management strategy will provide a basis for developing Inspection and Evaluation (I&E) Guidelines for utility applications.

Keywords

PWR internals
Aging management
License Renewal
Degradation mechanism
Threshold values
Screening Criteria

ABSTRACT

The purpose of this report is to develop age-related degradation mechanism screening criteria and document their technical bases for evaluation of PWR internals component items. Related MRP documents include a Framework and Strategy for Managing Aging Effects in PWR Internals (MRP-134) and Inspection and Flaw Evaluation Strategies for Managing Aging Effects in PWR Internals (MRP-153).

The screening criteria developed in this report are to be used to categorize all PWR internals component items in accordance with the strategy developed in Figure 4-1 of MRP-134 (reproduced as Figure 1-5 in this report). A general overview description of the various age-related degradation mechanisms, observable thresholds, and the suggested screening criteria applicable to PWR internals is contained in this report. The age-related degradation mechanisms discussed in this report are as follows:

- Stress Corrosion Cracking (SCC), which includes intergranular SCC (IGSCC), transgranular SCC (TGSCC), primary water SCC (PWSCC), and low-temperature crack propagation (LTCP)
- Irradiation-assisted SCC (IASCC)
- Wear
- Fatigue, which includes high-cycle fatigue (HCF) and low-cycle fatigue (LCF)
- Thermal aging embrittlement (TE)
- Irradiation embrittlement (IE)
- Void swelling (VS)
- Irradiation-enhanced stress relaxation and creep (SR/IC)

In addition, this report contains a roadmap for tying aging effects to age-related degradation mechanisms. Suggestions are included in the report for compiling and tabulating the screening criteria parameters to be used in determining the potential significance of age-related degradation effects on PWR internals component items. The screening criteria can be used to screen component items on either a plant-specific or vendor design-specific (generic) basis.

ACKNOWLEDGMENTS

The author would like to acknowledge the valuable input, review comments and report editing from the following core members of the EPRI MRP RI-ITG Expert Panel:

- P. Scott (Framatome ANP)
- R. Shogan and R. Lott (Westinghouse)
- F.A. Garner (PNNL)

The discussions, challenges and the consensus process leading to endorsement of the screening criteria by the expert panel members is a rewarding experience.

Suggestions from S. Byrne (Westinghouse), especially the threshold and screening criteria definitions, and editing suggestions from R. Gold (Westinghouse) are gratefully acknowledged.

The author would like to acknowledge the critical review and comments by the MRP RI-ITG members led by its Chairman, C. Griffin, of Progress Energy.

Finally, the support and efforts of H.T. Tang (EPRI MRP RI-ITG Project Manager), W.R. Gray (Framatome ANP RI-ITG Project Manager), C. Boggess (Westinghouse RI-ITG Functionality Project Manager), and T. Meyer (Westinghouse RI-ITG Functionality Project Lead) are acknowledged.

ACRONYMS AND ABBREVIATIONS

Acronym/Abbreviation	Definition
AEC	Atomic Energy Commission
AGR	Advanced Gas-Cooled Reactor
AIME	American Institute of Mining, Metallurgical, and Petroleum Engineers
AISI	American Iron and Steel Institute
AMS	Aerospace Materials Specification (Society of Automotive Engineers International)
ANL	Argonne National Laboratory
ASM	American Society for Metals (currently known simply as ASM International)
ASME	American Society of Mechanical Engineers
ASTM	American Society for Testing and Materials
ATR	Advanced Test Reactor
B&PV	Boiler & Pressure Vessel Code
B&W	Babcock & Wilcox (NSSS vendor)
BWR	Boiling Water Reactor
CASS	Cast Austenitic Stainless Steel
C&W	Corrosion and Wear
CE	Combustion Engineering (NSSS vendor)
CEA	Control Element Assembly or French Atomic Energy Commission (Commissariat à l'Énergie Atomique)
CEDM	Control Element Drive Mechanism
CMTR	Certified Material Test Report
CRDM	Control Rod Drive Mechanism

Acronym/Abbreviation	Definition
CT	Compact Tension (fracture toughness test specimen)
CUF	Cumulative Usage Factor
CW	Cold-Work
DBTT	Ductile-to-Brittle Transition Temperature
DFR	Dounreay Fast Reactor
DM	Degradation Matrix
DPA	Displacements Per Atom
EBR	Experimental Breeder Reactor
ECP	Electrochemical Potential
EDF	Electricité de France (the French electric utility)
EFPY	Effective Full Power Year
EPFM	Elastic-Plastic Fracture Mechanics
EPRI	Electric Power Research Institute: manages industry research and development programs.
ETR	Experimental Test Reactor
FA	Fuel Assembly
FBR	Fast Breeder Reactor
FAC	Flow-Accelerated Corrosion
FANP	Framatome ANP, Inc., an AREVA and Siemens company
FIV	Flow-Induced Vibration
GALL	Generic Aging Lessons Learned
FATT	Fracture Appearance Transition Temperature
FCA	Flux-Cored-Arc welding process
FFTF	Fast Flux Test Facility
FN	Ferrite Number
GMA	Gas-Metal-Arc welding process
GTA	Gas-Tungsten-Arc welding process
HRC	Rockwell C Hardness value

Acronym/Abbreviation	Definition
HTH	High Temperature Heat-Treatment Condition
HAZ	Heat-Affected Zone
HCF	High-Cycle Fatigue
HFIR	High Flux Isotope Reactor
IASCC	Irradiation-Assisted Stress Corrosion Cracking
IC	Irradiation-enhanced Creep
IE	Irradiation Embrittlement or a generic bulletin issued by the NRC, depending on context
IGSCC	Intergranular Stress Corrosion Cracking
IMT	Issue Management Table: provides brief summary statements on the consequences of failure for specific pieces of equipment together with comments on mitigation options, inspection and evaluation guidance, repair/replacement options and overall priority.
IP	Issue Program: various industry funded programs that support the materials work.
I&E	Inspection & Evaluation
JOBB	Joint Owners Baffle Bolt Program
KAPL	Knolls Atomic Power Laboratory
LCF	Low-Cycle Fatigue
LEFM	Linear-Elastic Fracture Mechanics
LTCP	Low-Temperature Crack Propagation
LWR	Light Water Reactor
MDA	Materials Degradation Assessment
MEOG	Materials Executive Oversight Group: provides executive oversight for materials work, organized under NSIAC.
MMA	Manual-Metal-Arc welding process
MPC	Materials Property Council
MRP	Materials Reliability Program
MTAG	Materials Technology Advisory Group: provides technical oversight for materials work, organized under NSIAC.
MTI	Materials Technology Institute of the Chemical Process Industries,

Acronym/Abbreviation	Definition
	Inc.
NACE	National Association of Corrosion Engineers
NEI	Nuclear Energy Institute: is the policy organization of the nuclear energy and technologies industry and participates in both the national and global policy-making process. NEI's objective is to ensure the formation of policies that promote the beneficial uses of nuclear energy and technologies in the United States and around the world. (Framatome ANP is a member.)
NRC	Nuclear Regulatory Commission
NRL	Naval Research Laboratory
NSIAC	(NEI) Nuclear Strategic Issues Advisory Committee
NSSS	Nuclear Steam Supply System
NUREG	<u>N</u> uclear <u>R</u> egulatory Commission Technical Report Designation
OD	Outside Diameter
ORR	Oak Ridge Research Reactor
PH	Precipitation-Hardenable
PNNL	Pacific Northwest National Laboratory
PVP	Pressure Vessel and Piping Division Conference, an annual publication of ASME
PWSCC	Primary Water Stress Corrosion Cracking
PWR	Pressurized Water Reactor
RCS	Reactor Coolant System
RI-ITG	Reactor Internals-Issue Task Group
RIS	Radiation-Induced Segregation
RiT	Reduction in Toughness
RV	Reactor Vessel
SA	Solution-Annealed, Submerged-Arc (welding process), or ASME Code specification prefix (e.g., SA-350) depending on context
SCC	Stress Corrosion Cracking
SFE	Stacking Fault Energy
SFEN	Société Française d'Énergie Nucléaire

Acronym/Abbreviation	Definition
SMA	Shielded-Metal Arc welding process
SR	Stress Relaxation
SS	Stainless Steel
TE	Thermal Aging Embrittlement
TEM	Transmission Electron Microscope
TGSCC	Transgranular Stress Corrosion Cracking
TMS	The Minerals, Metals, and Materials Society
TT	Thermal Treatment
UNS	Unified Numbering System
USE	Upper Shelf Energy
VS	Void Swelling
W	Westinghouse (NSSS vendor)
WCAP	Westinghouse Commercial Atomic Power (report designation issued by Westinghouse Nuclear)
WOG	Westinghouse Owners Group
WRC	Welding Research Council (report designation issued by this organization)
YS	Yield Strength

CONTENTS

1 INTRODUCTION	1-1
1.1 Report Purpose	1-1
1.2 Background	1-1
1.3 Threshold and Screening Definitions	1-8
1.4 Materials and Age-Related Degradation Mechanisms	1-9
1.5 Report Structure	1-10
1.6 References	1-11
2 SCREENING FOR AGE-RELATED DEGRADATION	2-1
2.1 Cracking	2-1
2.2 Reduction of Fracture Toughness	2-5
2.3 Loss of Mechanical Closure Integrity	2-9
2.4 Loss of Material	2-10
2.5 Changes in Dimension	2-11
2.6 References	2-12
3 COMPILING SCREENING PARAMETERS AND SAMPLE TEMPLATE	3-1
3.1 Screening and Categorization for Significance	3-1
3.2 Screening Parameters for Age-Related Degradation	3-2
3.2.1 Material	3-2
3.2.2 Dose (Neutron Exposure)	3-4
3.2.3 Cold-Work	3-5
3.2.4 Multi-Pass Welds	3-5
3.2.5 Ferrite and Molybdenum Content	3-5
3.2.6 Applied Stress	3-6
3.2.7 Operating Temperature	3-6
3.2.8 Tempering Temperature	3-6
3.2.9 Wear Potential	3-7

3.2.10 Fatigue Usage Factor	3-7
3.3 Initial Screening Process.....	3-7
3.4 References	3-9

A APPENDIX A: STRESS CORROSION CRACKING (EXCLUDING IRRADIATION EFFECTS) A-1

A.1 General Description of Stress Corrosion Cracking	A-1
A.1.1 Austenitic Stainless Steels	A-4
A.1.2 Martensitic Stainless Steels	A-9
A.1.3 Martensitic Precipitation-Hardenable Stainless Steels.....	A-10
A.1.4 Austenitic Precipitation-Hardenable Stainless Steels and Nickel-Base Alloys....	A-11
A.1.5 Cast Austenitic Stainless Steels.....	A-13
A.1.6 Austenitic Nickel-Base Alloys	A-14
Low Temperature Crack Propagation	A-15
A.2 Summary and Discussion	A-16
A.3 SCC Threshold and Screening Criteria.....	A-17
Austenitic Stainless Steels.....	A-17
Martensitic Stainless Steels	A-18
Martensitic Precipitation-Hardenable Stainless Steels	A-18
Austenitic Precipitation-Hardenable Stainless Steels	A-18
Cast Austenitic Stainless Steels	A-18
Austenitic Nickel-Base Alloys.....	A-19
Austenitic Precipitation-Hardenable Nickel-Base Alloys	A-19
A.4 SCC References	A-19

B APPENDIX B: IRRADIATION-ASSISTED STRESS CORROSION CRACKING..... B-1

B.1 General Description of Irradiation-Assisted Stress Corrosion Cracking	B-1
B.1.1 Annealed vs. Cold-Worked Materials	B-2
B.1.2 Austenitic Stainless Steels	B-2
B.1.3 Martensitic and Martensitic Precipitation-Hardenable Stainless Steels	B-3
B.1.4 Austenitic Precipitation-Hardenable Stainless Steels	B-4
B.1.5 Cast Austenitic Stainless Steels.....	B-4
B.1.6 Austenitic Nickel-Base Alloys	B-4
B.1.7 Austenitic Precipitation-Hardenable Nickel-Base Alloys	B-4
B.2 IASCC Summary and Discussion	B-5
B.3 IASCC Threshold and Screening Criteria	B-5

B.4 IASCC References.....	B-8
C APPENDIX C: WEAR	C-1
C.1 General Description of Wear	C-1
C.2 PWR Internals Wear Events	C-4
C.2.1 Westinghouse Internals Designs	C-4
C.2.2 B&W Internals Design	C-5
C.2.3 CE Internals Designs	C-5
C.3 Potential Long Term Issues	C-6
C.4 Wear Threshold and Screening Criteria	C-6
C.5 Wear References.....	C-7
D APPENDIX D: FATIGUE	D-1
D.1 General Description of Fatigue	D-1
D.1.1 Low-Cycle Fatigue (LCF)	D-2
D.1.2 High-Cycle Fatigue (HCF).....	D-2
D.1.3 Environmental or Corrosion Fatigue	D-3
D.2 Application of ASME B&PV Code Rules.....	D-3
D.3 Fatigue Summary and Discussion	D-4
D.4 Fatigue Threshold and Screening Criteria	D-4
D.5 Fatigue References	D-5
E APPENDIX E: THERMAL AGING EMBRITTLEMENT.....	E-1
E.1 General Description of Thermal Aging Embrittlement.....	E-1
E.1.1 CASS	E-1
E.1.2 Austenitic Stainless Steel Welds	E-4
E.1.3 Martensitic Stainless Steel	E-6
E.1.4 Martensitic Precipitation-Hardenable Stainless Steel	E-10
E.2 TE Summary and Discussion.....	E-13
E.3 TE Threshold and Screening Criteria.....	E-15
E.4 TE References	E-16
F APPENDIX F: IRRADIATION EMBRITTLEMENT.....	F-1
F.1 General Description of Irradiation Embrittlement	F-1
F.2 Fracture Toughness of Irradiated Austenitic Stainless Steels.....	F-2
F.2.1 Type 304 and Type 316 in Fast Reactors	F-2

F.2.2	Type 347 and Type 348 in Fast Reactors	F-3
F.2.3	Austenitic Stainless Steel Weld Metals in Fast Reactors	F-3
F.2.4	Austenitic Stainless Steel and Weld Metals in PWRs and BWRs	F-5
F.3	Tensile Properties of Irradiated Austenitic Stainless Steels	F-7
F.4	IE Threshold and Screening Criteria	F-7
F.5	IE References	F-10
G	APPENDIX G: VOID SWELLING	G-1
G.1	General Description of Void Swelling	G-1
G.2	Descriptions of Void Swelling of Austenitic Stainless Steels Irradiated in EBR-II	G-4
G.2.1	Earlier Published Equations	G-4
G.2.2	New Type 304 Stainless Steel Equation	G-9
G.3	Void Swelling of Russian Stainless Steels in Other Fast Reactors	G-15
G.3.1	Void Swelling Reported in BN-350, BOR-60 and BR-10	G-15
G.3.2	BN-350 Void Swelling Database Analyzed by Yilmaz et al.	G-17
G.4	JOBB Void Swelling Data	G-19
G.4.1	JOBB BOR-60 Density Measurement	G-19
G.4.2	JOBB TEM Measurement of EBR-II Specimens	G-21
G.5	Void Swelling in Removed PWR Baffle Bolts	G-23
G.6	Factors Affecting Void Swelling	G-25
G.7	VS Threshold and Screening Criteria	G-28
G.8	VS References	G-30
H	APPENDIX H: STRESS RELAXATION AND IRRADIATION CREEP	H-1
H.1	General Description of Stress Relaxation and Irradiation Creep	H-1
H.1.1	Thermal Stress Relaxation	H-2
H.1.2	Irradiation-Enhanced Stress Relaxation and Creep	H-3
H.2	SR/IC Summary and Discussion	H-9
H.2.1	Summary of Thermal Stress Relaxation and Creep	H-10
H.2.2	Summary of Irradiation-Enhanced Stress Relaxation and Creep	H-10
H.3	SR/IC Threshold and Screening Criteria	H-10
H.4	SR/IC References	H-13

LIST OF FIGURES

Figure 1-1 Framework for Implementation of Aging Management Using Screening, Functionality Evaluations, and Inspections	1-2
Figure 1-2 General Arrangement of Babcock & Wilcox Designed Internals	1-4
Figure 1-3 General Arrangement of Combustion Engineering Designed Internals.....	1-5
Figure 1-4 General Arrangement of Westinghouse Designed Internals	1-6
Figure 1-5 Process for Categorization of PWR Internals Components.....	1-7
Figure A-1 Synergistic Effects Required for Stress Corrosion in Metals.....	A-2
Figure A-2 Crack Paths Describing Stress Corrosion Cracking in Metals	A-2
Figure A-3 Example of Intergranular Stress Corrosion Cracking	A-3
Figure A-4 Example of Transgranular Stress Corrosion Cracking	A-3
Figure A-5 Effect of Oxygen on Chloride SCC ^[A-1]	A-5
Figure A-6 The Effects of Oxygen and Chloride on the SCC of 300 Series Stainless Steels in High Temperature Water as Revealed by Slow Strain Rate Testing ^[A-10]	A-6
Figure A-7 Cracking of Sensitized 304 Stainless Steel in Water Without Chlorides ^[A-1]	A-7
Figure A-8 Effect of Yield Strength and Martensite on the Stress Corrosion Crack Growth Rate on Austenitic Stainless Steel in a Simulated PWR Environment ^[A-14]	A-9
Figure A-9 Failure Trend Line for Alloy A-286 SCC ^[A-39]	A-11
Figure A-10 Failure Trend Line for Alloy X-750 HTH SCC ^[A-39]	A-12
Figure A-11 Stress Required to Produce SCC in Several CASS Alloys with Varying Amounts of Ferrite ^[A-48]	A-13
Figure A-12 Ferrite Pools Blocking the Propagation of SCC in a Cast Austenitic Stainless Steel ^[A-48]	A-14
Figure B-1 Prediction of IASCC Time-to-Failure Versus Stress ^[B-38]	B-6
Figure B-2 Neutron Fluence Effects on IASCC Susceptibility in BWR and PWR Environments ^[B-39]	B-6
Figure B-3 Proposed Plot of Stress and Neutron Exposure Screening Criteria for IASCC.	B-7
Figure C-1 Abrasive Wear Example	C-2
Figure C-2 Adhesive Wear Example.....	C-3
Figure C-3 Fretting Wear Example	C-4
Figure D-1 Classical Fatigue Failure of a Bolt by Reverse Bending	D-1
Figure E-1 Typical Microstructures Of Centrifugally Cast Austenitic Stainless Steel, With Islands Of Ferrite In An Austenite Matrix ^[E-35]	E-3

Figure E-2 Comparison Of J_{IC} Of Unirradiated Stainless Steel Weld By Different Processes ^[E-19]	E-5
Figure E-3 Variation In Hardness As A Function Of Aging Time And Temperature For 13%Cr (Type 410), 13%Cr-1%Ni, And 16%Cr-4%Ni ^[E-26]	E-7
Figure E-4 Charpy V-Notch Impact Energy Transition Curves In The Unaged And Aged Conditions Of 13%Cr (Type 410) And 13%Cr-1%Ni (Longitudinal Orientation) ^[E-27]	E-8
Figure E-5 Typical Charpy V-Notch Transition Behavior of Unaged Type 410 Martensitic Stainless Steel ^[E-28]	E-9
Figure E-6 Izod Data for Unaged Type 410 after Quenching From 1800°F and Tempering At 1150°F (HB 228) ^[E-29]	E-10
Figure E-7 Type 17-4 PH (H-1100), Effect Of %Cr + %Si + %Cb On Exposure Time At 800°F To Cause A 50% Drop In Initial Room Temperature Charpy Impact Energy ^[E-28]	E-12
Figure E-8 Type 17-4 PH (H-1100), Effect Of %P + %S + 0.1%Cb + %N On The Initial Room Temperature Charpy Impact Energy ^[E-28]	E-12
Figure E-9 Effect Of Exposure On Charpy V-Notch Impact Properties At 800°F For Type 17-4 PH (H-1100) ^[E-28]	E-13
Figure E-10 Predicted Embrittlement of Type 17-4 PH (H-110) FATT ₅₀ -vs.-EFPYs and USE-vs.-EFPYs as a Function of Exposure Time at 600°F ^[E-3]	E-14
Figure F-1 Elevated Temperature Fracture Toughness K_{Jc} as a Function of dpa for Type 304 and Type 316 Irradiated in Fast Reactors (Based on Reference F-2)	F-4
Figure F-2 Elevated Temperature Fracture Toughness K_{Jc} of Austenitic Stainless Steels and Welds Irradiated in BWRs or PWRs as a Function of dpa ^[F-2]	F-6
Figure F-3 Elevated Temperature Total Elongation as a Function of dpa for Type 304, Type 304L, and Type 347 ^[F-2]	F-8
Figure F-4 Elevated Temperature Total Elongation as a Function of dpa for Type 316 ^[F-2]	F-8
Figure F-5 Elevated Temperature Total Elongation as a Function of dpa for Type 308 and 308L Weld, Type 304 HAZ, and Type CF-8 CASS ^[F-2]	F-9
Figure G-1 Swelling-vs.-dpa at Different Irradiation Temperatures for Several Empirical Swelling Equations (Based on Austenitic Stainless Steel Swelling Data From EBR-II, Except 1Cr18Ni10Ti(MTO) From BN-350 (The Bounding Swelling Line is Also Indicated)	G-6
Figure G-2 Swelling Predictions versus DPA Using the Stress-Free Swelling Equation Developed by Garner[G-34] [Note: F-F indicates predictions using the Foster-Flinn Equation[G-31] for Comparison]	G-11
Figure G-3 Volumetric Change from Density Measurements of JOBB Tensile Specimens Irradiated in BOR-60 at 320°C (608°F)	G-22
Figure H-1 Schematic Representation of Creep Curves Under Constant Load. ^[H-3]	H-1
Figure H-2 Thermal Stress Relaxation (Without Irradiation) of a 10% Cold-Worked and Solution-Annealed Type 304 Bar ^[H-4]	H-4
Figure H-3 Thermal Stress Relaxation (Without Irradiation) of Mill Annealed, Straightened, and 50% Cold-Worked & Solution-Annealed Type 304 Bar. ^[H-4]	H-5
Figure H-4 Thermal Stress Relaxation (Without Irradiation) of 10% Cold-Worked Type 304 Bar ^[H-4]	H-6

Figure H-5 Thermal Stress Relaxation (Without Irradiation) of 20% Cold-Worked Type 304 Bar ^[H-4]	H-7
Figure H-6 Comparison of Thermal Creep and Irradiation-Enhanced Creep of a 20% Cold-Worked Type 316 Stainless Steel Irradiated in EBR-II ^[H-5]	H-8
Figure H-7 Trend Line for Screening Irradiation-Enhanced Stress Relaxation Based on Available Test Data	H-11

LIST OF TABLES

Table 1-1 Materials and Procurement Specifications Used for PWR Internals.....	1-10
Table 2-1 Stress Corrosion Cracking Screening Criteria for PWR Internals Materials	2-3
Table 2-2 Irradiation-Assisted Stress Corrosion Cracking Screening Criteria for PWR Internals Materials.....	2-4
Table 2-3 Fatigue Screening Criteria for PWR Internals Materials	2-5
Table 2-4 Thermal Aging Embrittlement Screening Criteria for PWR Internals Materials.....	2-6
Table 2-5 Irradiation Embrittlement Screening Criteria for PWR Internals Materials	2-8
Table 2-6 Void Swelling Screening Criteria for PWR Internals Materials.....	2-9
Table 2-7 Thermal and Irradiation-Enhanced Stress Relaxation and Creep Screening Criteria for PWR Internals Materials.....	2-10
Table 2-8 Wear Screening Criteria for PWR Internals Materials.....	2-11
Table 3-1 Example Tabulation of Screening Parameters	3-3
Table 3-2 PWR Internals Age-Related Degradation Mechanism Screening Criteria	3-8
Table E-1 Temperature Izod Impact Values of Type 17-4 PH (H-1100) ^[E-24]	E-11
Table F-1 Fracture Toughness of Type 347/348 Irradiated in Fast Reactors ^[F-2]	F-5
Table G-1 Irradiation Conditions for the Empirical Equations Plotted in Figure G-1	G-5
Table G-2 Chemical Composition of Russian EI-847 Stainless Steel in BN-350 ^[G-35, G-36]	G-15
Table G-3 Swelling Parameters for Russian Stainless Steels by Yilmaz et al. ^[G-43]	G-18
Table G-4 Chemical Composition of JOBB Specimens ^[G-44]	G-20
Table G-5 Thermomechanical History of JOBB Specimens ^[G-44]	G-20
Table G-6 Swelling of JOBB Specimens Irradiated in EBR-II at 375°C (707°F) ^[G-46]	G-21
Table G-7 Plants with Baffle Bolts Removed and Inspected for Void Swelling ^[G-47, G-48]	G-23
Table G-8 Void Swelling in PWR Baffle-to-Former Bolts	G-24

1

INTRODUCTION

1.1 Report Purpose

The purpose of this report is to develop and provide the technical bases for screening criteria for age-related degradation evaluation of Pressurized Water Reactor (PWR) internals component items. This report was prepared under the direction and sponsorship of the EPRI Materials Reliability Program (MRP) Reactor Internals Issue Task Group (RI-ITG). Valuable input and review comments were received from many sources, in particular from the following RI-ITG Expert Panel core members:

- P. Scott and S. Fyfitch (Framatome ANP)
- R. Shogan and R. Lott (Westinghouse)
- F. Garner (PNNL)

This report is a key element in an overall strategy for managing the effects of aging in PWR internals using knowledge of internals design, materials and material properties, and applying screening methodologies for known aging degradation mechanisms. Related MRP documents include a Framework and Strategy for Managing Aging Effects in PWR Internals^[1-1] and Inspection and Flaw Evaluation Strategies for Managing Aging Effects in PWR Internals.^[1-2]

1.2 Background

The framework for the implementation of a PWR internals aging management program incorporating the degradation research results and using inspections and flaw tolerance evaluations to manage the degradation issues is given in Figure 1-1. The important elements of this framework are:

- Screening of component items for susceptibility to the age-related degradation mechanisms, performed by establishing a set of screening criteria for each relevant age-related degradation mechanism,
- Evaluating the most affected component items or regions of greatest impact for the aging effects of cracking, reduction of fracture toughness, loss of mechanical closure integrity, loss of material, or changes in dimensions, and
- Performing functionality analyses and safety assessment of the critical component items that exceed the screening criteria to determine the need for supplementary aging management.

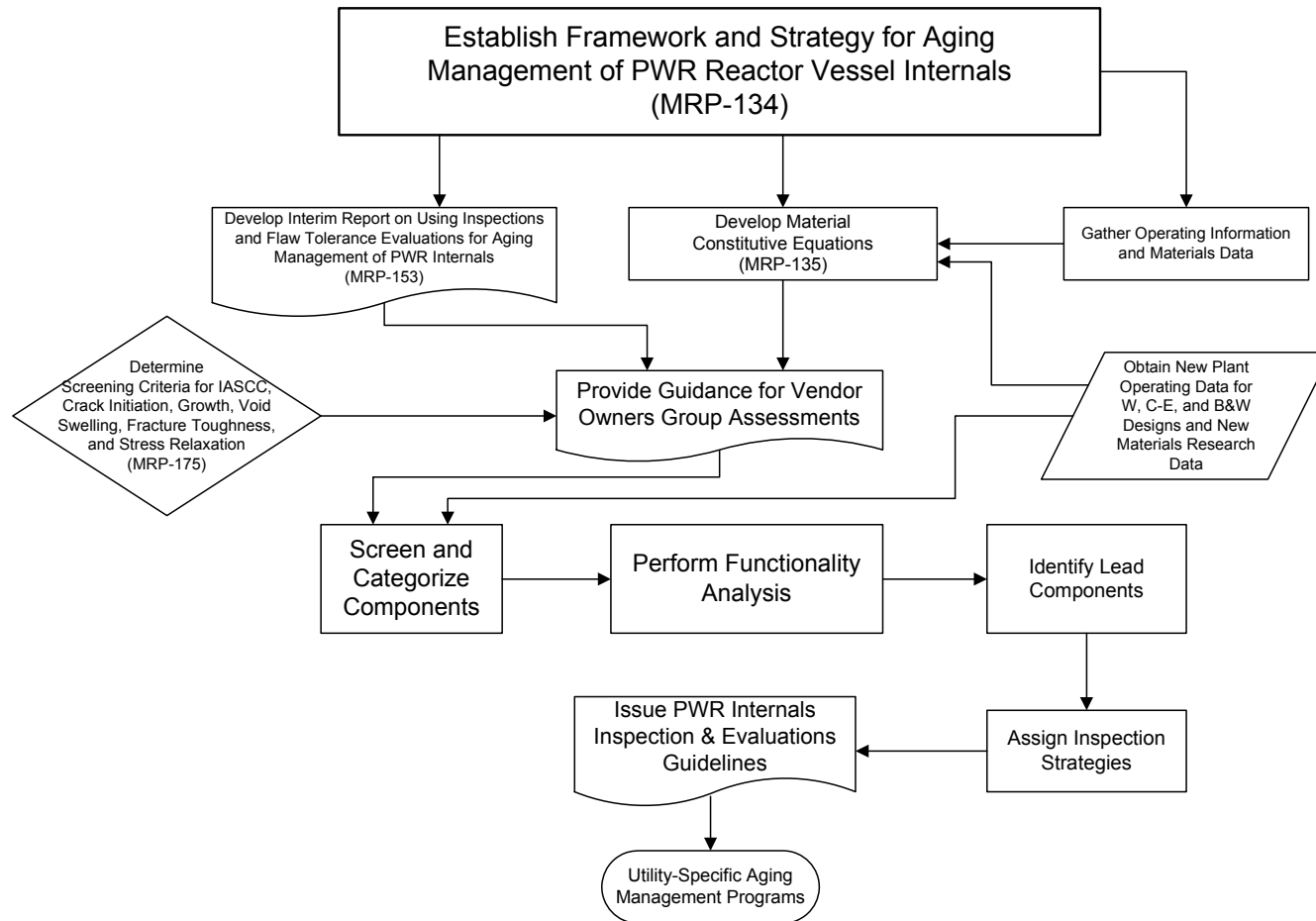


Figure 1-1
Framework for Implementation of Aging Management Using Screening, Functionality Evaluations, and Inspections

The reports discussed above provide a framework and strategy for management of these aging effects using screening, inspection methods and flaw tolerance evaluations that can be applied to the PWR internals component items. Figures 1-2, 1-3, and 1-4 generically illustrate the main component items of the Babcock & Wilcox, Combustion Engineering, and Westinghouse designed PWR internals, respectively. The screening criteria developed in this report will be used to categorize all PWR internals component items in accordance with the strategy developed in Figure 1-5 (Figure 4-1 of MRP-134).^[1-1] The categories defined therein are based on the significance of the aging effects and will be related to the type of inspections to be used for managing the effects:

Category A

Category A components are those for which aging effects are below the screening criteria, so that aging degradation significance is minimal. Typically, only the required ASME B&PV Code Section XI Examination Category B-N-3 ISI visual examinations (VT-3) will be performed on these components to assess potential aging effects.

Category C

Category C PWR internals components are those “lead” components for which aging effects are above screening levels, which have moderate or high susceptibility to degradation. Enhanced inspections (e.g., Enhanced VT-1, UT, etc.) and/or surveillance sampling will typically be warranted to assess aging effects and verify functionality of these components.

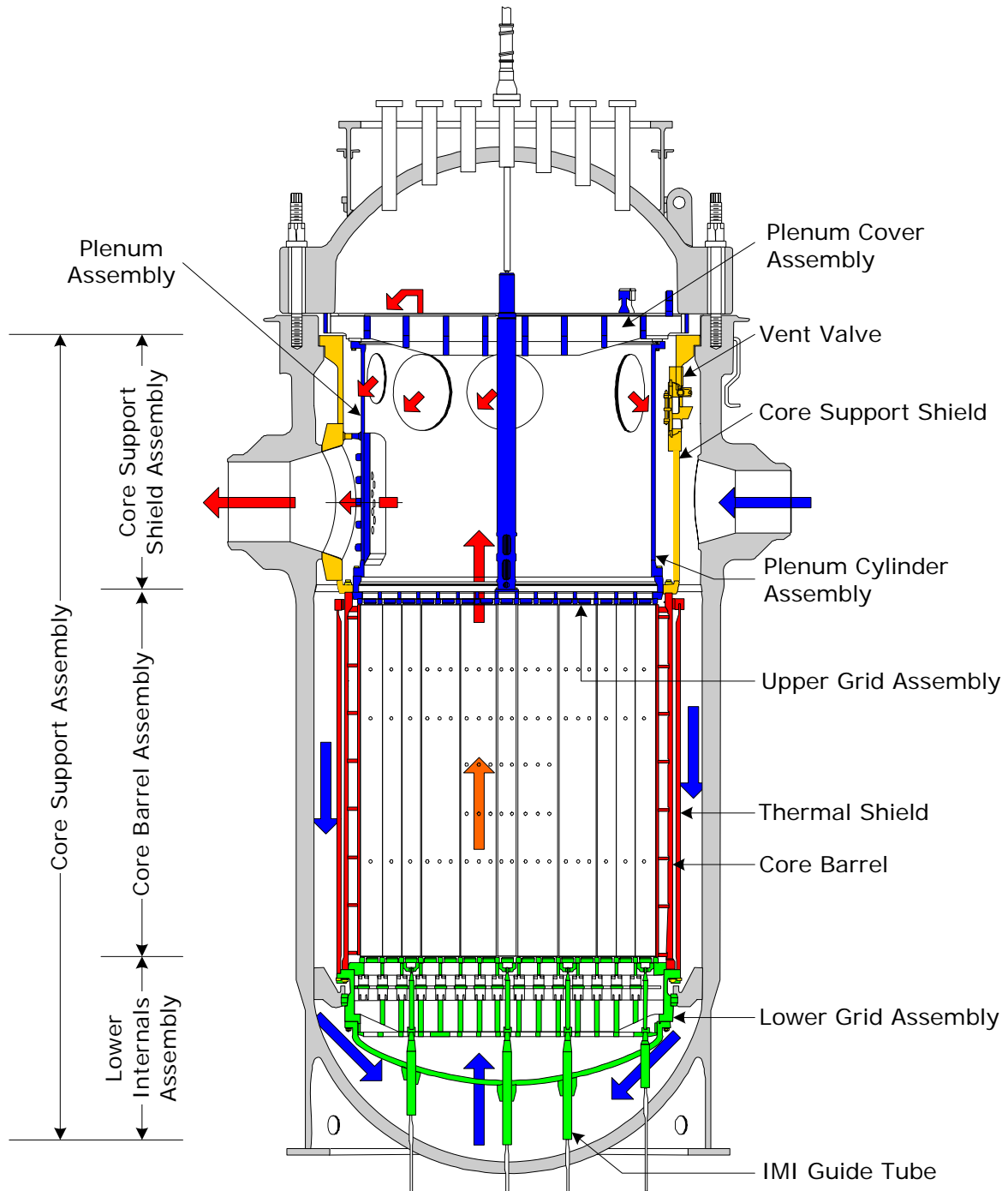
Category B

Category B includes those PWR internals components that are moderately susceptible to the aging effects, such that the effects on function cannot easily be dispositioned by screening and are not “lead” components. Category B components may require additional evaluations to be shown tolerant of the aging effects with no loss of functionality (i.e., damage tolerant).

Category B'

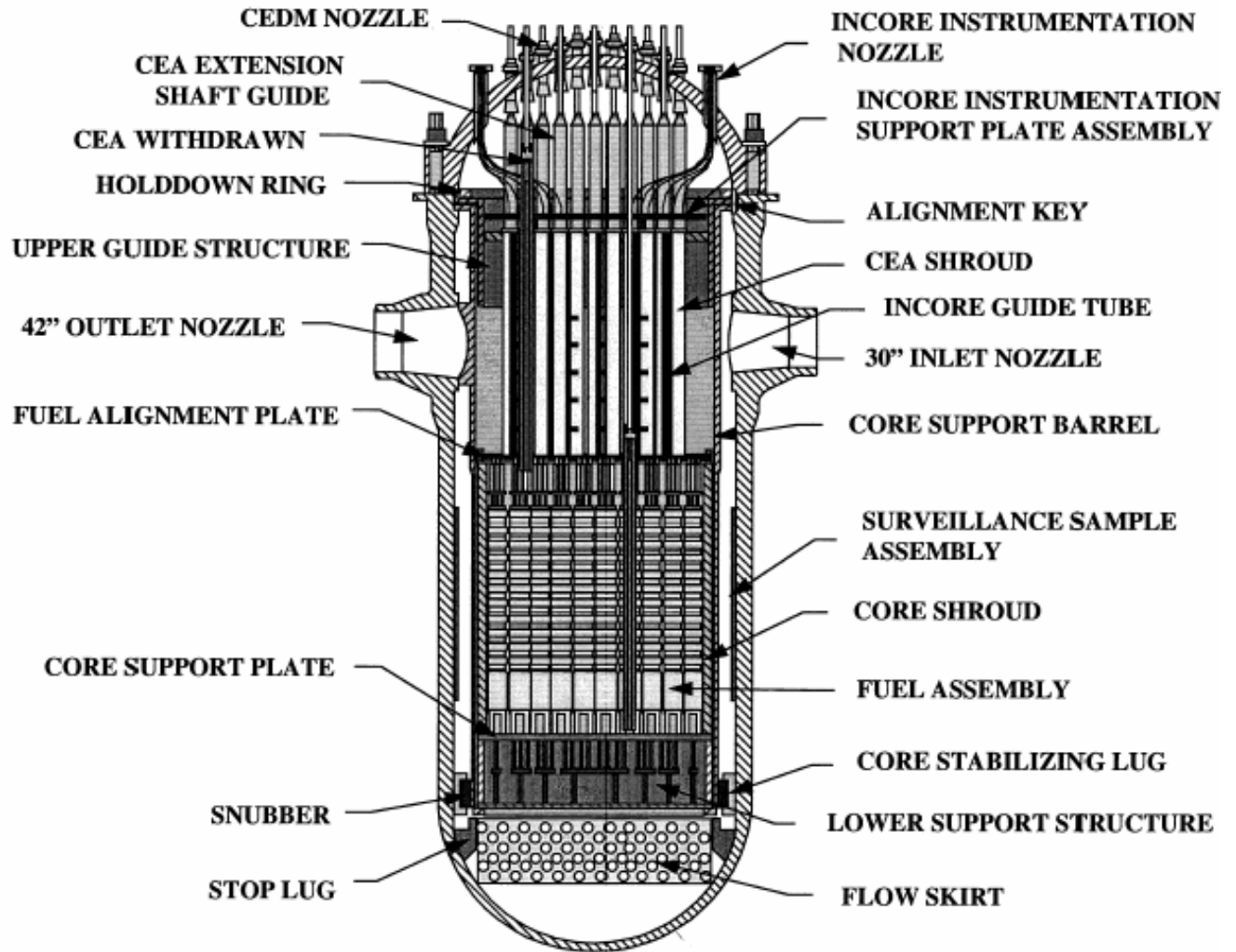
Category B' components are those “lead” components that can be shown to be tolerant of the aging effects through a functionality assessment. These components are candidates for an expanded inspection program.

This categorization depends on an initial screening for susceptibility and functionality of the component items. This report provides a general overview of the materials age-related degradation mechanisms and provides suggested screening criteria that can be used for an initial categorization of the potentially susceptible, or non-susceptible, PWR internals component items.



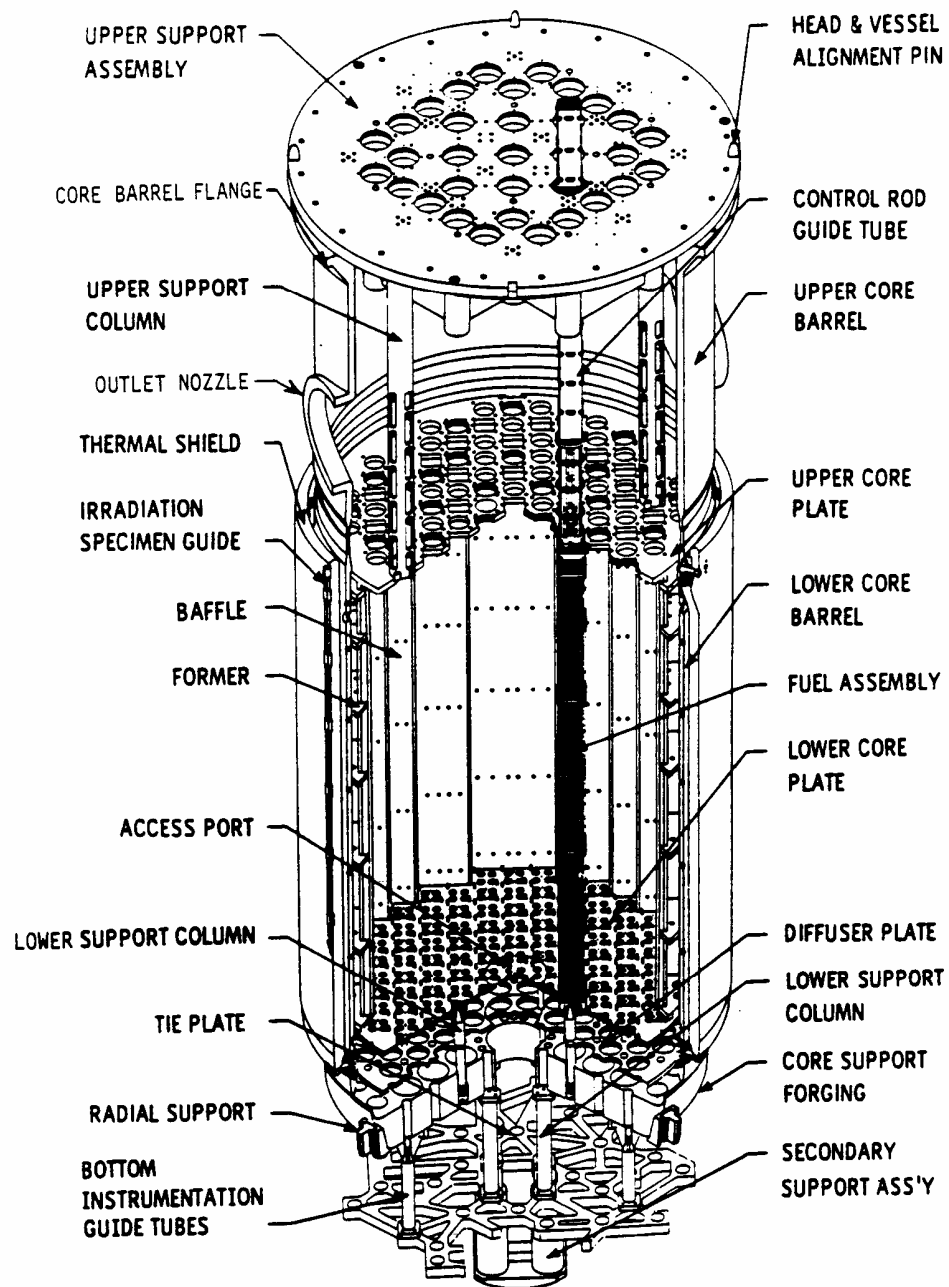
(Note: Typical configuration – unique variations may exist for individual plant designs; some items rotated for clarity)

Figure 1-2
General Arrangement of Babcock & Wilcox Designed Internals



(Typical configuration – unique variations may exist for individual plant designs; some items rotated for clarity)

Figure 1-3
General Arrangement of Combustion Engineering Designed Internals



(Typical configuration – unique variations may exist for individual plant designs)

Figure 1-4
General Arrangement of Westinghouse Designed Internals

Figure 1-5
Process for Categorization of PWR Internals Components

A key step in this process is to apply screening criteria (such as material chemical composition, neutron fluence, temperature history, and applied stress) to identify those PWR internals component items for which the effects of age-related degradation on functionality during the license renewal term are insignificant (i.e., Category A, as defined in MRP-134). For those locations that do not exceed the screening criteria, no further actions would be required, other than to continue existing plant inspection and maintenance programs.

The portion of the strategy that is covered by this report is identified in Figure 1-1. This includes the determination of screening criteria for each of the materials age-related degradation mechanisms identified for PWR internals (e.g., irradiation-assisted stress corrosion cracking, irradiation embrittlement, void swelling, and wear). These criteria for screening, based on an understanding of age-related degradation mechanisms and engineering judgment, will be instrumental in the evaluation and categorization of vendor-specific PWR internals component items. A significant aspect of the overall strategy is the differentiation between thresholds for susceptibility and screening criteria for potential loss of functionality (Section 1.3). In this application, loss of functionality is the primary concern, and appropriate screening criteria will be applied. Since all lead component items (i.e., Category C, as defined in MRP-134) will undergo some inspection and other potentially susceptible component items (i.e., Categories B and B') will be available for inspection as necessary, there is no need to include any additional conservatism in the screening criteria to require augmented inspections for minimally susceptible component items. Therefore, the screening criteria should be the best estimate criteria that will identify potential component items for further evaluation of the effects of degradation on functionality. Functionality evaluations may include expert opinions, engineering judgments, or detailed stress evaluations.

The models used in future functionality evaluations for those component items that cannot be screened out and construed as lead items will include irradiation-dependent material properties data, behavior equations and models for stress-strain curves, creep equations, void swelling equations, and irradiation-assisted stress corrosion cracking susceptibility and damage formulation.^[1-3] Parametric and special-effects studies, using these models (either simplified or more detailed), will be carried out, to examine the effects of individual mechanisms and phenomena on functionality. These might include such considerations as void swelling effects on irradiation-enhanced creep and stress relaxation, stress concentration effects on bolt loading, bolt-load relaxation and loss of pre-load, differential swelling, potential irradiation-assisted stress corrosion cracking (IASCC) susceptibility considering statistical material variability, effects of high doses at re-entrant corners, re-creation of residual stresses in welded joints and the effects of irradiation-enhanced creep and stress relaxation on residual stresses and IASCC susceptibility of welded joints.

From the results of the screening and subsequent analyses, a technical basis can be documented for PWR internals inspection and flaw evaluation guidance applicable to plants throughout the license renewal term.

1.3 Threshold and Screening Definitions

Understanding the mechanisms of aging degradation is important for managing the potential aging effects in PWR internals. PWR internals aging management involves monitoring or predicting the levels of degradation, evaluating mitigation and/or repair techniques, and using inspections or some other type of surveillance to assure component integrity. An age-related degradation mechanism is considered significant if it cannot be shown that the component would maintain its function when the degradation mechanism is allowed to continue without additional preventive or mitigative measures. Thus, there is a distinct difference between threshold values

for observing the onset of an aging effect and screening values for evaluating the significance of age-related degradation mechanisms. The following are working definitions agreed upon by the RI-ITG, which will be utilized in this report:

- **Threshold Value** - The level of susceptibility when an aging effect is first observed or quantifiable.
- **Screening Value** - The level of susceptibility when an aging effect may be significant to functionality or safety.

Quantification of the screening values, referred to here as criteria, will require knowledge of the specific age-related degradation mechanisms, degradation effects, some engineering judgment, and possibly empirical extrapolations where data may be lacking. The screening criteria provided in this report will be used by those organizations performing the screening and categorization of component items.

1.4 Materials and Age-Related Degradation Mechanisms

NEI 03-08^[1-4] is a materials management guideline that became effective on January 2, 2004. This document outlines the policy and practices that the industry has committed to follow in managing materials aging issues. Two standing committees were established to assist the utilities and the issue programs (IPs) they fund. The Materials Technology Advisory Group (MTAG) provides technical oversight and the Materials Executive Oversight Group (MEOG) provides executive oversight. Neither of these groups is directly involved in the technical work, which resides in the IPs. (The degradation matrix and issue management table IPs discussed below are being managed through EPRI.) For example, one of the current IPs that is governed by this guideline is the EPRI MRP.

Recently, an industry Ad Hoc Committee was tasked by the MTAG to prepare a generic Degradation Matrix (DM) applicable to all PWR internals designs.^[1-5] Expert elicitation, laboratory studies, and field experience were used to identify potential mechanisms by which each of the PWR internals materials, among other materials and component items, might degrade. The current DM groups the age-related degradation mechanisms into several broad categories such as Stress Corrosion Cracking (SCC), Corrosion and Wear (C&W), Fatigue (Fat.) and Reduction in Toughness (RiT). Each of these is comprised of various subcategories of degradation. For example, the RiT category includes thermal aging embrittlement and void swelling.

Screening criteria are included in this report for the various age-related degradation mechanisms identified as potentially applicable to PWR internals from the DM effort. Age-related degradation mechanisms may be removed or new ones may be added as a result of continuing programs on aging of PWR internals. The currently identified age-related degradation mechanisms discussed in this report are as follows:¹

¹ The more generally known acronyms provided in this list will be used throughout the remainder of this report, in lieu of the acronyms defined in the industry DM.

- Stress Corrosion Cracking (SCC), which includes
 - Intergranular SCC (IGSCC)
 - Transgranular SCC (TGSCC)
 - Primary water SCC (PWSCC)
 - Low-temperature crack propagation (LTCP)
- Irradiation-assisted SCC (IASCC)
- Wear
- Fatigue, which includes
 - High-cycle fatigue (HCF)
 - Low-cycle fatigue (LCF)
- Thermal aging embrittlement (TE)
- Irradiation embrittlement (IE)
- Void swelling (VS)
- Irradiation-enhanced stress relaxation and creep (SR/IC)

The DM was used as input to a Materials Degradation Assessment / Issue Management Table (MDA/IMT) Ad-Hoc Committee. This committee developed the IMTs for reactor coolant system components, one of which was the PWR internals IMT.^[1-6] The IMT is intended to be a living document and will be updated as necessary. It is expected to be used by the industry to document the state of the art, identify priority changes, map progress, determine conclusions, and assess results on an on-going basis. The materials and procurement specifications utilized in PWR internals for Babcock & Wilcox (B&W), Combustion Engineering (CE), and Westinghouse (W) designs, as identified by the IMT effort, are provided in Table 1-1.

Table 1-1
Materials and Procurement Specifications Used for PWR Internals

1.5 Report Structure

A general overview description of the various age-related degradation mechanisms, observable thresholds, and the suggested screening criteria for each is contained in the Appendices. Chapter 2 provides a roadmap for tying aging effects to age-related degradation mechanisms and summarizes the thresholds and screening criteria developed in the Appendices, including discrete screening tables for each mechanism and material combination. Chapter 3 provides a summary listing of the screening criteria parameters and suggestions for their compilation and tabulation. In addition, Chapter 3 also provides an example screening template. Included in Chapter 3 is a simplified screening criteria table for use in performing the initial screening process.

1.6 References

- 1-1 Materials Reliability Program: Framework and Strategies for Managing Aging Effects in PWR Reactor Vessel Internals (MRP-134), EPRI 1008203, 2005.
- 1-2 Materials Reliability Program: Inspection and Flaw Evaluation Strategies for Managing Aging Effects in PWR Internals (MRP-153), EPRI 1012082, 2005.
- 1-3 Materials Reliability Program: Development of Material Constitutive Model for Irradiated Austenitic Stainless Steels (MRP-135), EPRI 1011127, 2004.
- 1-4 NEI Document NEING0620033926, “NEI 03-08, Guideline for the Management of Materials Issues,” May 2003.
- 1-5 “Materials Degradation Matrix,” Enclosure to NEI Letter from M.S. Fertel to Chief Nuclear Officers, November 2, 2004.
- 1-6 Pressurized Water Reactor Issue Management Table, PWR-IMT Consequence of Failure (MRP-156), EPRI 1012110, 2005.

2

SCREENING FOR AGE-RELATED DEGRADATION

The age-related degradation mechanisms described in Chapter 1 and discussed in detail in the Appendices may lead to aging effects that could result in a loss of function or loss of structural integrity of the PWR internals. Whether or not the age-related degradation mechanisms are active depends on the material type and composition, manufacturing process, product form, operational environment (i.e., neutron fluence, neutron flux, temperature, and water chemistry), stress (operating and residual), etc. It then follows that the possibility of each mechanism must be established using specific and quantifiable screening criteria (to the extent possible). Tables 2-1 through 2-8 summarize the age-related degradation mechanism screening criteria developed in the Appendices that are suggested for use by the RI-ITG for evaluating PWR internals component items. The screening criteria are intended to be indicators of the level of degradation that, degradation below the screening criteria, may clearly be tolerated without compromise of the component functionality. Component items initially screened in by the screening criteria require additional evaluation for proper categorization, as described in MRP-134.^[2-1] Follow-on evaluations, possibly including an assessment of functionality, will be performed.

The license renewal application process involves screening of component items for potential significance of aging effects, and this has been recommended by the Nuclear Regulatory Commission (NRC) in the Generic Aging Lessons Learned (GALL) report.^[2-2] The aging effects that must be considered can be categorized for discussion into the following broad general groups: (1) cracking (initiation and growth); (2) reduction of fracture toughness; (3) loss of material; (4) change in dimension (including mechanical deformation, distortion, and/or ratcheting); and (5) loss of mechanical closure integrity for bolted connections. The following sections identify each of these and list suggested data to be tabulated in order to evaluate each of the potential age-related degradation mechanisms.

2.1 Cracking

Age-related degradation mechanisms that may lead to cracking of the PWR internals items include IASCC, PWSCC/LTCP, and fatigue. Cracking due to SCC is not expected to be a significant aging mechanism for the PWR internals because of the rigorousness of the reactor coolant chemistry controls, as required by plant Technical Specifications. However, some component items (such as crimped locking devices and weld heat-affected zones) will initially be screened in due to potentially high cold-work or weld shrinkage strains and possibly evaluated for functionality concerns.

Examples of concern for cracking as a result of IASCC are the austenitic stainless steel alloy component items (plates, bolts and welds) that will experience high fluence exposures due to

their proximity to the core. Cracking concerns from PWSCC/LTCP exist with the nickel-base materials used in the PWR internals.

Environmental effects on fatigue are also one of the cracking concerns for license renewal.

The currently identified potential materials and age-related degradation mechanisms of concern for cracking are addressed separately as follows:

- SCC (Table 2-1)

- Wrought austenitic stainless steels

Component items having high stress (operating and residual) and high cold-work from fabrication (bending or grinding) or welded locations with potentially high heat-affected zone (HAZ) weld shrinkage strains will be screened in as potentially susceptible to SCC.

- Austenitic stainless steel welds

Highly stressed (operating and residual) and low ferrite welds will be screened in as potentially susceptible to SCC. Long-term thermal aging embrittlement may also lead to an SCC concern (Table 2-4).

- Martensitic stainless steels and martensitic PH stainless steels

Component items having high stress (operating and residual) will be screened in as rendering these materials potentially susceptible to SCC. Long-term thermal aging embrittlement may also lead to an SCC concern (Table 2-4).

- Austenitic PH stainless steels

Component items having high stress (operating and residual) and surface cold-work will be screened in as rendering these materials potentially susceptible to SCC. In particular, bolts fabricated with hot-heading or shot-peened in the head-to-shank area that meet the stress criterion are to be evaluated for potential SCC susceptibility.

- Cast Austenitic Stainless Steel (CASS)

Component items having high stress (operating and residual) and low ferrite contents will be screened in as contributors to SCC susceptibility by analogy with austenitic stainless steel welds. Long-term thermal aging embrittlement may also be a concern because the effects of long-term aging on SCC resistance are unknown. However, thermal aging embrittlement is a concern only for CASS materials that exceed the criteria in Table 2-4.

Table 2-1
Stress Corrosion Cracking Screening Criteria for PWR Internals Materials

- Austenitic Ni-base alloys

Component items having high stress (operating and residual) will be screened in as potential contributors to PWSCC, particularly items where the annealing temperatures were insufficient to ensure carbide precipitation on the grain boundaries.

- Austenitic PH Ni-base alloys

Component items having high stress (operating and residual) will be screened in as rendering these materials potentially susceptible to SCC.

- IASCC (Table 2-2)

- All applicable alloys

For component items beyond a lower limit screening dose of 3 dpa (2.0×10^{21} n/cm², E > 1.0 MeV), IASCC is a potential age-related degradation mechanism. Screening depends on stress (operating and residual) level and expected dose (Appendix B, Figure B-3).

Table 2-2

Irradiation-Assisted Stress Corrosion Cracking Screening Criteria for PWR Internals Materials

- Fatigue (Table 2-3)
 - All applicable alloys

Currently, the industry has no clearly defined criteria, but a cumulative usage factor ≥ 0.1 (calculated at the end of the original 40-year license) is suggested for screening component items at this time. In some instances, fatigue was qualified through testing, and these component items should initially be screened in for potential fatigue concerns and evaluated further (e.g., for functionality). In addition, all bolted or spring items for which SR/IC is screened as applicable may also be susceptible to fatigue and should be screened in. In those cases of early plant designs for which fatigue analyses were not performed, it may be necessary to invoke a process known as similitude using more recent design analyses to estimate cumulative usage factors.

Table 2-3
Fatigue Screening Criteria for PWR Internals Materials

2.2 Reduction of Fracture Toughness

Age-related degradation mechanisms that may lead to a reduction of fracture toughness of the PWR internals materials include thermal aging embrittlement (TE), irradiation embrittlement (IE), and void swelling (VS). A consequence of reduced fracture toughness is a reduction in a materials critical crack size. Aging management of items with reduced fracture toughness need to rely upon observations of flaw length and the magnitude of stress/loading. Of particular concern would be a case of VS exceeding approximately 10% where the material would be exceptionally brittle after the reactor has cooled down and the material temperature is below about 392°F

(200°C). The currently identified potential materials and age-related degradation mechanisms of concern for reduction of fracture toughness are addressed separately as follows:

- TE (Table 2-4)

Only CASS, austenitic SS welds, martensitic SS, and martensitic PH SS materials are potentially susceptible to TE.

- CASS

Criteria for CASS materials are based on the type of casting (centrifugal vs. static), ferrite content, and molybdenum content (for static castings only). Some CASS locations will be screened in for further evaluation of a potential synergistic effect of flux or fluence on TE proposed by the NRC based on the irradiation embrittlement screening criteria (Table 2-5).

- Austenitic SS welds

Criteria for austenitic SS welds are based on static CASS castings, due to similarity in composition, and ferrite and molybdenum contents. Due to the range of procurement specification ferrite contents (5-15 %) in the American Society of Mechanical Engineers (ASME) Boiler and Pressure Vessel (B&PV) Code, austenitic stainless steel welds will generally not be screened in as susceptible to thermal aging embrittlement. However, some austenitic SS weld locations will be screened in for further evaluation of a potential synergistic effect of flux or fluence on TE proposed by the NRC based on the irradiation embrittlement screening criteria (Table 2-5).

- Martensitic SS and martensitic PH SS

All martensitic SS and martensitic PH SS component items are considered potentially susceptible to TE.

Table 2-4
Thermal Aging Embrittlement Screening Criteria for PWR Internals Materials

- IE (Table 2-5)

IE is only relevant to materials that are used in relatively high fluence locations (e.g., austenitic SS, austenitic SS welds, and CASS). If other materials are used in a location that exceeds the austenitic stainless steel criterion, they also are considered potentially susceptible to IE.

- Austenitic SS

Component items that achieve dose levels ≥ 1.5 dpa (1.0×10^{21} n/cm², $E > 1.0$ MeV) will be screened in for potential concern with IE.

- Austenitic SS welds and CASS

Component items that achieve dose levels ≥ 1 dpa (6.7×10^{20} n/cm², $E > 1.0$ MeV) will be screened in for potential concern with IE. This lower value accounts for the large initial variability in fracture toughness for these materials and potential synergistic effects with thermal aging embrittlement.

Table 2-5
Irradiation Embrittlement Screening Criteria for PWR Internals Materials

- VS (Table 2-6)

Only austenitic SS and austenitic SS welds are typically used in locations where the combined screening criteria for dose and temperature will be exceeded. If other materials are used in locations that exceed the criteria, they also are potentially susceptible to VS.

- Austenitic SS and welds

Component items that achieve temperatures $\geq 608^{\circ}\text{F}$ (320°C) and ≥ 20 dpa (1.3×10^{22} n/cm², $E > 1.0$ MeV) will be screened in for potential concern with VS. Follow-on functionality evaluations may be needed.

Table 2-6
Void Swelling Screening Criteria for PWR Internals Materials

2.3 Loss of Mechanical Closure Integrity

Loss of mechanical closure integrity may result from stress relaxation / irradiation creep (SR/IC) of those component items (i.e., bolting or springs) where maintaining a preload is important to the structural integrity function of the PWR internals. Neutron fluence, temperature and the degree of preloading are the key parameters. Thus the identified potential materials and age-related degradation mechanisms of concern for loss of mechanical closure integrity are:

- SR/IC (Table 2-7)
 - All applicable alloys used for bolts or springs

Thermal SR is a concern with all bolts or springs, particularly those that require maintaining a preload for functionality. Irradiation-enhanced SR/IC is a concern with all bolted or spring locations that achieve dose levels ≥ 0.2 dpa (1.3×10^{20} n/cm², E > 1.0 MeV).

Table 2-7
Thermal and Irradiation-Enhanced Stress Relaxation and Creep Screening Criteria for PWR Internals Materials

2.4 Loss of Material

The only known aging degradation mechanism that results in significant loss of material is wear due to mechanical abrasion in circumstances where items are physically in contact and able to move in relation to each other, either by design or due to flow-induced vibration or loss of preload. Plant operating conditions usually determine the severity of wear. Loss of material due to wear is not considered a potential aging effect for bolted items provided the bolts continue to maintain sufficient preload, as discussed in Appendix C, or do not sever as a result of cracking. Therefore, the identified potential materials and age-related degradation mechanism of concern for loss of material is:

- Wear (Table 2-8)
 - All applicable alloys

Wear is influenced by a number of parameters and no clear screening values exist. Screening is performed by evaluating locations where relative motion may occur, where clamping force is required, and with bolted or spring locations where SR/IC is screened as applicable.

Table 2-8
Wear Screening Criteria for PWR Internals Materials

2.5 Changes in Dimension

Changes in dimension due to VS could lead to loss of component function if the required clearances of the PWR internals items cannot be maintained for: 1) the orientation, guidance, and protection of the control element assemblies, 2) distribution of the reactor coolant flow to the reactor core, or 3) support, guidance, and protection of the in-vessel core instrumentation. Differential VS could also introduce stresses in bolted joints that could lead to other complications such as IASCC. If VS does occur in the PWR internals, it is most likely to be a localized phenomenon in regions of peak temperature and neutron fluence. If sufficient amounts of VS were to occur during the period of extended operation, the dimensional changes would need to be managed. The currently identified potential materials and age-related degradation mechanism of concern for change in dimension are as follows:

- VS (Table 2-6)

Only austenitic SS and austenitic SS welds are typically used in locations where the combined screening criteria for dose and temperature will be exceeded. If other materials are used in locations that exceed the criteria, they also are potentially susceptible to VS.

- Austenitic SS and austenitic SS welds

Component items that achieve temperatures $\geq 608^{\circ}\text{F}$ (320°C) and ≥ 20 dpa (1.3×10^{22} n/cm², $E > 1.0$ MeV) will be screened in for potential concern with VS.

2.6 References

- 2-1 Materials Reliability Program: Framework and Strategies for Managing Aging Effects in PWR Reactor Vessel Internals (MRP-134), EPRI 1008203, 2005.
- 2-2 Generic Aging Lessons Learned (GALL) Report, NUREG-1801, Rev. 1, Vol. 1, U.S. Nuclear Regulatory Commission, September 2005.

3

COMPILING SCREENING PARAMETERS AND SAMPLE TEMPLATE

3.1 Screening and Categorization for Significance

A key aspect of the aging management strategy using periodic inspections is to identify the PWR internals component items of greatest significance due to the effects of age-related degradation. For the screening and categorization for significance, aging susceptibility factors are examined to identify those conditions that could contribute to the effects listed in Chapter 2: (1) cracking, (2) reduction of fracture toughness, (3) loss of mechanical closure integrity, (4) loss of material, and (5) changes in dimension.

A prioritization of the significance of age-related degradation in PWR internals was provided in MRP-134^[3-1] for the screening process such that the significance is a combination of the susceptibility to aging and potential for loss of function because of materials degradation. This process is exemplified by the equation below.

$$\text{Significance} \cong \left[\begin{array}{c} \text{Potential for Aging Based} \\ \text{on Susceptibility Factors} \end{array} \right] \times \left[\begin{array}{c} \text{Potential for Loss of Function} \\ \text{With Materials Degradation} \end{array} \right]$$

Susceptibility Factors

* Fluence

* Stress

* Temperature

* Material

Functionality Assessment

Results

As described in MRP-134, component items are to be placed into four categories: (1) **Category A**, (2) **Category B**, (3) **Category B'**, or (4) **Category C**. A component item is designated as **Category A** if it can be shown to initially be below a screening limit for susceptibility or if the age-related degradation has been shown to be insignificant through a functionality assessment. A component item may be designated as **Category B** or **Category B'** if a functionality assessment shows the component to be flaw tolerant with no loss of function. The remaining component items with high significance are designated as **Category C**.

3.2 Screening Parameters for Age-Related Degradation

This section provides a listing of screening parameters for determining the potential significance of age-related degradation effects on PWR internals component items. The use of a screening matrix to screen out component items for which age-related degradation effects are not significant was first proposed in the PWR License Renewal Industry Report for Vessel Internals.^[3-2] More recently, as the result of experience gained during the license renewal application review process, screening of component items for potential significance of aging effects is the accepted methodology given in the Generic Aging Lessons Learned (GALL) report.^[3-3]

Based on the criteria established in the Appendices and Chapter 2, the following parameters should be compiled prior to performing the screening and categorization of PWR internals (as detailed in MRP-134):

- Material
- Dose (Neutron Exposure)
- Cold-Work
- Multi-Pass Welds
- Ferrite Content (where applicable, including Molybdenum Content for CASS Static Castings)
- Applied Stress (Operating and Residual)
- Operating Temperature (including Gamma Heating)
- Tempering Temperature (where applicable)
- Wear Potential
- Fatigue Usage Factor

Table 3-1 provides an example of a screening template with the parameters listed for determining the potential significance of age-related degradation effects on PWR internals component items. A discussion of each of these is provided in the sections below.

3.2.1 Material

The materials of construction for PWR internals have recently been summarized by an MTAG Ad-Hoc Committee, consisting of vendor and utility representatives.^[3-4] This effort generically provides a summary of PWR internals component items and materials for initial screening and categorization. In some instances, plant-specific variations or material alternatives will exist; if the information is readily available, it should be included.

Table 3-1
Example Tabulation of Screening Parameters

The suggested information to be compiled for each component item follows:

- **Material System**

The materials used in PWR internals (as provided in Chapter 1) include: Austenitic stainless steels, CASS, austenitic stainless steel welds, martensitic stainless steels, martensitic PH stainless steels, austenitic nickel-base alloys, austenitic PH nickel-base alloys, and cobalt-base alloys.

- **Material Specification**

Specifications used in PWR internals include: ASTM, ASME, AMS, Mil-spec., etc.

- **Type, Grade, or Class**

The various alloys used in PWR internals include examples such as: Type 304, Grade B8, Type 17-4PH, Class RCoCr-A (Stellite #6), etc.

- **Product Form**

The product forms used in PWR internals include: Bars, plates, forgings, etc.

3.2.2 Dose (Neutron Exposure)

Accumulated dose (neutron exposure) for PWR internals component items will be compiled. Component items well removed from the core, where it is known that the accumulated dose will be below the screening criteria, should be noted as such. The range of estimated fluence values (resulting from best estimate fluence calculations) for each component item (through thickness or along the length) should be summarized. The peak surface fluence value, and the fluence value at the peak surface temperature and peak through thickness temperature locations for each of these component items will eventually be identified. It is understood that dose rate varies both within an operating cycle due to fuel burn-up and from cycle-to-cycle according to core design and power generation requirements. Initial screening should be performed on the best available values. Should additional calculations be needed to refine the dose estimates, these should be performed during the follow-on functionality evaluation efforts. Dose estimates calculated for 32 EFPYs (effective full power years), representing 40 calendar years of operation, should be linearly extrapolated to 60 calendar years of operation.

Dose should be provided in units of n/cm^2 ($E > 1.0 \text{ MeV}$) and/or dpa, as the screening criteria are expressed in both of these units. (Note that 10^{22} n/cm^2 , $E > 1.0 \text{ MeV}$ is approximately equivalent to 15 dpa for a PWR internals neutron spectrum.) Dose, in units of n/cm^2 ($E > 0.1 \text{ MeV}$), may also be needed for future functionality evaluations as lower energy levels are more relevant for some age-related degradation mechanisms.

3.2.3 Cold-Work

Manufacturing records and practices, to the extent that these are recoverable, should be reviewed to determine locations that may have been cold-worked during fabrication. Alternatively, this information may be available through expert knowledge. Cold-work (giving rise to an elevation of material yield strength) results from a number of things, including procurement in the cold-worked condition (e.g., cold-worked bolting), intentional grinding or bending during fabrication, and shrinkage strains associated with welded component items. The screening criterion applies to anything that creates the equivalent of $\geq 20\%$ cold-work in an austenitic stainless steel component item or weld. For austenitic PH stainless steel (Alloy A-286) material, hot-heading of bolts, which can create a HAZ between the head and shank, is another known adverse factor. Shot-peened bolts that are preloaded to high stress levels, where a stress reversal of the compressively stresses layer might occur, are also of concern. Component items that fall into these categories should be regarded as having potentially high residual tensile stresses for the screening process.

3.2.4 Multi-Pass Welds

Manufacturing records and drawings should be reviewed to determine locations where welding would have been performed. Multi-pass full-penetration, partial-penetration, or fillet joint weld type locations are of a similar concern (as high cold-work noted in the previous section) due to potentially high weld shrinkage strains in the HAZ. Small weld joint types such as tack or plug welds are excluded. Weld shrinkage deformation and the resultant increase in yield strength due to strain hardening, increase the residual stress that together with operational stresses could potentially provide a driving force for crack initiation and growth. Therefore, all HAZs of welded component items where high weld shrinkage strains are plausible should be compiled.

3.2.5 Ferrite and Molybdenum Content

The ferrite content of cast austenitic stainless steels and austenitic stainless steel welds is an important parameter for screening of thermal aging embrittlement and perhaps stress corrosion cracking. Ferrite contents (volume percentage) should be estimated based on known chemical compositions, specifications, or taken from fabrication records where measured prior to service. For example, ferrite contents required in ASME B&PV Code specifications for austenitic stainless steel weld materials range from 5 to 15% and for cast austenitic stainless steels 15 to 25%.

For static castings, molybdenum content is also an important screening parameter that should be tabulated. This, however, can only be found on component item-specific certified material test reports (CMTRs). The recovery process for these records may hinder this tabulation. If this information is not readily available for a particular component item and the remaining screening criteria for the material is met, that component item should be screened in as potentially susceptible to aging degradation.

3.2.6 Applied Stress

Applied stresses (normal operating and residual) acting on PWR internals component items are typically very low; however some instances of high applied stresses do exist and must be accounted for in the screening evaluation.

The total applied stresses of concern are tensile, and they will normally approach the yield strength of the component item to be of concern. The total applied stress must not only consider operating stresses, but residual stresses as well. Therefore, anytime a component item is cold-worked (e.g., bent or straightened), the residual stress may, by definition, approach or exceed the yield strength of the non-deformed material. Residual stress (in the heat-affected zone of a weld from weld shrinkage, or from grinding, for example) must also be considered. In the case of bolts, the area between the bolt head and shank represents a particular concern because the stress concentration, which depends on the radius in this area, multiplies the local stress by several times, resulting in a stress that may be well above the original as-recorded tensile yield strength.

Since operating stress values are most likely not calculated for every component item in the PWR internals, engineering judgment and assumptions must be made from available stress reports and fabrication knowledge. It is important that highly stressed component items be screened in for further evaluation. Therefore, many component items can simply be compiled with operational stresses listed as significantly below the criteria being evaluated (e.g., < 5 ksi, < 20 ksi, etc.) or simply less than the screening criterion. Residual stress should be indicated as “yes” or “no” depending upon whether or not it has been welded, intentionally cold-worked beyond the 20% criterion by being bent or ground, etc. during fabrication. For other locations, such as bolts, both the peak stress due to the stress concentration factor and nominal shank stress should be calculated or estimated and compiled.

3.2.7 Operating Temperature

Operating temperatures for the PWR internals component items need to be compiled. The range of temperatures (resulting from best estimate, steady state calculations) for each component item (through-thickness or along the length) should be summarized. Best estimate gamma heating calculations, where applicable, should also be included with the operating temperature. It is understood that temperature varies both within an operating fuel cycle and from cycle-to-cycle, because gamma heating rates vary. Initial screening should be performed using best available values. Should additional calculations be needed to refine the temperature estimates, this can be performed during the follow-on functionality evaluation efforts.

3.2.8 Tempering Temperature

Knowledge of the tempering temperature is important for SCC screening of martensitic and martensitic PH stainless steels. If this information is unavailable at this time, and the applied stress meets the screening criterion, the component item should be screened in as potentially susceptible to SCC.

3.2.9 Wear Potential

The parameters used in the criteria for wear are simply to identify three locations: 1) where relative motion may occur between component items (e.g., control rod guide tubes), 2) where clamping force is required for functionality (e.g., mating ledge between the internals and the RV), and 3) bolts or springs where SR/IC is applicable (e.g., baffle-to-former bolts). Thus, the wear index should be compiled as yes or no, depending on the above criteria.

3.2.10 Fatigue Usage Factor

Fatigue usage is typically evaluated by calculating a cumulative usage factor (CUF) for 40 years of operation. The fatigue screening criterion utilizes this CUF value, which should be compiled. Calculated CUF values will not be available for many locations, and engineering judgment and assumptions must be made regarding an estimated CUF. Other locations may have been qualified to 40 years of service by testing. In cases where a CUF or a reasonable estimate is unavailable, it is suggested that the component item be initially screened in as potentially susceptible to fatigue and evaluated further.

3.3 Initial Screening Process

The initial screening process, shown near the top of Figure 1-5, consists of using the screening criteria to either “screen in” or “screen out” component items and age-related degradation mechanisms. A simplified summary of the screening criteria developed in the Appendices and tabulated in Chapter 2 is provided as Table 3-2 as a quick reference of the age-related degradation mechanism screening criteria. Using Table 3-2, the initial screening process is to be performed as follows:

- A component item/degradation mechanism is “screened in” when the compiled parameter(s) meet or exceed the screening criteria for the age-related degradation mechanism and component item material being evaluated.
- A component item/degradation mechanism is “screened out” when the compiled parameters(s) do not meet the screening criteria for the age-related degradation mechanism and component item material being evaluated.

Example component items where the age-related degradation mechanism screening criteria are met or exceeded, therefore being “screened in,” are highlighted in Table 3-1. Using the parameters in Table 3-1 and the screening criteria summarized in Table 3-2, a compilation of component items and potential age-related degradation mechanisms can be prepared (e.g., in a tabular form using an Excel spreadsheet). Table 3-3 is an example using the listed example component items in Table 3-1. The “yes” signifies that a particular age-related degradation mechanism has been “screened in” and a “no” signifies that a degradation mechanism has been “screened out.” This process is performed for each component item in the PWR internals design being evaluated.

Table 3-2
PWR Internals Age-Related Degradation Mechanism Screening Criteria

3.4 References

- 3-1 “PWR Reactor Pressure Vessel Internals License Renewal Industry Report; Revision 1,” EPRI TR-103838s, 1994.
- 3-2 Generic Aging Lessons Learned (GALL) Report, NUREG-1801, Rev. 1, Vol. 1, U.S. Nuclear Regulatory Commission, September 2005.
- 3-3 Materials Reliability Program: Framework and Strategies for Managing Aging Effects in PWR Reactor Vessel Internals (MRP-134), EPRI 1008203, 2005.
- 3-4 Pressurized Water Reactor Issue Management Table, PWR-IMT Consequence of Failure (MRP-156), EPRI 1012110, 2005.

A

APPENDIX A: STRESS CORROSION CRACKING (EXCLUDING IRRADIATION EFFECTS)

A.1 General Description of Stress Corrosion Cracking

As shown in Figure A-1, stress corrosion cracking (SCC) occurs when the following synergistic conditions are present: 1) a tensile stress (both applied and/or residual stresses), 2) a corrosive environment, and 3) a susceptible material. SCC will not occur if any one of these three factors is out of the range of susceptibility. SCC can occur either as intergranular stress corrosion cracking (IGSCC) or as transgranular stress corrosion cracking (TGSCC), depending upon the environment/material combination (Figure A-2). (Note: irradiation as it affects SCC, known as irradiation-assisted SCC, is discussed separately in Appendix B.) Low temperature crack propagation (LTCP) refers to the propagation of intergranular stress corrosion cracking at low temperatures (~ 130-170°F) due probably to the embrittlement by hydrogen of the grain boundaries ahead of an advancing crack; however, no information currently exists in the open literature describing such an effect in alloy systems other than for nickel-base materials.

PWR internals items that have exhibited IGSCC are highly-stressed Alloy A-286 fasteners and Alloy X-750 support pins. The Alloy X-750 IGSCC failures though are generally described as primary water stress corrosion cracking (PWSCC), which is a term traditionally used for IGSCC of nickel-base materials in PWR primary coolant systems.

IGSCC is characterized by cracks propagating along the grain boundaries of the material. An example of IGSCC is shown in Figure A-3. It is often not clear why an intergranular path is preferred over a transgranular one. One clear example of IGSCC is associated with sensitized stainless steel in oxygenated water. In this case, preferential grain boundary precipitation of carbides in austenitic stainless steels and nickel-base alloys leads to a localized depletion of chromium in the vicinity of the grain boundary, which oxidizes (or corrodes) more quickly than the grains. Sensitization is generally caused by slow cooling from elevated temperatures. (Typically, the elevated temperature is from welding or other processing.)

Grain boundary segregation of impurities such as phosphorus, sulfur, and silicon is another metallurgical phenomenon that promotes IGSCC. In many other material-environment conditions, the reason for IGSCC is unclear. Alloy X-750 is a classical example.

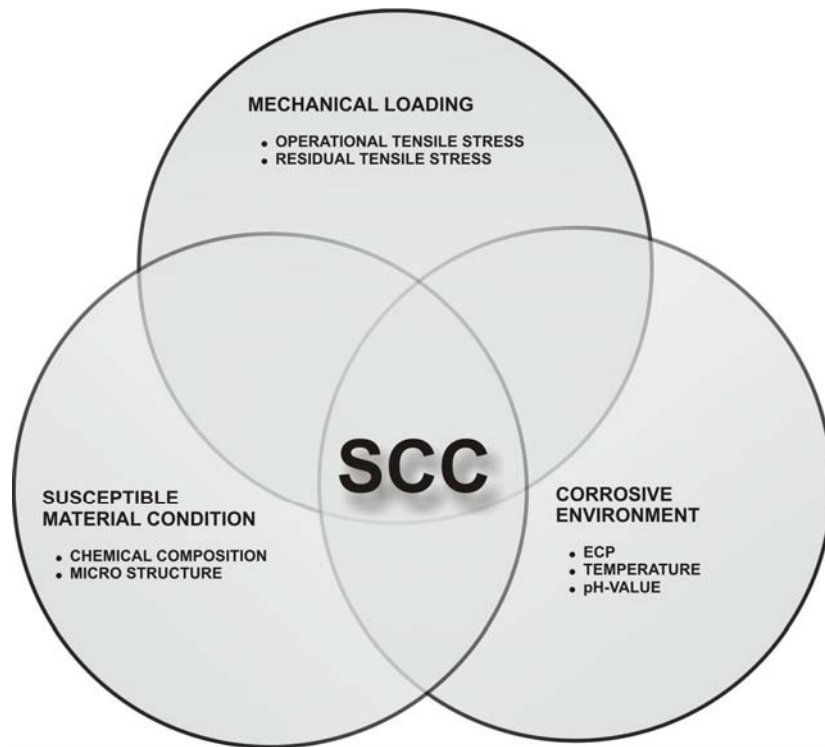


Figure A-1
Synergistic Effects Required for Stress Corrosion in Metals

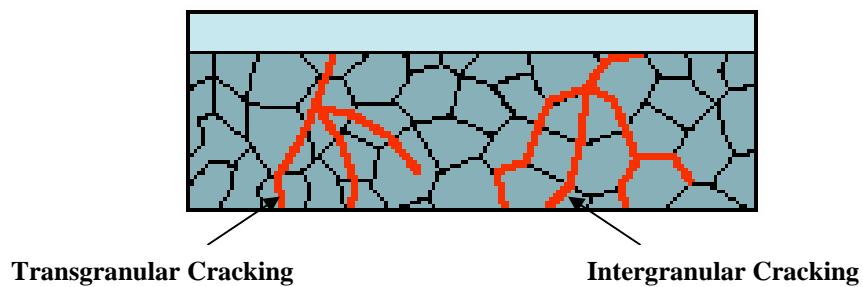


Figure A-2
Crack Paths Describing Stress Corrosion Cracking in Metals



Figure A-3
Example of Intergranular Stress Corrosion Cracking

TGSCC is characterized by cracks that propagate through (or across) the grains of the material. Numerous metallurgical factors, such as crystal structure, grain size and shape, dislocation density and geometry, and phase composition, affect TGSCC. A notable example is austenitic stainless steels exposed to chlorides and oxygenated environments. However, TGSCC has been reported as occurring in sensitized material in the total absence of chlorides and low oxygen environments at temperatures above about 120°C (248°F).^[A-1] Figure A-4 shows a typical example of TGSCC.

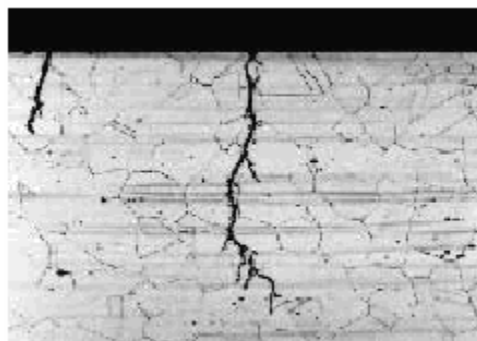


Figure A-4
Example of Transgranular Stress Corrosion Cracking

Despite years of research and testing, many mechanisms of SCC are not well understood. This is mainly due to the complex interplay of the metal, interface, and environmental properties. As a result, different combinations of aqueous environments and stresses are seldom comparable

and the most reliable information is usually obtained from empirical experiments. One of the results of improvements in experimental data quality and sensitivity is the conclusion that SCC immunity and thresholds probably only rarely exist, if at all. Threshold values for various alloys and environments that were once widely accepted have almost all been discredited in recent years.

The following subsections provide a summary of available information on SCC conditions for each of the alloys listed in Table 1-1. However, a separate section on cobalt--base alloys is not provided since these materials are not known to be susceptible to SCC in applications in PWR internals.

A.1.1 Austenitic Stainless Steels

Austenitic stainless steels are generally susceptible to SCC in elevated temperature environments where impurities such as halogens (e.g., chlorides and fluorides) and/or dissolved oxygen are significant (see below). As noted above, it is well known that sensitized austenitic stainless steels are very susceptible to IGSCC in various levels of chloride and oxygen environments, or in thiosulfate environments. Copious literature papers and reviews exist on the effects of these environmental impurities, some of which are referenced herein.^[A-2 – A-7]

The review performed by Williams in 1957 may be viewed as one of the earliest definitive descriptions of the conditions necessary for TGSCC.^[A-8] The author performed this work in support of the Navy's use of austenitic stainless steels in heat transfer equipment. He noted that IGSCC can be controlled by the use of low carbon versions of stainless steels and careful control of its heat treatment to avoid sensitization.

In 1980, the Materials Technology Institute of the Chemical Process Industries issued a manual summarizing the combined effects of oxygen and chloride content on SCC of austenitic stainless steels at high temperatures. Figure A-5 shows the results from this effort.^[A-1]

Gordon's 1980 literature review not only included Williams' efforts, but also collected and evaluated all "chloride-oxygen stress corrosion cracking mechanisms of austenitic chromium-nickel steels in high purity water at 482°F (250°C) to 662°F (350°C)."^[A-9] Gordon concluded that the oxygen content is the critical parameter for SCC in high temperature water. He further noted that chloride SCC of austenitic stainless steels will propagate transgranularly unless the material is sensitized. In the latter case, the cracking will be either intergranular or mixed mode. (The experience in boiling water reactor (BWR) piping systems indicates overwhelmingly that cracking has been predominantly intergranular occurring in weld heat-affected zones.)

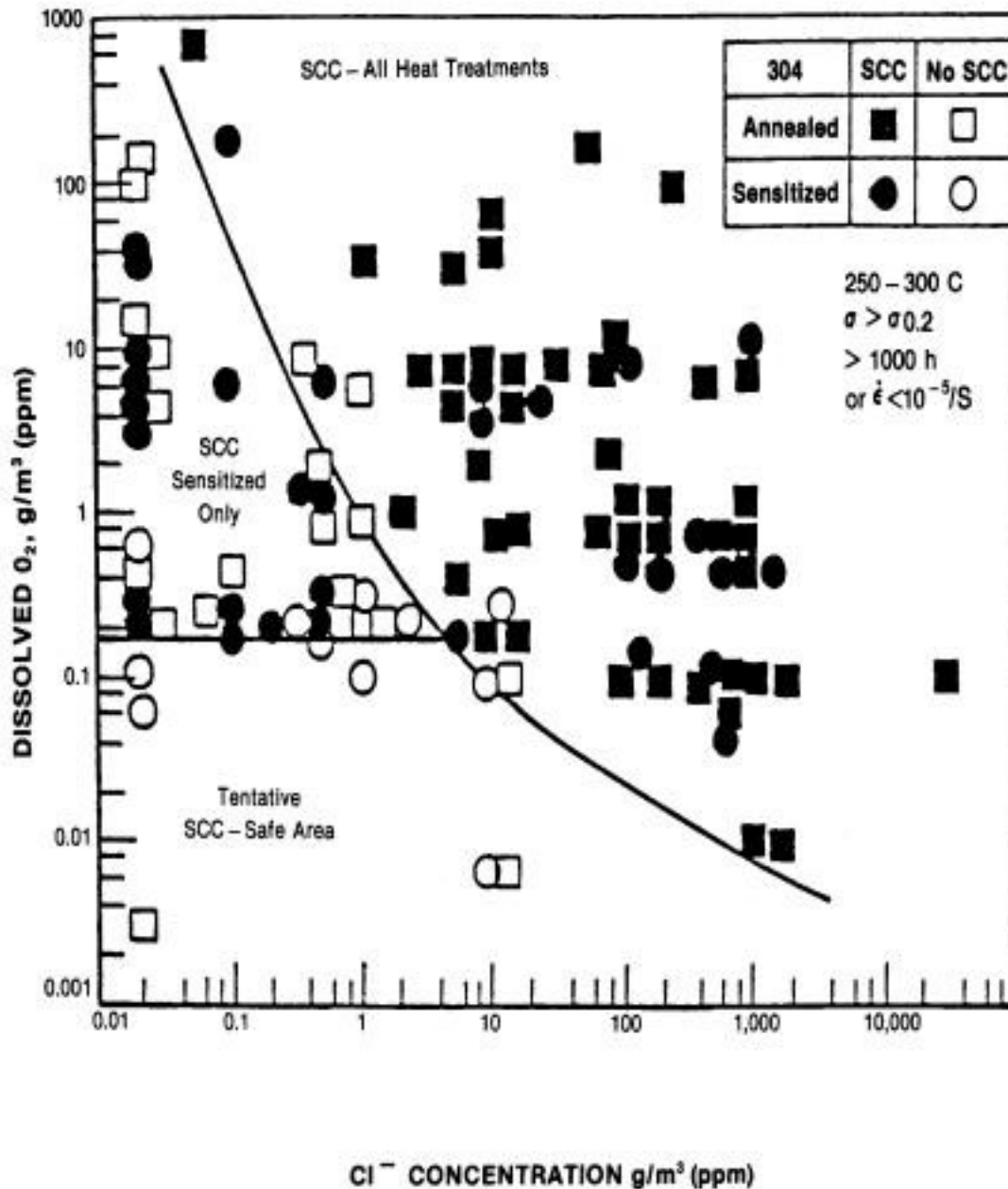


Figure A-5
Effect of Oxygen on Chloride SCC^[A-1]

Gordon's relationship, Figure A-6, was reproduced and used by the original authors of the EPRI primary water guidelines^[A-10] to illustrate that normal PWR water chemistry conditions (dissolved oxygen and chloride levels) are well below any known IGSCC or TGSCC concerns. However, more recent data indicate that sensitized austenitic stainless steel material may be susceptible to TGSCC at high temperatures in low oxygen environments (Figure A-7).^[A-1] While current EPRI PWR water chemistry guidelines^[A-11] continue to limit dissolved impurities (chlorides, fluorides, sulfates, and oxygen) to very low levels, and IGSCC has not been observed in a significant database of test environments using such levels, some concern,

albeit apparently with very low probability, still exists with the long-term potential for IGSCC or TGSCC of austenitic stainless steels in PWR internals. This is particularly true if the cold-working exceeds the current ASME B&PV Code limits (see below).

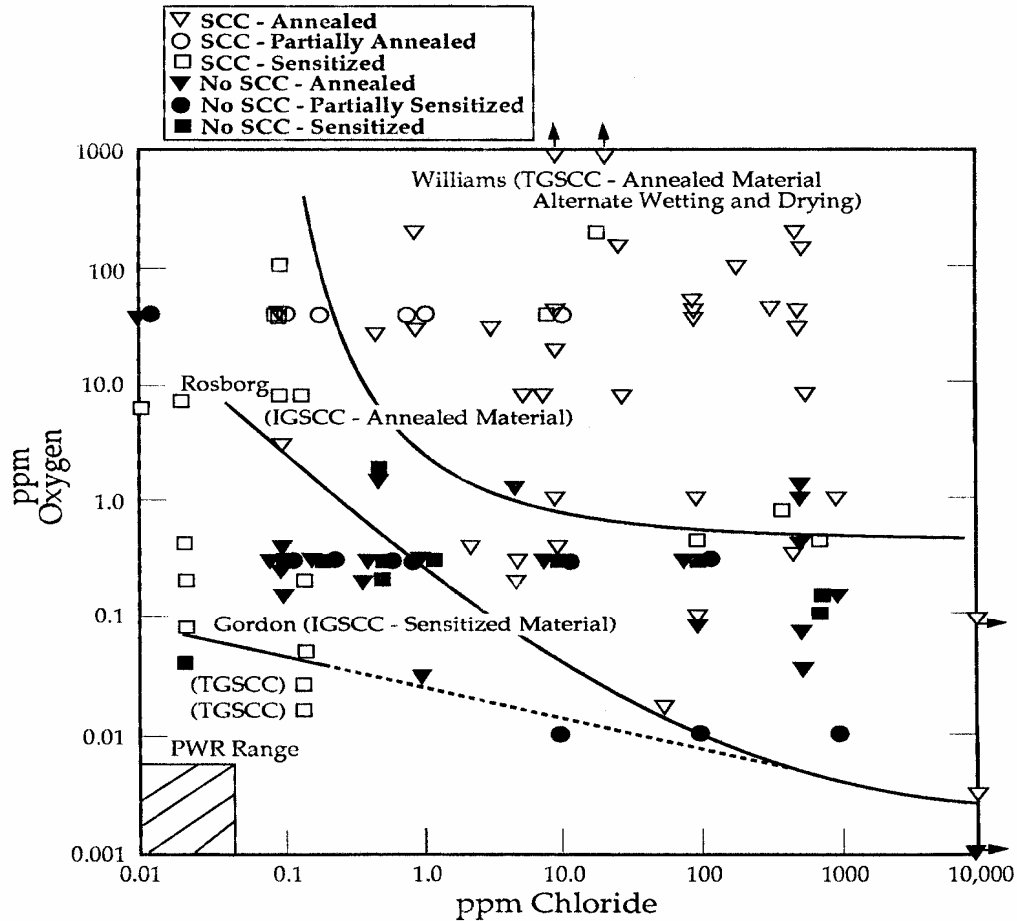


Figure A-6
The Effects of Oxygen and Chloride on the SCC of 300 Series Stainless Steels in High Temperature Water as Revealed by Slow Strain Rate Testing^[A-10]

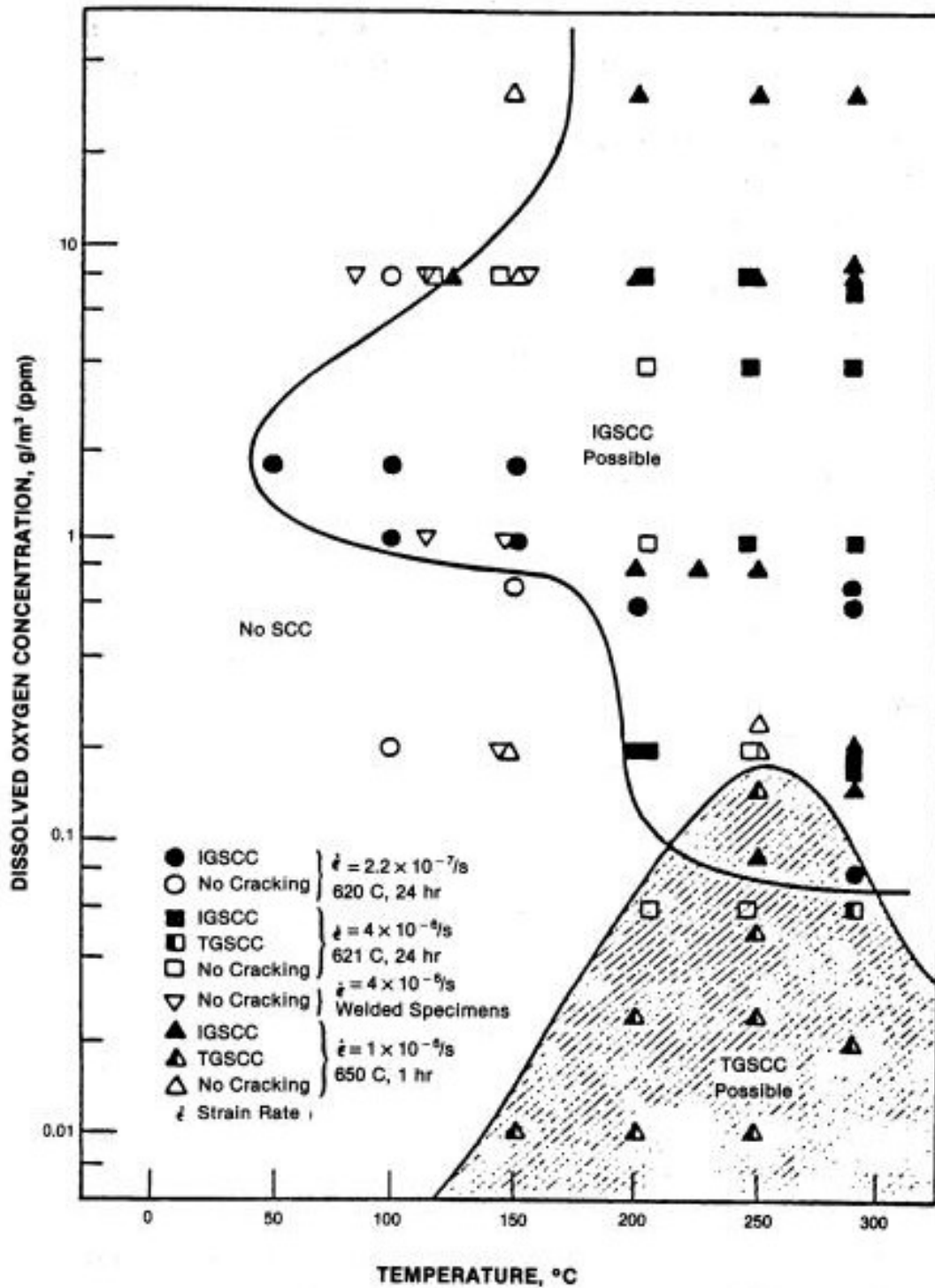


Figure A-7
Cracking of Sensitized 304 Stainless Steel in Water Without Chlorides^[A-1]

The stress needed to promote SCC is more subtle. The total applied stresses of concern are tensile, and must approach the proportional limit of the material to be of concern. The total

applied stress must not only consider operating stresses, but residual stresses as well. Therefore, whenever a component item is cold-worked (e.g., bent or straightened), the residual stress may, by definition, approach or exceed the yield strength of the non-deformed material. Residual stress (in the heat-affected zone of a weld, weld shrinkage, or from grinding, for example) must also be considered. Elevation in yield strength has been shown to have a strong adverse effect on SCC resistance and growth rates in all water chemistries.^[A-12] Another complicating factor for consideration is the presence of a pit or other sharp notches. This multiplies the residual stress by several times, resulting in a local stress potentially far in excess of the originally specified tensile yield strength.

Very limited testing of low and medium (< approximately 20%) cold-worked austenitic SS in environments simulating PWR reactor coolant has been reported in the open literature. The limited data^[A-13] indicate that low and medium cold-worked SS is satisfactory for PWR internals service, but detailed data on long-term testing are not available. Data on highly (approximately 20%) cold-worked material from another EPRI program^[A-14] indicate that IGSCC or TGSCC may be possible for such highly cold-worked material in PWR internals environments (Figure A-8). Although the ASME B&PV Code prohibits the intentional use of > 20% cold-worked materials, there still exists much controversy in the industry regarding the SCC potential of highly cold-worked materials in PWR environments. Recent work shows that cracking of these cold-worked materials in the absence of oxygen in acceptable purity water is observed either in CERT or crack growth experiments, never at constant load.^[A-15 – A-19] Furthermore, one of these papers by Tice, et al., showed that crack growth of semi-elliptical cracks occurred on the surface at about the same rates as observed in compact tension (CT) specimens but almost no growth occurred in the depth direction. This suggests that there is a problem with lack of constraint in laboratory testing that probably leads to unintentional dynamic loading that has little relevance to component items in service.

Multi-pass full-penetration, partial-penetration, or fillet joint weld type locations are of a similar concern (as high cold-work noted in the previous section) due to potentially high weld shrinkage strains in the HAZ. Small weld joint types such as tack or plug welds are excluded. During welding, the magnitude of the residual stress or strain is mainly dominated by the cooling rate after welding, the heat input during each pass and the order for multi-pass welding layers, the binding force of the welded joint, etc. The cooling rate after welding is dominated by the heat input, inter-pass temperature, and the temperature, thickness and thermal conductivity of the base material. The heat input during each welding pass is determined by the electric current, voltage, and torch travel speed. The binding force of the welding joint is affected by the thickness and groove shape of the base metal. In addition, the residual stress of the weld metal can be significantly affected by subsequent repair welding of the joint, if required to be carried out. Weld shrinkage deformation and the resultant increase in yield strength due to strain hardening, increase the residual stress that together with operational stresses could potentially provide a driving force for IGSCC or TGSCC crack initiation and growth.

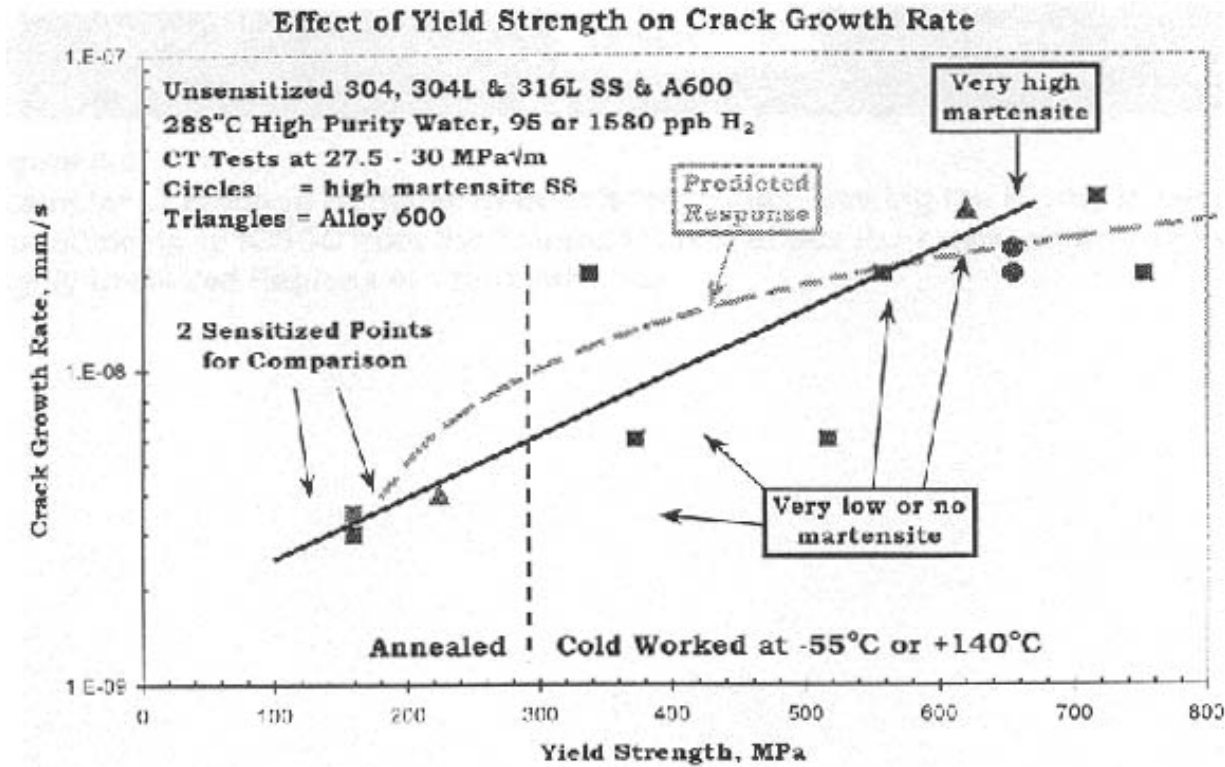


Figure A-8
Effect of Yield Strength and Martensite on the Stress Corrosion Crack Growth Rate on Austenitic Stainless Steel in a Simulated PWR Environment^[A-14]

Also, in 1973, Regulatory Guide 1.44^[A-20] was issued to describe acceptable methods of controlling processing of austenitic stainless steels to avoid sensitization. The position in this Regulatory Guide is that austenitic stainless steels (excluding low-carbon or stabilized grades) subjected to sensitizing temperatures (800 to 1500°F [427 to 816°C]) during fabrication could result in SCC. Many PWR internals were fabricated prior to issuance of this Regulatory Guide and therefore may have been subjected to such sensitizing temperatures.

Therefore, although no SCC has been observed to date in PWR internals fabricated with austenitic stainless steel, a remote potential exists for IGSCC or TGSCC of PWR internals component items fabricated with austenitic stainless steels that may have been severely cold-worked (e.g., $\geq 20\%$) as a result of localized deformation (from bending or grinding) or high shrinkage strains in HAZs from welding that are highly stressed (levels greater than the room temperature material yield strength).

A.1.2 Martensitic Stainless Steels

Martensitic stainless steels contain enough chromium ($> 11\%$) to be corrosion resistant and also have chemical compositions that make them hardenable by a martensitic transformation. The most common type of martensitic stainless steels used in PWR internals contains about 12% chromium and about 0.1% carbon, and are identified as Type 403 or Type 410 stainless

steel. Type 431 stainless steel, also used in PWR internals, contains slightly higher chromium and some nickel to improve the corrosion resistance and toughness.

Martensitic stainless steels are widely used in Light Water Reactors (LWRs), in applications such as turbine blades, bolting, valve stems and hardware, and pump shafts and hardware. These alloys have performed satisfactorily in many of these applications. However, there have been some failures, often related to use of material with improper heat treatment for the application involved. The most common problem has been use of material with too low a tempering temperature, with a resultant high hardness and relatively high susceptibility to SCC. Another related problem has been temper embrittlement. This occurs due to tempering in, or slow cooling through, the temperature range of about 750 - 1020°F (399-549°C), which results in embrittlement and poor corrosion resistance. The exact cause(s) of the embrittlement are not clear, and may involve precipitation of second phases or ordered phases.^[A-21] Other sequences of improper thermo-mechanical processing or heat treatment also apparently can result in material meeting specified mechanical properties but nevertheless having poor corrosion resistance and/or low ductility.

The SCC susceptibility of martensitic stainless steels (mainly Type 410) has been extensively studied in various temper conditions.^[A-22 – A-24] Samples tempered between 1125°F (607°C) and 1350°F (732°C) for four hours minimum with subsequent hardness levels of HRC \leq 26 show resistance to SCC after exposure to elevated temperatures in high purity water. Thermal aging embrittlement (Appendix E) however, is also capable of decreasing the resistance of martensitic stainless steel alloys to SCC.

A.1.3 Martensitic Precipitation-Hardenable Stainless Steels

Type 17-4 PH materials have experienced SCC in BWRs where there is a higher oxygenated environment in the coolant than in PWRs. Applications in valves (bolts and stems) have also failed in PWRs. In a number of instances, failed Type 410 valve parts were replaced with Type 17-4 PH material.^[A-25] Thermal aging embrittlement (Appendix E) however, is also capable of decreasing the resistance of precipitation-hardenable alloys to SCC.^[A-13, A-26, A-27]

Studies have shown that if Type 17-4 PH is aged (tempered) to the H1100 condition, it will be very resistant to SCC at high levels of applied stress.^[A-28 – A-33]

Type 15-5 PH is a delta-ferrite-free compositional modification of Alloy 17-4 PH, containing less chromium and slightly higher nickel. No known data have been identified in the open literature on SCC resistance of Type 15-5 PH material in PWR environments. However, the corrosion resistance of Type 17-4 PH material is comparable and therefore the SCC resistance would be expected comparable too.

A.1.4 Austenitic Precipitation-Hardenable Stainless Steels and Nickel-Base Alloys

In 1983, McIlree^[A-34] reviewed the experience in LWRs with Alloys X-750, 718, and A-286. He identified a number of failures with these materials, and concluded that each is susceptible to IGSCC when fabricated with certain heat treatments and loaded to high operational stresses. He also concluded that with proper heat treatment and control of the overall stress on the component item, these materials will show improved IGSCC resistance. Since then, a number of SCC test programs have been carried out with these materials.^[A-35 – A-37]

The most notable PWR internals component items to have experienced degradation are thermal shield bolts and split pins. The thermal shield bolts were fabricated from Alloy A-286 material and the split pins were fabricated from Alloy X-750 material. Both have experienced degradation due to IGSCC in the high-stressed regions.

Laboratory tests have shown that Alloy A-286 materials, when processed by cold-working prior to heat treatment (cold reduction of 40-50%) or by hot heading during bolt fabrication, are more susceptible to IGSCC.^[A-38, A-39] The most recent testing performed for the industry, which includes both in-reactor and autoclave test data, show that peak stress levels below 70-80% of room temperature yield strength perform well in PWR environments. Figure A-9 shows an empirical lower bound line drawn that approximates the threshold between cracking and acceptable performance.^[A-39, A-40]

Figure A-9
Failure Trend Line for Alloy A-286 SCC^[A-39]

Alloy 718 materials have been reported to be susceptible to IGSCC with heat treatments that produce delta and Laves phases.^[A-41 – A-44] However, work by P. Scott has shown this to be erroneous, the observation of delta phase, in particular, being entirely dependent on the magnification used in microscopy.^[A-45] In addition, the presence of surface defects is known to initiate cracking in PWR environments. When given a high temperature anneal (~2000°F) followed by a two-step aging treatment (~1324°F and 1150°F), significantly better IGSCC growth resistance from pre-cracks is achieved. In general, use of this material in PWR environments has been excellent, even at stresses significantly exceeding the nominal yield strength. The extremely low failure rates that have been observed were shown to be associated with surface defects. Thus careful attention to manufacturing detail is required to maintain SCC resistance.

High temperature annealing (~2000°F) followed by aging at about 1300°F (the HTH condition) improves the SCC resistance of Alloy X-750 in PWR environments.^[A-39, A-40, A-46] Another study performed by Framatome and Electricité de France (EDF) showed that the sensitivity of Alloy X-750 to crack initiation was strongly dependent upon the surface condition and surface oxide layers.^[A-47] Hence, service endurance is as much, if not more, related to manufacturing procedures as it is to heat treatment.

Test data show that for Alloy X-750 HTH condition material, peak stress levels up to two times the room temperature yield strength performed well in PWR environments; however, maintaining peak stresses below yield strength would seem to be a prudent practice for long-term use. Figure A-10 shows an empirical lower bound line drawn that approximates the threshold between cracking and acceptable performance.^[A-39, A-40]

Figure A-10
Failure Trend Line for Alloy X-750 HTH SCC^[A-39]

As noted below in Section A.1.6, LTCP is an issue with the nickel-base materials. It is particularly an issue with Alloy X-750, regardless of the heat treatment. In the AH and BH heat treatment conditions, Alloy X-750 is very susceptible to LTCP. However, testing of Alloy X-750 HTH material seems to show somewhat less LTCP susceptibility.

A.1.5 Cast Austenitic Stainless Steels

SCC resistance of CASS has been investigated for a very limited number of environments, heat treatments, and test conditions. In general, SCC resistance tends to improve as the composition is adjusted (e.g., lower nickel content) to provide greater amounts of ferrite in the austenitic matrix. This trend appears to continue to approximately 50% ferrite (Figure A-11). At low and medium stress levels, the ferrite tends to block the propagation of SCC (Figure A-12). However, as the stress level increases, the preferred crack propagation mode may change from IGSCC to TGSCC.^[A-48]

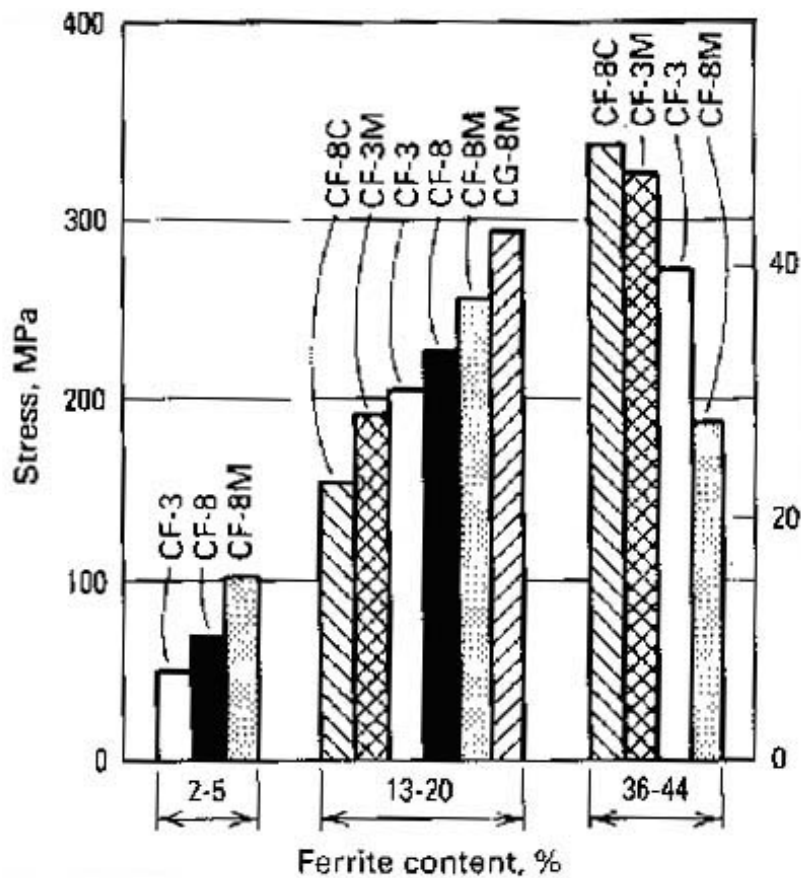


Figure A-11
Stress Required to Produce SCC in Several CASS Alloys with Varying Amounts of Ferrite^[A-48]



Figure A-12
Ferrite Pools Blocking the Propagation of SCC in a Cast Austenitic Stainless Steel^[A-48]

Under normal PWR conditions, CASS materials and welded CASS materials have shown excellent resistance to SCC. Generally, the ferrite contents are $> 5\%$. However, if very low levels of ferrite are present in any CASS weld, because of the filler materials or weld procedures used, those welds could be susceptible to SCC, as seen in BWR conditions.^[A-38]

Therefore, low ferrite ($< 5\%$) CASS material or CASS welds that are highly stressed (levels greater than the room temperature material yield strength) may be of concern for SCC. Additionally, an unresolved issue with CASS materials is the potential for reduced SCC resistance in the thermally aged condition (Appendix E).

A.1.6 Austenitic Nickel-Base Alloys

In general, austenitic nickel-base alloys are much more resistant to SCC in the presence of impurities and oxygenated water than austenitic stainless steel. However, austenitic nickel-base alloys are susceptible to SCC (i.e., PWSCC) when exposed to high-purity deaerated, hydrogenated, water at elevated temperatures. Many studies of Alloy 600 in PWR environments^[A-49 – A-55] show that PWSCC occurs when high tensile stress, high temperature, and a susceptible microstructure are simultaneously present. All failures of Alloy 600 component items reported in the field resulted from high residual tensile stresses introduced during fabrication. Other factors that may possibly influence susceptibility include the hydrogen concentration and possibly high lithium concentration, although the latter is a very weak effect within the permissible range in PWR primary water. Recent industry experience indicates that Alloy 82 and Alloy 182 weld metals are also susceptible to PWSCC.

Considerable research efforts have been made to identify the mechanism responsible for PWSCC of Alloy 600. These investigations, reviewed by Was,^[A-56] have shown that PWSCC is primarily dependent on the heat treatment received by the material. For instance, a heat treatment after mill-annealing (MA) in the temperature range of 1200°F to 1380°F (649 to 749°C) has been found to cause a drastic improvement of the resistance of Alloy 600 to PWSCC. This has been termed “thermal treatment” (TT), the improvement being mainly associated in the literature with an improved grain boundary decoration by carbides. Although the exact mechanism of enhanced resistance to PWSCC is unclear and still under debate, there is general agreement that the chemical composition and structure of grain boundaries are of crucial importance. In this connection, chromium depletion, segregation of impurities to grain boundaries, intergranular carbides and their mechanical effect on stress concentrations, and grain boundary misorientation appear to be important for the PWSCC resistance of the material.

Operating temperature appears to be an important parameter in determining the susceptibility of nickel-base alloys to PWSCC.^[A-57] PWSCC has occurred quite often at temperatures $\geq 600^\circ\text{F}$. However, some failures by PWSCC in nickel-base alloys have occurred when exposed to temperatures $\leq 600^\circ\text{F}$ (316°C) and to reactor coolant chemistry conditions described in the EPRI Water Chemistry Guidelines for the Reactor Coolant System (RCS).^[A-11]

Low Temperature Crack Propagation

The observation of low temperature crack propagation (LTCP) with austenitic nickel-base alloy materials in PWRs has been described in several publications.^[A-58 – A-62] LTCP refers to the propagation of intergranular stress corrosion cracking at low temperatures ($\sim 130\text{--}170^\circ\text{F}$ [$54\text{--}77^\circ\text{C}$]) due to the embrittlement by hydrogen of the grain boundaries ahead of an advancing crack. This is a potential issue for the Alloy 82 welds, and perhaps the Alloy 182 welds, although much less data is available for the latter. LTCP is characterized as a significant degradation in fracture toughness in low temperature hydrogenated water at K-levels as low as $40\text{ MPa}\sqrt{\text{m}}$ ($36\text{ ksi}\sqrt{\text{in}}$) for nickel-base material. This effect is attributed to a hydrogen-induced intergranular cracking mechanism, and is considered to be a form of hydrogen embrittlement.

The literature data suggest that LTCP could be a potential concern with all nickel-base alloys; however, testing of Alloy 600 wrought materials appear to indicate it to be relatively immune to this mechanism. Alloy 600 materials demonstrate about a 30% drop in toughness in hydrogenated low temperature water environments with sufficient fracture resistance remaining. In addition, the operative cracking mechanism is ductile dimple rupture.

The available literature data suggest that four conditions must be satisfied simultaneously for LTCP:

- a. Relatively high concentrations of hydrogen must be present (in the environment and therefore in the metal). The early work by Mills, et al., suggested the most significant effects were observed at hydrogen concentrations 3 to 5 times the normal PWR operating concentrations. Some of the more recent data suggests that, under lower hydrogen concentrations, this degradation mechanism may also be seen.

- b. Low temperatures; typically in the range from 130 to 200°F (54 to 93°C).
- c. The presence of a "sharp" crack tip.
- d. The presence of sustained high loads – the loads must be capable of creating stresses in the metal which approach the yield stress.

A.2 Summary and Discussion

The literature data and field experience show that chloride-induced SCC in austenitic stainless steels can only occur in the presence of oxygen, either as IGSCC or TGSCC. IGSCC failures in BWR service have been associated with sensitized weld HAZs and cold-worked, solution-annealed, stainless steels. All forms of 300 series austenitic stainless steels can experience SCC in water containing chlorides, certain forms of sulfur (e.g., thiosulfate, which was previously used in building spray systems) and oxygen. Tensile stress is required, which can be induced by material manufacturing processes, grinding, welding (especially multiple weld repairs) and cold-work in bending. The magnitude of these stresses need not be particularly high, depending on the combined concentrations of oxygen and chloride.

During normal PWR operating conditions, radiolytic dissolved oxygen concentration in primary water is maintained at <5 ppb by injecting externally-supplied hydrogen. The hydrogen addition serves to suppress radiolysis and to shift the electrochemical potential (ECP) into a regime in which cracking of stainless steels (whether sensitized or not) is not favored. During refueling outages, however, the primary water system will by necessity be exposed to oxygen when the reactor head is removed, and also briefly during cool-down, as described below. The shift in environmental conditions during cool-down, from a highly reducing environment (hydrogen) to oxidizing conditions, is used to oxidize and release corrosion products (particularly Ni and Co-58) intentionally into the primary water system. The material released into solution can then be removed by the letdown demineralizers. During plant cool-down, hydrogen peroxide is added to the primary coolant at temperatures typically <180°F (<80°C) to dissolve Co-58 and Ni out of the oxides. The temperature limitation on hydrogen peroxide addition is two-fold, the primary reason being to limit exposure of the primary water system to oxidizing conditions while at temperatures high enough to possibly crack sensitized austenitic alloys. The secondary reason for the temperature limit is that peroxide is more stable at lower temperature, allowing the plant to maintain a residual peroxide concentration following the addition. At shutdown conditions, the primary coolant is exposed to air, which maintains the coolant under mildly oxidizing conditions. However, shutdown periods are relatively short and the temperatures are much lower compared with the time and temperatures of normal operation when oxygen levels are negligible.

The above coolant chemistry controls (i.e., hydrogen injection during operation and limiting oxygen exposure until Mode 5 during shutdown) have historically eliminated the potential for SCC of austenitic SS PWR internals component items although continued surveillance should be practiced. Highly cold-worked (> 20%) materials appear to be cause for particular surveillance. Sensitized material may also be present in PWR internals due to welding and post-weld stress relief operations. While sensitized material may potentially be susceptible to

SCC, both service experience and extensive test data under normal PWR (hydrogenated) primary operating conditions indicate that the probability is extremely low.

The literature data for precipitation-hardenable materials seems to indicate that high temperature tempers (for martensitic SS alloys) or high temperature annealing and aging (for austenitic SS and Ni-base alloys) and stress levels below the room temperature proportional limit should perform well in PWR environments.

CASS stainless steels and austenitic stainless steel weld metals appear to be immune to SCC in PWR environments (in the non-thermally aged condition) provided that ferrite levels are within specified limits (i.e., > 5% and < ~25%). It is currently not known if thermal aging has an effect on SCC susceptibility of CASS materials.

Austenitic Ni-base alloys are potentially susceptible to PWSCC in PWR environments, particularly at temperatures seen in PWR internals and at stress levels near or above the room temperature yield strength of the material. Metallurgical and manufacturing factors play a large role in determining potential susceptibility. LTCP may be a mechanism of concern under certain conditions for nickel-base alloys (with Alloy 600 apparently the least susceptible); however, to date, no occurrences have been noted in service or in the literature at PWR-relevant conditions.

A.3 SCC Threshold and Screening Criteria

As noted in Section A.1, no acceptable threshold values seem to exist for SCC and therefore, no threshold criteria are proposed. The development of PWR internals screening criteria for SCC (encompassing IGSCC, TGSCC, PWSCC, and LTCP) are based on the following assumptions:

- a. Water chemistry conditions, in accordance with EPRI guidelines, ^[A-11] are maintained.
- b. Co-base alloys are not known to be susceptible to SCC in applications in PWR internals.
- c. Neutron flux or fluence dependencies associated with SCC are accounted for in the IASCC degradation mechanism described in Appendix B.

Screening criteria for parameters that produce potentially susceptible materials and the necessary stress levels for SCC are identified below:

Austenitic Stainless Steels

Austenitic stainless steels are concluded to have a very high resistance to SCC in PWR primary water conditions due to the absence of dissolved oxygen and the impurity limits placed by the PWR primary water specification. The notable exceptions though are the remote potential for IGSCC of severely cold-worked (> 20% from grinding, bending, etc.) or highly strained material in HAZs from multi-pass welding. For material that is stressed near or beyond the annealed room temperature yield strength, the probability increases for the occurrence of SCC.

Thus, a screening criterion of ≥ 30 ksi (207 MPa) is suggested for those component items in operation in the severely cold-worked (equivalent to $> 20\%$) or multi-pass welded conditions.

Austenitic stainless steel weld materials that contain low ferrite levels and are highly stressed are potentially susceptible to SCC in the presence of oxygen based on BWR experience. Thus, screening criteria of ferrite $< 5\%$ and yield strength stress levels of ≥ 30 ksi (207 MPa) are established here. [Note: A potential concern exists that SCC could affect austenitic stainless steel welds that meet or exceed the above stress criterion and the thermal aging embrittlement criteria (Appendix E).]

Martensitic Stainless Steels

Martensitic stainless steel material loaded beyond approx. 70% of the room temperature yield strength (≥ 88 ksi/607 MPa) is potentially susceptible to IGSCC. However, martensitic stainless steels not subject to gamma heating with tempers $> 1125^{\circ}\text{F}$ (607°C) generally are not considered susceptible to SCC. [Note: A potential concern exists that SCC could affect martensitic stainless steel materials that meet or exceed the above stress criterion and the thermal aging embrittlement criteria (Appendix E).]

Martensitic Precipitation-Hardenable Stainless Steels

Martensitic PH stainless steel material loaded beyond approx. 70% of the room temperature yield strength (≥ 88 ksi/607 MPa) is susceptible to IGSCC. However, martensitic PH stainless steels not subject to gamma heating with tempers $> 1100^{\circ}\text{F}$ (593°C) generally are not considered susceptible to SCC. [Note: A potential concern exists that SCC could affect martensitic PH stainless steel materials that meet or exceed the above stress criterion and the thermal aging embrittlement criteria (Appendix E).]

Austenitic Precipitation-Hardenable Stainless Steels

Surface cold work and tensile loading $\geq 70\%$ of room temperature yield strength (approx. ≥ 70 ksi [483 MPa]) will promote IGSCC of austenitic PH SS materials. (Note: This is particularly relevant for highly stressed bolts that were fabricated by a hot-heading process or that were shot-peened.)

Cast Austenitic Stainless Steels

CASS materials that contain low ferrite levels and are highly stressed are potentially susceptible to IGSCC or TGSCC. Thus, screening criteria of ferrite $< 5\%$ and yield strength stress levels of ≥ 35 ksi (241 MPa) are established. [Note: A potential concern exists that SCC could affect CASS materials that meet or exceed the above stress criterion and the thermal aging embrittlement criteria (Appendix E).]

Low ferrite levels ($< 5\%$) in CASS welds that are highly stressed will also potentially make them susceptible to IGSCC.

Austenitic Nickel-Base Alloys

Austenitic Ni-base alloys are susceptible to PWSCC at stress levels near or exceeding the yield strength (i.e., approximately ≥ 30 ksi [207 MPa]).

Austenitic Ni-base alloy weld materials that are highly stressed are also potentially susceptible to PWSCC. Thus, a screening criterion for stress levels near or exceeding the yield strength of ≥ 35 ksi (241 MPa) is established.

Austenitic Precipitation-Hardenable Nickel-Base Alloys

Austenitic PH Ni-base alloys are potentially susceptible to PWSCC at stress levels exceeding the yield strength depending on heat treatment and manufacturing details. The surface condition is also critical to PWSCC susceptibility. Therefore, for Alloy X-750 material the suggested screening criterion is ≥ 100 ksi [689 MPa]. For Alloy 718 material, which has been shown both by testing and in-service experience to be very resistant to PWSCC, the suggested screening criterion is ≥ 130 ksi [896 MPa].

A.4 SCC References

- A-1 McIntyre, D.R., "Experience Survey of Stress Corrosion Cracking of Austenitic Stainless Steels in Water," MTI publication No. 27, February 1987.
- A-2 "Component Life Estimation: LWR Structural Materials Degradation Mechanisms," EPRI NP-5461, Project 2643-5, September 1987.
- A-3 Jones, R. H., Stress-Corrosion Cracking, American Society for Metals International, Copyright 1992.
- A-4 Boursier, J.M., et al. "Stress Corrosion Cracking of Austenitic Stainless Steels in PWR Primary Water: An Update of Metallurgical Investigations Performed on French Withdrawn Components," Fontevraud V, September 2002.
- A-5 Herbsleb, G., "Preventing Intergranular Stress Corrosion Cracking of Austenitic Stainless Steels," Mannesmann Forschungsinstitut GmbH, Duisburg, 1984.
- A-6 Kilian, R., et al. "Parameters Influencing the Transgranular Stress Corrosion Cracking Behaviour of Austenitic Stainless Steels in Systems Conveying Reactor Coolant," Fontevraud V, September 2002P.
- A-7 Berge, J.P., et al. "Corrosion and Cracking of Stainless Steels and Cobalt Alloys in Primary Circuit Piping of Light Water Reactors," Proceedings of the Fourth

- International Symposium on Environmental Degradation of Materials in Nuclear Power Systems-Water Reactors, Jekyll Island, GA, August 1989, edited by D. Cubicciotti, NACE, Houston, TX.
- A-8 Williams, W.L., "Chloride and Caustic Stress Corrosion of Austenitic Stainless Steel in Hot Water and Steam," Corrosion—National Association of Corrosion, Engineers Vol. 13, August 1957.
- A-9 Gordon, B. M., "The Effect of Chloride and Oxygen on the Stress Corrosion Cracking of Stainless Steels: Review of Literature," Materials Performance, Vol. 19, No. 4, April 1980.
- A-10 "PWR Primary Water Chemistry Guideline," EPRI NP-4762-SR, 1986.
- A-11 "PWR Primary Water Chemistry Guideline: Revision 4," EPRI TR-105714-V1R4, March 1999.
- A-12 Andresen, P.L., et al., "Effects of PWR Primary Water Chemistry and Deaerated Water on SCC," Proceedings of the Twelfth International Symposium on Environmental Degradation of Materials in Nuclear Power Systems-Water Reactors, August 2005 (to be published).
- A-13 Materials Handbook for Nuclear Plant Pressure Boundary Applications, TR-109668-SA-R1, Final Report, Revision 1, EPRI, Palo Alto, CA, December 1998.
- A-14 "Stress Corrosion Crack Growth Behavior of Cold Worked 304L and 316L Stainless Steels," EPRI, Palo Alto, CA: 2002. 1007379.
- A-15 Guerre, C., Raquet, O., et al., "SCC Crack Growth Behavior of Austenitic Alloys in PWR Primary Water Conditions," 12th International Conference on Environmental Degradation of Materials in Nuclear Power Systems – Water Reactors, August 2005 [to be published].
- A-16 Tice, D.R., Platts, N., et al., "Environmentally Assisted Crack Growth of Cold-Worked Type 304 Stainless Steel in PWR Environments," 12th International Conference on Environmental Degradation of Materials in Nuclear Power Systems – Water Reactors, August 2005 [to be published].
- A-17 Herms, E., Couvant, T., et al., "SCC of Cold-Worked Austenitic Stainless Steels in Primary Water of PWRs," 12th International Conference on Environmental Degradation of Materials in Nuclear Power Systems – Water Reactors, August 2005 [to be published].
- A-18 Arioka, K., Chiba, G., et al., "Influence of Orientation of Cold Work and Carbide Precipitation on IGSCC Behaviors of SUS 316 in Hydrogenated High Temperature

- Water,” 12th International Conference on Environmental Degradation of Materials in Nuclear Power Systems – Water Reactors, August 2005 [to be published].
- A-19 Couvant, T., Vaillant, F., et al., “Stress Corrosion Cracking of 304L Stainless Steel in PWR Environment,” 12th International Conference on Environmental Degradation of Materials in Nuclear Power Systems – Water Reactors, August 2005 [to be published].
- A-20 Regulatory Guide 1.44, “Control of the Use of Sensitized Stainless Steel,” 1973, available from U.S. Nuclear Regulatory Commission.
- A-21 ASM Specialty Handbook, ASM International, 1994, p. 50-51.
- A-22 Suss, H., “A Discussion of the Susceptibility of AISI 410 to SCC, and a Means of Eliminating the Stress Corrosion Problem,” KAPL-2155, March 10, 1961.
- A-23 Suss, H., “Practicality of Establishing Threshold Values to Eliminate Stress Corrosion Failures in metals and Alloys,” Corrosion, NACE, Feb. 1951, Vol. 17, pp. 61t-66t.
- A-24 Lillys, P., and Nehrenberg, A.E., “Effect of Tempering Temperature on SCC and Hydrogen Embrittlement of Martensitic Stainless Steels,” Transactions of ASM, Vol. 48, 1955, pp. 327-355.
- A-25 Jordan, E.L., “Valve Stem Corrosion Failures,” Information Notice 85-59, U.S. Nuclear Regulatory Commission, Washington, D.C., July 17, 1985.
- A-26 Xu, H., and Fyfe, S., “Aging Embrittlement Modeling of Type 17-4 PH at LWR Temperatures,” Proceedings of the Tenth International Symposium on Environmental Degradation of Materials in Nuclear Power Systems-Water Reactors, August 2001.
- A-27 Xu, H., and Fyfe, S., “Fracture of Type 17-4 PH CRDM Leadscrew Male Coupling Tangs,” Proceedings of the Eleventh International Symposium on Environmental Degradation of Materials in Nuclear Power Systems-Water Reactors, August 2003.
- A-28 Rowland, M.C., and Smith, W.R., Jr., “Precipitation-Hardening Stainless Steels in Water-Cooled Reactors,” NE, Jan. 1962, pp. 14-22.
- A-29 Suss, H., “Stress Corrosion and Hydrogen Embrittlement Properties of 17-4PH in 600°F Waters,” KAPL-M-6580, April 1967.
- A-30 Boyd, W.K., and Peoples, R.S., “Corrosion in Borated and Deionized Water at Temperatures up to 500°F,” BMI-1047, October 14, 1955.
- A-31 Jackson, R.P., “Stress-Corrosion Cracking of 17-4PH Stainless Steel,” DP-779, Sept. 1962.

- A-32 Williams, W.L., and Eckel, J.F., ed., "Stress Corrosion," Corrosion and Wear Handbook, AEC TID-7006, 1957, pp. 187-225.
- A-33 Gras, J. M., et al., "Corrosion by Concentrated Boric Acid of Materials for Bolting of Components of the Primary Circuit," International Symposium, 2-6 September 1985, Fontevraud, SFEN, pp. 178-187.
- A-34 McIlree, A.R., "Degradation of High Strength Austenitic Alloys X-750, 718, and A-286 in Nuclear Power Plants," Proceedings: International Conference on Environmental Degradation of Materials in Nuclear Power Systems--Water Reactors, 1983, NACE.
- A-35 Miglin, M. T., et al., Microstructure and Stress Corrosion Resistance of Alloys X-750, 718, and A-286 in LWR Environments, EPRI NP-6392-SD, June 1989.
- A-36 Daret, J., "CEA Experience on Alloy X-750 and Alternate Materials (Alloy 718 and A-286) After 27,000 Hours Testing of Actual Pins and Tensile Specimens," Proceedings: 1986 Workshop on Advanced High-Strength Materials, Paper 16, EPRI NP-6363, May 1989.
- A-37 Hall, J. F., "Stress Corrosion Cracking of A-286 Stainless Steel," Proceedings: 1986 Workshop on Advanced High-Strength Materials, paper 22, EPRI NP-6363, May 1989.
- A-38 Shah, V.N., and MacDonald, P.E., Eds., Aging and Life Extension of Major Light Water Reactor Components, Elsevier, New York, 1993.
- A-39 Material Reliability Program: Stress Corrosion Cracking of High Strength Reactor Vessel Internals Bolting in PWRs (MRP 88), 1003206, EPRI, Palo Alto, CA, 2003. 1003206.
- A-40 Hall, J.B., Fyfitich, S., and Moore, K.E., "Laboratory and Operating Experience with Alloy A-286 and Alloy X-750 RV Internals Bolting Stress Corrosion Cracking," 11th International Conference on Environmental Degradation of Materials in Nuclear Power Systems--Water Reactors, August 2003, NACE.
- A-41 Miglin, B.P., et al., "Stress Corrosion Cracking of Commercial-Grade Alloy 718 in Pressurized-Water-Reactor Primary Water," Proceedings of the Fourth International Symposium on Environmental Degradation of Materials in Nuclear Power Reactors, 1989.
- A-42 Miglin, M.T., et al., "Effect of Heat Treatment on Stress Corrosion of Alloy 718 in Pressurized-Water-Reactor Primary Water," Proceedings of the Fifth International Symposium on Environmental Degradation of Materials in Nuclear Power Reactors, 1991.
- A-43 Miglin, M.T., et al., "Stress Corrosion Cracking of Chemistry and Heat Treat Variants of Alloy 718 Part 1: Stress Corrosion Test Results," Proceedings of the Sixth

International Symposium on Environmental Degradation of Materials in Nuclear Power Reactors, 1993.

- A-44 Burke, M.G., et al., "Stress Corrosion Cracking of Chemistry Variants of Alloy 718 Part 2: Microstructural Characterization," Proceedings of the Sixth International Symposium on Environmental Degradation of Materials in Nuclear Power Systems – Water Reactors, 1993.
- A-45 Scott, P.M., "Stress Corrosion Cracking in Pressurized Water Reactors – Interpretation, Modeling, and Remedies," Corrosion, Vol. 56, pp. 771-782, 2000.
- A-46 Hanninen, H. and Aho-Mantila, I., "Environment-Sensitive Cracking of Reactor Internals," Proceedings of the Third International Symposium on Environmental Degradation of Materials in Nuclear Power Systems – Water Reactors, American Nuclear Society, La Grange Park, IL. 1987, p. 77.
- A-47 Foucault, M., and Benhamou, C., "Influence of the Surface Condition on the Susceptibility of Alloy X-750 to Crack Initiation in PWR Primary Water," Proceedings of the Sixth International Symposium on Environmental Degradation of Materials in Nuclear Power Systems – Water Reactors," TMS, 1993.
- A-48 Monroe, R.W., and Pawel, S.J., "Corrosion of Cast Steels," from Metals Handbook, Vol. 13, Corrosion, 9th Editions, ASM International, Materials Park, OH, 1987.
- A-49 Campbell, C.A., and Fyfe, S., "PWSCC Ranking Model for Alloy 600 Components," Proceedings of the Sixth International Symposium on Degradation of Materials in Nuclear Power Systems-Water-Reactors, San Diego, CA, August 1-5, 1993.
- A-50 Stiller, K., et al., "Structure, Chemistry, and Stress Corrosion Cracking of Grain Boundaries in Alloys 600 and 690," Metallurgical and Materials Transactions A, Volume 27A, February 1996, pp. 327-341.
- A-51 Briant, C.L., et al., "The Effect of Microstructure on the Corrosion and Stress Corrosion Cracking of Alloy 600 in Acidic and Neutral Environments," Corrosion, Vol. 42, No. 1, January 1986, pp. 15-27.
- A-52 Hall, E.L., and Briant, C.L. "The Microstructural Response of Mill-Annealed and Solution-Annealed INCONEL 600 to Heat Treatment," Metallurgical Transactions A, Vol. 16A, July 1985, pp. 1225-1236.
- A-53 "Specially Prepared Alloy 600 Tubing," EPRI NP-5072, Project S303-17, February 1987.
- A-54 Norring, K., et al., "Intergranular Stress Corrosion Cracking in Steam Generator Tubing, Testing of Alloy 690 and Alloy 600 Tubes," Proceedings of the Third

International Symposium on Environmental Degradation of Materials in Nuclear Power Systems, National Association of Corrosion Engineers, 1987.

- A-55 Bruemmer, S., et al., "Microstructure and Microdeformation Effects on IGSCC of Alloy 600 Steam Generator Tubing," *Corrosion*, November 1988, pp. 782-788.
- A-56 Was, G.S., "Grain-Boundary Chemistry and Intergranular Fracture in Austenitic Nickel-base Alloys—A Review," *Corrosion*, Vol. 46, 1990, pp. 319-330.
- A-57 Bamford, W. and Hall, J., "A Review of Alloy 600 Cracking in Operating Nuclear Plants: Historical Experience and Future Trends," 11th Int. Conf. on Environmental Degradation of Materials in Nuclear Systems – Water Reactors, August 10-14, 2003.
- A-58 Mullen, J.V., and Parrington, R.J., "Stress Corrosion of Alloy 600 Weld Metal in Primary Water," presentation F3, Proceedings: 1992 EPRI Workshop on PWSCC of Alloy 600 in PWRs, EPRI TR-103345, December 1993.
- A-59 Brown, C.M., and Mills, W.J., "Fracture Toughness, Tensile and Stress Corrosion Cracking Properties of Alloy 600, Alloy 690, and Their Welds in Water," Paper 90, *Corrosion96*, NACE, 1996.
- A-60 Mills, W.J., and C.M. Brown, "Fracture Behavior of Nickel-based Alloys in Water," Ninth International Conference on Environmental Degradation of Materials in Nuclear Power Systems—Water Reactors, August 1-5, 1999, Newport Beach, CA, TMS/NACE.
- A-61 Mills, W.J., Brown, C.M., and Burke, M.G., "Effect of Microstructure on Low Temperature Cracking Behavior of EN82H Welds," Tenth International Conference on Environmental Degradation of Materials in Nuclear Power Systems—Water Reactors, August 2001, NACE.
- A-62 Mills, W.J., Lebo, M.R., and Kearns, J.J., "Hydrogen Embrittlement, Grain Boundary Segregation and Stress Corrosion Cracking of Alloy X-750 in Low and High Temperature Water," *Metallurgical and Materials Transactions*, Vol. 30A, 1999, pp. 1579-1596., ITG White Paper on LTCP.

B

APPENDIX B: IRRADIATION-ASSISTED STRESS CORROSION CRACKING

B.1 General Description of Irradiation-Assisted Stress Corrosion Cracking

Irradiation-assisted stress corrosion cracking (IASCC) is an age-related degradation mechanism where materials exposed to neutron radiation become more susceptible to SCC with increasing fluence.^[B-1] IASCC, like PWSCC, is a distinctive subset of SCC. Despite numerous investigations and research efforts, details of the IASCC mechanism in PWR internals remain hypothetical.^[B-2 – B-9] The current consensus is that IASCC results from a synergistic effect of irradiation damage to the material, water environment with possible radiolysis effects, and stress state. At present, interactions between these variables have not adequately been quantified and no primary IASCC controlling mechanism has been identified.

There are three major ways that irradiation affects the structure of a PWR internals component item:

- a. Irradiation changes the dislocation population, leading to radiation-induced hardening and, at very high neutron exposures, dislocation channeling with stress.^[B-10]
- b. Irradiation changes the local alloy chemistry near point defect traps, especially around the grain boundaries.^[B-11]
- c. Irradiation produces transmutation products, including hydrogen and helium.

Irradiation can also lead to precipitation of new phases^[B-12] or destabilization of the phases already present.^[B-13] However, these are generally considered secondary effects. Although the exact mechanism of IASCC in PWRs is not yet known, both hardening and radiation-induced segregation (RIS) could play a role.^[B-14] Operating experience and irradiated material test results suggest that IASCC may be of most concern in the later stages of PWR internals life.

Much of the existing IASCC knowledge comes from BWR experience and advanced gas-cooled reactor (AGR) and fast breeder reactor (FBR) test programs, whose neutron spectra, flux and fluence levels, radiation temperature, and environmental chemistry differ significantly from those of PWRs. Systematic study of IASCC in the PWR environment has not been conducted in the past, but the Joint Owners Baffle Bolt (JOBB) program, with participation by various institutions in the U.S. and Europe, coordinated by the Electric Power Research Institute (EPRI) through the MRP RI-ITG, has recently completed such a program,^[B-15] the results are discussed herein. In addition, the MRP RI-ITG has been conducting tests in hot cell to study IASCC since 2001 to expand the JOBB investigation and findings.^[B-40 – B-43]

Changes in tensile and yield strengths, ductility and fracture toughness results from changes in the microstructure due to irradiation damage (see Appendix F). Many investigations^[B-2 – B-5, B-16, B-17, B-40 – B-43] have studied the evolution of mechanical properties and microstructure of austenitic stainless steels with increasing neutron fluence. Irradiation-induced hardening, transmutation, segregation, creep, and healing are among the factors suspected to have a significant impact on IASCC, hence they are the most widely studied. A more thorough discussion of these is contained in References B-9, B-18 and B-44.

IASCC was first observed in Type 304 SS fuel cladding in the early 1960s in both BWRs and PWRs.^[B-4] Since then, IASCC failures have been reported for a number of other reactor internals component items made from various stainless steels and nickel-based alloys in various types of reactors. More detailed historical reviews of intergranular cracking attributed to IASCC in the BWRs and PWRs can be found in References B-3 and B-4. The most recent and potentially significant IASCC events in PWRs are the observed cracking of baffle/former bolts and control rod cladding in some early French built PWR units.^[B-3, B-4, B-15, B-19, B-20, B-21] Both irradiated Type 304 and Type 316 stainless steel materials can show high sensitivity to cracking in the PWR environment although strong heat-to-heat variability has been observed. As demonstrated in tests on irradiated materials with constant loading, constant deformation, and slow strain rates, a conservative threshold fluence of approximately 7×10^{20} n/cm² ($E > 1.0$ MeV), or ~ 1 dpa, can be considered as the lower limit for the PWR primary environment.^[B-22, B-23, B-24, B-25, B-40 – B-43]

B.1.1 Annealed vs. Cold-Worked Materials

Cold-working (CW) produces a dislocation density in stainless steel many orders of magnitude higher than that of solution-annealed (SA) material. This initial difference has a strong impact on subsequent radiation-induced microstructural evolution. Cold work slows down the development of irradiation damage and hardening, as explained later, but in this case the improvement in flow localization suppression is due to a pre-existing dislocation network.^[B-26] Studies have also shown that prior CW also suppresses void nucleation and swelling during irradiation.^[B-27, B-28] Cold-working introduces a higher dislocation density, which leads to an increase in the nucleation density of helium bubbles, thus a decrease in the individual bubble growth rates.^[B-29]

Nevertheless, recent failure of baffle bolts and control rod cladding in the French PWRs were made of CW 316 and SA 304 stainless steel, respectively.^[B-8] It has therefore been suggested that at significantly high fluence levels (> 10 to 20 dpa or 6.7×10^{21} to 1.3×10^{22} n/cm² [$E > 1.0$ MeV]), there is little difference in IASCC behavior between CW and SA stainless steels.^[B-6, B-15]

B.1.2 Austenitic Stainless Steels

Type 304 and Type 316 stainless steels are the most extensively used material in the fabrication of baffle bolts and plates of PWR internals designs. Type 316 is generally regarded as superior to Type 304 in IASCC resistance, at least for doses < 10 dpa.^[B-2, B-6, B-15] Mechanical tests show that, for a given dose, increases in yield strength, and decreases in uniform and total elongations were greater for Type 304 than for Type 316.^[B-2, B-6, B-15] Irradiation hardening is strongly

believed to be directly linked to IASCC, though no unambiguous correlation has yet been established.^[B-26]

The formation of martensite along a grain boundary may contribute toward IASCC in PWR internals. Low austenite stability against martensite formation is facilitated by a low stacking fault energy (SFE) and a high deformation-induced martensite formation temperature, M_d . The influence of composition on austenite stability can be seen from SFE values of $\sim 20 \text{ mJ/m}^2$ for Type 304 and $\sim 80 \text{ mJ/m}^2$ for Type 316.^[B-9] The Ni concentration of Type 316 is generally 3% higher than Type 304 and Ni is a strong austenite stabilizer that depresses M_d . New investigations on the possibility of martensite formation at grain boundaries are reportedly in progress.^[B-21]

New experiments to evaluate possible replacement materials have included some Ti and Nb stabilized austenitic stainless steels.^[B-6, B-15] Data collected from swelling capsule experiments after exposure to two PWR fuel cycles gave a mixed result with only Type 348 (Nb stabilized) material appearing to outperform Types 304 and 316.^[B-3] A low level of undersized impurities (Si, N, P), which reduces irradiation-induced dislocation loop sizes and increases loop density, are cited as reasons for improvement. However, it has been shown that low levels of Si and P are insufficient, as similar results were not reproduced by subsequent tests on high purity heats.^[B-30, B-31, B-32, B-33] Oversize solutes (like Ti and Nb) can serve as trapping sites for point defects. A reduction in the availability of point defects reduces the diffusion rate to other trap sites such as grain boundaries, thus diminishing RIS at grain boundaries. Hence, it is possible that they could improve IASCC resistance by reducing RIS.^[B-32] Based on fast breeder reactor experience, Type 316-Ti is being pursued as a possible candidate replacement material.^[B-6, B-15]

There is a paucity of IASCC-related studies of welding materials. Toughness tests of weld materials (Type 308) removed from BWRs ($\sim 10 \text{ dpa}$ or $\sim 6.7 \times 10^{21} \text{ n/cm}^2$ [$E > 1.0 \text{ MeV}$]) indicate a substantially lower toughness value of $\sim xx \text{ MPa}\cdot\sqrt{\text{m}}$ compared to $xxx \text{ MPa}\cdot\sqrt{\text{m}}$ for Type 304 stainless steel.^[B-34] The same study also found the tearing modulus of the weld material after irradiation to be very low, which could, upon crack initiation, lead to immediate failure without stable crack growth. The above data correlate well with results obtained in other BWR experiments.^[B-35] When irradiated at 427°C (801°F) it has also been shown that the saturation fracture toughness for the weld (Type 308) was below that for the wrought material (Types 316 and 304).^[B-36] However, there is a lack of testing data related to weld metals at PWR operating conditions. Recently, SSRT tests of 308 TIG weldments and 308 SAW specimens, irradiated in the Bor-60 fast reactor to 10.4 dpa and 20 dpa , respectively, were performed in PWR waters.^[B-43] The fracture surfaces of these specimens show very small amount of intergranularity.

B.1.3 Martensitic and Martensitic Precipitation-Hardenable Stainless Steels

No studies of martensitic PH stainless steel IASCC susceptibility have been identified in the open literature.

B.1.4 Austenitic Precipitation-Hardenable Stainless Steels

No studies of IASCC susceptibility for Alloy A-286 have been identified in the open literature.

B.1.5 Cast Austenitic Stainless Steels

The MRP RI-ITG tested statically cast 11 7/8 x 7 1/8 x 1 3/4 inch plates of CF8.^[B-43] The ferrite number of this material is 18. These plates first underwent three different thermal treatments: as cast, aged 100 hours at 400°C, and aged 950 hours at 400°. Subsequently, they were irradiated in the Bor-60 fast reactors to a level of ~10 dpa.

SSRT specimens fabricated from these plates tested in PWR waters showed varying fracture morphologies. Despite some degree of indication of columnar structure in their fracture morphology, as-cast CASS and “fully aged” CASS (950 hours at 400°) showed zero or negligible susceptibility to stress corrosion cracking, as their fracture faces were almost entirely ductile.^[B-43]

B.1.6 Austenitic Nickel-Base Alloys

Many PWR reactor coolant system component items, fabricated from Alloy 600 (e.g., pressurizer nozzles and control rod drive mechanism [CRDM] nozzles), have experienced PWSCC.^[B-37] Appendix A contains additional discussion of PWSCC. However, radiation is not considered to be a factor in these failures. No known IASCC-related studies have been reported in the open literature.

B.1.7 Austenitic Precipitation-Hardenable Nickel-Base Alloys

There is a lack of IASCC data for Alloy X-750 at high neutron fluence level. Results obtained from swelling capsule tests indicate that IASCC resistance of Alloy X-750 is approximately the same as Types 304 and 316 stainless steel.^[B-3,B-4] Some tensile test data of small scale Alloy X-750, HTH Condition bolts irradiated in a PWR to 1.4×10^{19} n/cm² ($E > 1.0$ MeV) performed without any failure up to 0.95% strain.^[B-45] Simulated BWR testing demonstrated an irradiation-enhanced IGSCC susceptibility of Alloy X-750 HTH Condition as a function of fluence and boron content.^[B-46] Fluence at 10^{19} n/cm² versus 10^{14} to 10^{18} n/cm² ($E > 1.0$ MeV) showed an increase in susceptibility.

Alloy 718 has an excellent record in PWR primary water applications often at operating stresses close to or exceeding the yield point that can be approximately 145 to 160 ksi (1000 to 1100 MPa). In fuel applications, very high neutron fluxes are also experienced. The few failures that have occurred have been attributed to a manufacturing defect that allowed components to enter service with pre-existing intergranular defects. Alloy 718 is known to be highly resistant to crack initiation but IGSCC will propagate rapidly in PWR primary water from pre-existing defects.

B.2 IASCC Summary and Discussion

While IASCC susceptibility is recognized to be affected by bulk composition and microstructure, no consistent or quantitative correlation has been established between the two. Experiments to isolate individual contributions to IASCC are difficult with different heats and grades of commercial purity in various thermal or cold-worked conditions. Efforts to address this issue have been attempted and are ongoing.^[B-44] To date, most data are pertinent to Type 304 and Type 316 austenitic stainless steels with variation in impurity levels and additions of a stabilizing element. Few data are related to other PWR internals alloys. Studies of different alloys have produced data too scattered to substantiate claims that one grade or thermal condition is superior in IASCC resistance than another. Heat-to-heat variations in behavior for the same alloy have been shown to be large.

While the mechanical properties, such as yield strength and fracture toughness appear to saturate around 10 to 20 dpa of irradiation, laboratory test data indicates that IASCC susceptibility appears to continue to increase. IASCC studies by Conermann and Shogan et al.^[B-38, B-41] were performed using a highly irradiated CW Type 316 flux thimble material removed from a commercial PWR after ~23 years of operation. Based on the studies, a proposed plot of applied stress versus time-to-failure was prepared from the results of O-ring crack initiation specimens for the various neutron exposures examined. Data were then plotted on a curve showing time-to-failure as a function of applied stress and fluence, which is provided as Figure B-1. From this figure, IASCC susceptibility appears to increase with irradiation and the stress levels needed to initiate IASCC decrease with neutron dose. It is noted, however, that this figure is based on a limited data set for one heat of material.

The development of PWR internals threshold and screening criteria for IASCC are based on the following assumptions:

- a. Water chemistry conditions, in accordance with EPRI guidelines, are maintained.
- b. No differences are assumed between CW and SA materials in screening.
- c. Insufficient data are available to determine the variations in IASCC susceptibility of the alloys or between heats of the same material used in PWR internals. Therefore, it is assumed that the threshold and screening criteria presented below apply to all alloys.

B.3 IASCC Threshold and Screening Criteria

It is recognized that a certain neutron fluence level is a necessary precondition for the occurrence of IASCC in LWRs. Approximate fluence levels for the observed occurrences of IASCC in both BWRs and PWRs are plotted in Figure B-2.^[B-39] Due to different water chemistry and operational conditions, a neutron fluence threshold for IASCC in PWRs differs considerably from that in BWRs. For austenitic stainless steels, a review of literature data indicates that a threshold value of $\sim 7 \times 10^{20} \text{ n/cm}^2$ ($E > 1.0 \text{ MeV}$) or $\sim 1 \text{ dpa}$ exists for PWRs.

Failure would be predicted after a significant time above the “Long term” curve and in a short time above the “Short time” curve.

Figure B-1
Prediction of IASCC Time-to-Failure Versus Stress^[B-38]

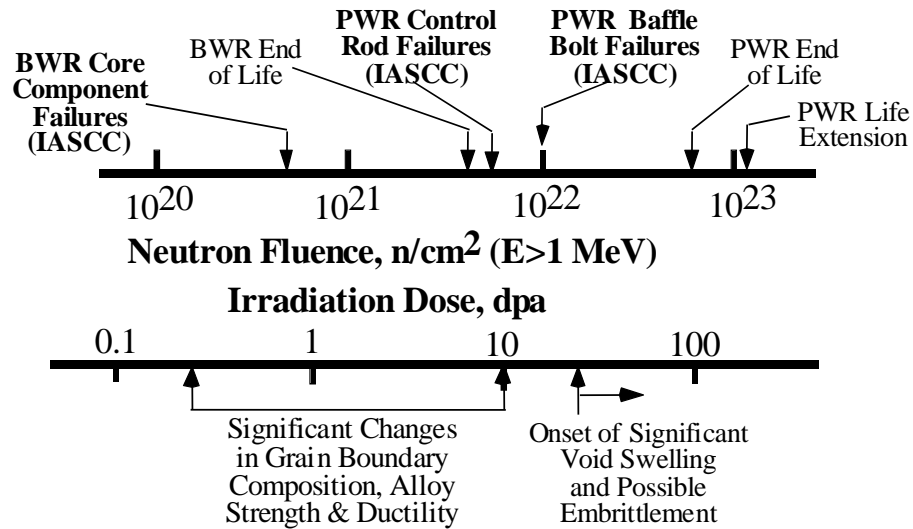


Figure B-2
Neutron Fluence Effects on IASCC Susceptibility in BWR and PWR Environments^[B-39]

The known IASCC incidents (failure of baffle bolts) observed in the European PWRs have indicated an IASCC threshold level at $\sim 2 \times 10^{21}$ n/cm² ($E > 1.0$ MeV) or ~ 3 dpa.^[B-15] It should be pointed out that, since there is much variation in PWR internals design, material composition, fabrication methods, and operating characteristics, an all encompassing threshold fluence level may prove to be inadequate for different PWR internals component items of different PWR designs. It should also be noted that full susceptibility to IASCC does not appear suddenly at a threshold level. Instead, susceptibility begins at this threshold fluence level and increases with increasing fluence over several tens of dpa.

IASCC can be forced in the laboratory by slow strain rate tensile tests at neutron exposures as low as 1 dpa. This effect however, can only be seen after extremely high strains near 40% reduction in area of the test specimens. Such conditions should not exist in actual component items of PWR internals. A better measure of the threshold for initial concern would be the fluence at which cracking can be initiated at above the yield stress of the material. Shogan demonstrated that this level was about 3 dpa for various heats of cold-worked 316 stainless steel.^[B-23, B-41] This level corresponds to that found in the French Bugey plant, referenced above, which has been found to be the most IASCC susceptible material tested to date.

No one, as of yet, has developed a sufficient understanding of IASCC to predict with certainty the effects of thermo-mechanical history and the chemical composition of a material on the threshold for IASCC, if any. Threshold values for IASCC in PWR internals materials are expected to vary considerably with material, heat, temperature, and neutron spectrum. Developing a single value for all materials and Nuclear Steam Supply System (NSSS) designs can only be done in a fairly conservative manner. Therefore, it is suggested that a fluence threshold of 2×10^{21} ($E > 1.0$ MeV) [3 dpa] be utilized for highly stressed component items such as bolts, springs, and multi-pass welds.

At the current time, the understanding of IASCC is not sufficiently advanced to suggest reliable predictive rules for PWR internals materials. As shown in Figure B-1, IASCC appears to correlate fairly well with stress and neutron dose for a given heat of material. This figure indicates that a saturation in the stress vs. IASCC initiation curve of approximately 100 MPa (14 ksi) at neutron exposures greater than 80 dpa may exist.

Figure B-3 is a proposed screening curve for IASCC initiation of austenitic stainless steels. This curve is based on a shifting of the Figure B-1 curve to account for the observed baffle bolt failures in Europe. It is suggested that stress and dose levels from this curve be utilized as screening criteria for IASCC at neutron doses $\geq 2 \times 10^{21}$ ($E > 1.0$ MeV) [3 dpa].

Figure B-3
Proposed Plot of Stress and Neutron Exposure Screening Criteria for IASCC.

B.4 IASCC References

- B-1 McNeil, M.B., "Irradiation Assisted Stress Corrosion Cracking," *Nuclear Engineering and Design*, 181, 1998, pp. 55-60.
- B-2 Scott, P., "A Review of Irradiation Assisted Stress Corrosion Cracking of Austenitic Materials for PWR Core Internals", Framatome, France, Eurocorr, Sept. 1996.
- B-3 Scott, P., "A Review of Irradiation Assisted Stress Corrosion Cracking", *Jour. Of Nuclear Materials*, 211 (1994), pp. 101-122.
- B-4 Andresen, P.L., "Irradiation-Assisted Stress-Corrosion Cracking," in *Stress Corrosion Cracking - Materials Performance and Evaluation*, ed. R.H. Jones (American Society for Metals, Metals Park, OH, 1992), pp. 182-210.
- B-5 Nelson, J.L., and Andresen, P.L., "Review of Current Research and Understanding of Irradiation-Assisted Stress Corrosion Cracking," *Proc. 5th Int. Symp. on Environmental Degradation of Materials in Nuclear Power Systems - Water Reactors*, Monterey California, August, 1991, NACE, pp. 10-26.

- B-6 Meeting Notes of the JOBB Task Team With EDF on Baffle/Former Bolts, April 3-4, 1997, Moret-Sur-Loing, France, EPRI.
- B-7 Andresen, P.L., Ford, F.P., Murphy, S.M., and Perks, J.M., "State of Knowledge of Radiation Effects on Environmental Cracking in Light Water Reactor Core Materials," Proc. 4th Int. Symp. on Environmental Degradation of Materials in Nuclear Power Systems - Water Reactors, Jekyll Island, Georgia, August, 1989, NACE, pp. 1-83 - 1-121.
- B-8 Hanninen, H., and Aho-Mantilla, I., "Environmental-Sensitive Cracking of Reactor Internals", Proc. 3rd Int. Symp. on Environmental Degradation of Materials in Nuclear Power Systems - Water Reactors, Traverse City, Michigan, August 30 - September 3, 1987, AIME, pp. 77-92.
- B-9 Bruemmer, S.M., et al., "Reviews for the Understanding and Evaluation of Irradiation-Assisted Stress Corrosion Cracking," Critical Issue Reviews for the Understanding and Evaluation of Irradiation-Assisted Stress Corrosion Cracking, EPRI TR-107159, 4068, Final Report, November, 1996.
- B-10 Cole, J.I., et al., "Deformation Temperature, Strain Rate, and irradiation Microstructure Effects on Localized Plasticity in 304L SS," Proc. 7th Int. Symp. On Environmental Degradation of Materials in Nuclear Power Systems – Water Reactors, NACE, 1995.
- B-11 Simonen, E.P., and Bruemmer, S.M., "Kinetic Evaluation of Intergranular Fracture in Austenitic Stainless Steels," Proc. 7th Int. Symp. On Environmental Degradation of Materials in Nuclear Power Systems – Water Reactors, NACE, 1995.
- B-12 Garner, F.A., "Irradiation Performance of Cladding and Structural steels in Liquid Metal Reactors," Materials Science and Technology, Vol. 10A, VCH, Weinheim, 1994, pp. 422-543.
- B-13 Yang, W.J.S., "Grain boundary segregation in Solution-Treated Nimonic PE16 During Irradiation," J. Nucl. Mater., 108-109, 1982, pp. 339-346.
- B-14 "Critical Issue Reviews for the Understanding and Evaluation of Irradiation-Assisted Stress Corrosion Cracking," EPRI TR-107159, November 1996.
- B-15 Joint Owners Baffle Bolt Program, JOBB-CD, Version 05.12, EPRI 1012083, 2005.
- B-16 Jacobs, A.J., Wozadlo, G.P., Nakata, K., Yoshida, T., and Masaoka, I., "Radiation Effects on The Stress Corrosion and Other Selected Properties of Type-316 Stainless Steels," Proc. 3rd Int. Symp. on Environmental Degradation of Materials in Nuclear Power Systems - Water Reactors, Traverse City, Michigan, August 30 - September 3, 1987, AIME, pp. 673-681.

- B-17 Lucas, G.E., "The Evolution of Mechanical Property Change in Irradiated Austenitic Stainless Steels," *Journal of Nuclear Materials*, Vol. 206 (1993), pp. 287-305.
- B-18 Xu, H., "Current Understanding of the Irradiation-Assisted Stress Corrosion Cracking Potential for PWRs," BAW-2314, FANP, November 1997.
- B-19 Cauvin, R., et al., "Damage to Lower Internals Structures Subject to Heavy Fluence: Expert Evaluations," *Contribution of Materials Investigation to the Resolution of Problems Encountered in Pressurized Water Reactors*, Vol. 1, Sept. 12-16, 1994, France.
- B-20 Cauvin, R., Rouillon, Y., Meylogan, T., and Goltrant, O., "Intergranular Cracking of Irradiated Austenitic Stainless Steels Core Materials in PWR," *Effects of Radiation on Materials: 18th International Symposium*, ASTM, STP 1325, R.K. Nanstad, M.L. Hamilton, F.A. Garner, and A.S. Kumar, Eds., ASTM, 1997.
- B-21 Bourgoïn, J., et. al., "Contribution a la Connaissance du Comportement Sous Irradiation des Crayons de Grappes de Commande," *Contribution of Materials Investigation to the Resolution of Problems Encountered in Pressurized Water Reactors, Fontevraud III*, Volume 2, 1994.
- B-22 Scott, P., Deydier, D., Trenty, A., "Analysis of Baffle/Former Bolt Cracking in French PWRs," ASTM-1401, R.D. Kane, Ed., 2000.
- B-23 Shogan, R.P., and Mager, T.R., "Susceptibility of Type 316 Stainless Steel to Irradiation Assisted Stress corrosion Cracking in a PWR Environment," *Proc. 10th Int.Conference on Environmental Degradation of Materials in Nuclear Power Systems - Water Reactors*, 2002.
- B-24 Kanasaki, H., et al., "Fatigue and Stress Corrosion Cracking Behaviors of Irradiated Stainless steels in PWR Primary Water," *Proceedings of ICON 5: 5th International Conference on Nuclear Engineering*, 1997.
- B-25 Fukuya, K., et al., "IASCC Susceptibility and Slow Tensile Properties of Highly-Irradiated 316 Stainless Steels," *Journal of Nuclear Science and Technology*, Vol. 41, No. 6, p. 673-681, June 2004.
- B-26 Lucas, G.E., and Hamilton, M.L., "Small Specimen Testing For Irradiated Austenitic Stainless Steels," *Critical Issue Reviews for the Understanding and Evaluation of Irradiation-Assisted Stress Corrosion Cracking*, EPRI TR-107159, 4068, Final Report, November, 1996.
- B-27 Eyre, B.L., and Matthews, J.R., "Technological Impact of Microstructural Evolution During Irradiation," *Journal of Nuclear Materials*, 205 (1993), pp. 1-15.

- B-28 Garner, F.A., Black, C.A., and Edwards, D.J., "Factors Which Control the Swelling of Fe-Cr-Ni Ternary Austenitic Alloys," *Journal of Nuclear Materials*, 245 (1997), pp.124-130.
- B-29 Wang, Y.S., et al., "The Study of Bubble Formation in 316L Stainless Steel Irradiated With Helium Ions at 873 K," *Journal of Nuclear Materials*, 240 (1996), pp. 70-74.
- B-30 Hide, K., Onchi, T., Oyamada, R., Kayano, H., "Mechanical Response of Irradiated Thermally-Sensitized Type 304 Stainless Steels," *Journal of Nuclear Materials*, 232 (1996), pp. 30-43.
- B-31 Garzarolli, F., Deves, P., Hahn, R., and Nelson, J.L., "Deformability of High-Purity Stainless Steels and Ni-Based Alloys in the Core of A PWR," *Proc. 6th Int. Symp. on Environmental Degradation of Materials in Nuclear Power Systems - Water Reactors*, San Diego, California, August, 1993, AIME, pp. 607-613.
- B-32 Tsukada, T., Miwa, Y., Nakajima, H., "Stress Corrosion Cracking of Neutron Irradiated Type 304 Stainless Steels," *Proc. 7th Int. Symp. on Environmental Degradation of Materials in Nuclear Power Systems - Water Reactors*, Breckenridge, Colorado, August, 1995, NACE, pp. 1009-1019.
- B-33 Kasahara, S., et al. "The Effects of Minor Elements on IASCC Susceptibility in Austenitic Stainless Steels Irradiated with Neutrons," *Proc. 6th Int. Symp. on Environmental Degradation of Materials in Nuclear Power Systems - Water Reactors*, San Diego, California, August, 1993, AIME, pp. 615-623.
- B-34 Pettersson, K., and Simonen, E.P., "Radiation Effects on Deformation of Austenitic Alloys in Light Water Reactors," *Critical Issue Reviews for the Understanding and Evaluation of Irradiation-Assisted Stress Corrosion Cracking*, EPRI TR-107159, 4068, Final Report, November, 1996.
- B-35 PWR Reactor Pressure Vessel Internals, License Renewal Industry Report; Revision 1, TR-103838, Research Project 2643-32, Final Report, July 1994.
- B-36 Mills, W.J., "Fracture toughness of Irradiated Stainless Steel Alloys," Westinghouse Hanford Company, P.O. Box 1970, Richland, Washington, 99352.
- B-37 The 4th EPRI Workshop on PWSCC of Alloy 600 in PWRs, February, 1997, Daytona, Florida.
- B-38 Conermann, J., et al., "Irradiation Effects in a Highly Irradiated Cold Worked Stainless Steel Removed from a Commercial PWR," *Proc. of the 12th Int. Symp. on Environmental Degradation of Materials in Nuclear Power Systems - Water Reactors*, TMS, August 2005 (to be published).
- B-39 Bruemmer, S.M., et al., *J. Nuclear Materials*, Vol. 274, 1999, pp. 299-314.

- B-40 Materials Reliability Program: Hot Cell Testing of Baffle/Former Bolts Removed From Two Lead Plants (MRP-51), EPRI Report 1003069, 2001.
- B-41 Materials Reliability Program: Characterization of Type 316 Cold-Worked Stainless Steel Highly Irradiated Under PWR Operating Conditions (MRP-73), EPRI Report 1003525, 2002.
- B-42 Materials Reliability Program: Characterization of Decommissioned PWR Vessel Internals Material Samples - Tensile and SSRT Testing (MRP-129), EPRI Report 1008205, 2004.
- B-43 Materials Reliability Program: Crack Initiation Testing and Slow Strain Rate Tensile (SSRT) Testing of Boris-60 Irradiated Materials, and Effect of Hydrogen on IASCC Susceptibility (MRP-159), EPRI Report 1010096, 2005.
- B-44 Materials Reliability Program: A Review of the Cooperative Irradiation Assisted Stress Corrosion Cracking Research Program (MRP-98), EPRI Report 1002807, 2003.
- B-45 Materials Reliability Program: Stress Corrosion Cracking of High Strength Reactor Vessel Internals Bolting in PWRs (MRP-88), EPRI Report 1003206, 2003.
- B-46 R. Bajaj, W. J. Mills, M. R. Lebo, B. Z. Hyatt, and M. G. Burke “Irradiation-Assisted Stress Corrosion Cracking of HTH Alloy X-750 and Alloy 625,” Proceedings of Seventh International Symposium on Environmental Degradation of Materials in Nuclear Power Systems—Water Reactors, American Nuclear Society, 1997.

C

APPENDIX C: WEAR

C.1 General Description of Wear

Wear in metals is the localized damage and material loss that results from the relative motion between two surfaces in contact.² Abrasive wear, fretting wear, or mechanical wear are names for different types (or processes) of wear. Wear may occur in one or a combination of the following interactions between two materials (materials couple): 1) contact between surface asperities where the weaker material would suffer local yielding and ultimately asperity failure (microscopic level); 2) shearing of surface oxides; 3) local welding (due to friction) and subsequent separation of the weld zone (like galling in a bolted joint) or by; 4) local work hardening of two materials with the same or similar mechanical properties (e.g., a couple consisting of Type 304 materials, typical of many PWR internals situations).^[C-1] The forces of interest in assessing the potential for wear in PWR internals are generally due to sliding (momentary such as during installation) or excitations due to flow-induced vibration (FIV). These forces produce wear as described in either 1 or 4 above. (Note: “welding” or “galling” referred to here is not a common occurrence.) Examples of wear are provided in Figures C-1 through C-3. Classic examples of a form of wear in a PWR are between steam generator tubes and tube support plates and fuel cladding and fuel cladding assembly grid spacers. This particular form of wear is referred to as fretting; the result of oscillatory relative motion between the tubes (i.e., FIV), in each case, and the mating part.^[C-2]

Generally, (as noted here and in referenced license renewal reports^[C-3,C-4] the main component items, in the various PWR internals designs, subject to damage are austenitic stainless steels (e.g., Types 304 and 316). However, component items fabricated from other materials have also been affected. It is worth noting that a rather complete data set on the wear rates of various material couples typically used in light water reactor applications can be found in Reference C-1. The environment is virtually the same in all designs as well with the exception of the neutron fluence (or, dpa) achieved in each design. Despite the similarities in materials, environment and basic design configurations, there are some significant features in each PWR internals design that end up being far more important in identifying wear susceptible locations. The next subsection provides examples of wear induced failures and notes some of the changes made to avoid future problems.

² Erosion, erosion-corrosion, and flow-accelerated corrosion (FAC) are not anticipated to be of concern for the materials used in PWR internals.

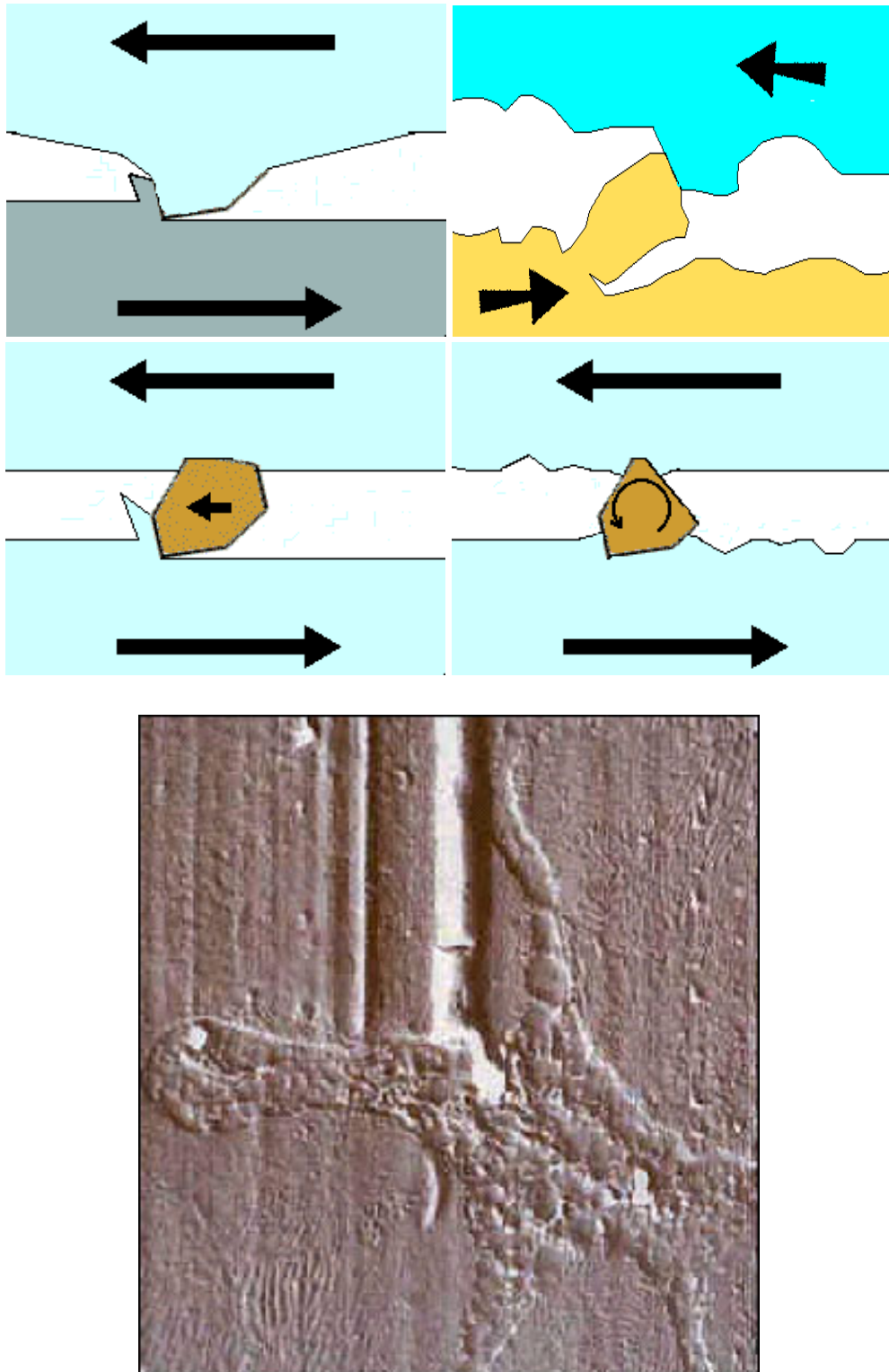


Figure C-1
Abrasive Wear Example

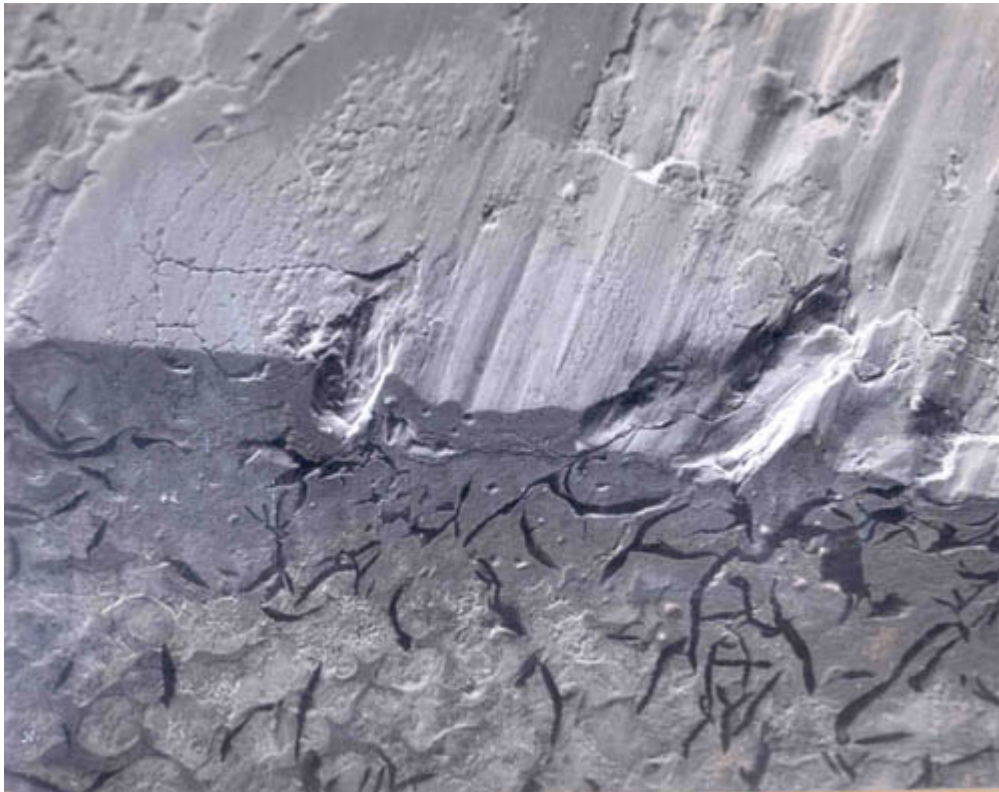
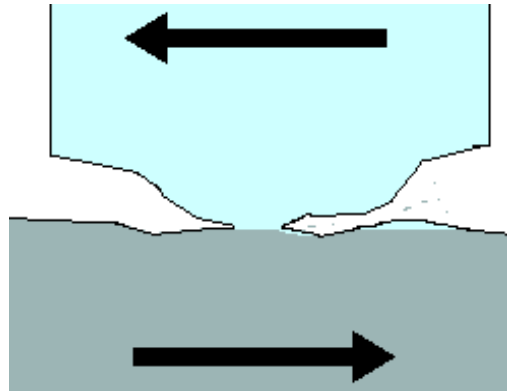


Figure C-2
Adhesive Wear Example

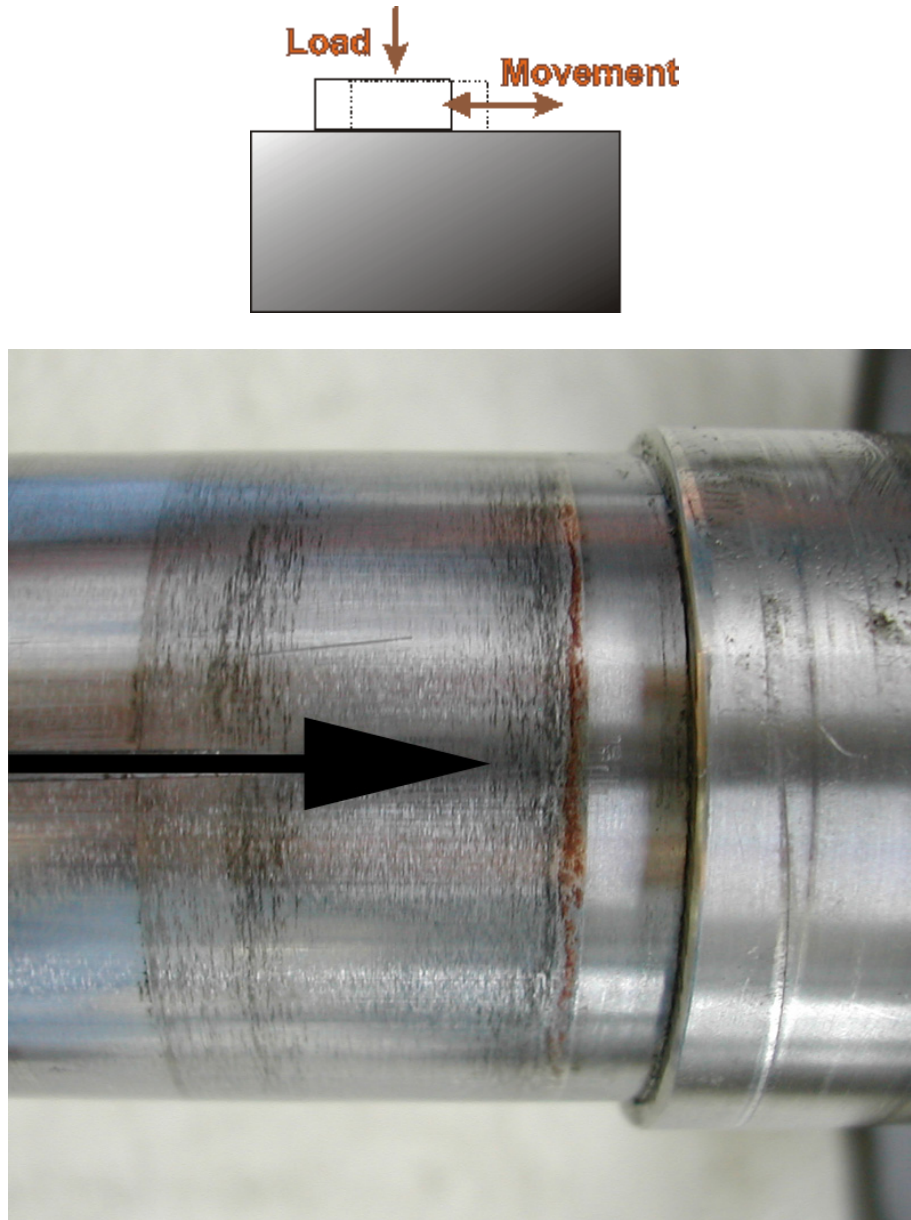


Figure C-3
Fretting Wear Example

C.2 PWR Internals Wear Events

C.2.1 Westinghouse Internals Designs

The flux thimble and guide tubes, part of the in-core neutron monitors in Westinghouse designed PWR internals, have experienced thinning and leaks due to wear. The wear was identified as fretting wear produced by FIV excitations (IE Information Notice No. 87-44).^[C-5] The thimble tubes extend from the seal table (~100 feet from the bottom of the reactor vessel), through

stainless steel piping and then through nozzles in the bottom of the reactor vessel up through the lower PWR internals and into the bottom of selected fuel assemblies. The portion of the guide tube between the bottom of these fuel assemblies and the top of the “lower core plate” is subjected to FIV forces (refer to Figure 1-4 in the main text of this report). This is the location where fretting damage has been observed. Various measures have been taken in response to IE Bulletin 88-09 resulting in plant-specific changes.^[C-5, C-6] Basically, eddy current methods have been used to monitor the extent of thinning. The problem with this situation, currently being managed through inspection strategies, is that a leak could become a breach in the pressure boundary that requires closing a valve manually.

C.2.2 B&W Internals Design

The B&W designed 177-FA(fuel assembly) PWR internals also use incore instrumentation in a configuration similar to the Westinghouse design.^[C-3] However, to this point, no significant wear-induced damage has been observed.

Vent valves are located in the upper plenum in the B&W 177-FA plant design (refer to Figure 1-2 in the main text of this report). During the 1978-1980 time period, routine visual inspections revealed signs of wear in the “jacking screw” locking cup in a few cases. The source of the wear was FIV in the locking cup, which consists of a spring and cup arrangement. The locking cup, fabricated from Type 304 SS, was subsequently modified on the affected vent valves. No further significant wear has been detected in either the original or modified configurations.

During the 1972-1973 time period, the initial design of the RV Surveillance Program holder tubes suffered significant FIV-induced wear. This resulted in complete re-design of the holder tubes and the reactor vessel materials surveillance program.^[C-7]

C.2.3 CE Internals Designs

The CE designed PWR internals use incore instrumentation that is inserted through the RV closure head with exception of 1 or 2 plants. No problems have been reported.

The CE designed units have, however, experienced excessive wear due to FIV early in life in the Type 304 SS holddown ring used to provide clamping forces of the PWR internals at the RV flange. The material in the holddown ring was changed to Type 403 SS to provide additional spring force; this has corrected the problem.^[C-8]

Other areas of potential concern were identified in License Renewal Reports covering the various designs supplied by Westinghouse, Combustion Engineering and, Babcock and Wilcox including control rod guide tubes, supports pads located on the outside diameter (OD) of the upper grid assembly, clevises, guide blocks (radial support blocks) and mating surfaces in the junction formed by the core support assembly, the reactor vessel flange and closure head.

C.3 Potential Long Term Issues

Wear in the PWR internals may occur during installation and subsequent inspection operations where there is sliding motion, and potential impact of adjacent parts may occur. These particular situations are monitored through periodic inspections either by utility inspection instituted plans or Section XI of the ASME B&PV Code.^[C-9] The consequences of the localized fit-up type of wear has the potential of leading to more serious forms of damage should the localized metal loss exceed design allowances. The same could be asserted for the other materials aging degradation mechanisms discussed in other portions of this document. While FIV damage can accumulate quickly (e.g., during hot functional testing), bolted joints present particular areas of concern. For example, if sufficient irradiation-induced stress relaxation were to occur and result in gaps, hydrodynamic forces from FIV could produce significant damage in a short period of time after many years of trouble-free operation. Some of the PWR internals are subjected to neutron fluence levels for which stress relaxation of bolted joints is a concern (Appendix H). This could lead to significant wear in portions of the core support assembly and structural instability. However, the more likely failure mechanism would be expected to be fatigue.

General corrosion, induced from localized environmental conditions in a crevice (e.g., a bolted connection), is not an issue in oxygen-free environments and so has no potential to result in metal loss of significance in the structure's response to FIV. Similarly, flow-accelerated corrosion (FAC) of stainless alloys is unknown in LWR coolants and so cannot influence FIV response. One potentially important source of unusually high FIV loadings can be changes in the manner in which a plant is operated, i.e., pump operation, uprate, etc. Distortions produced in the PWR internals resulting from localized irradiation-induced swelling and growth (Appendix G) could also alter structural response to FIV loadings.

C.4 Wear Threshold and Screening Criteria

The development of PWR internals threshold and screening criteria for wear are based on the following assumptions:

- a. There are no flux or fluence dependencies associated with wear, per se. [Note however that SR/IC, covered in Appendix H, could affect wear rates in bolted connections, for example.]
- b. Wear is affected by the mechanical properties of the surfaces in contact. Wear rates could change with the local temperature and degree of IE, but neither is quantifiable at this time.
- c. Wear (from erosion, erosion-corrosion, and FAC) is not a concern for PWR internals materials.

It is known that wear is influenced by a variety of parameters. These parameters, in general, include the following:

- Material parameters include composition, grain size, modulus, thermal conductivity, degree of work hardening, hardness, etc.
- Design parameters include shape, loading, type of motion, roughness, vibration, cycle time, etc.

- Environmental parameters include temperature, humidity, atmosphere, contamination, corrosion potential, etc.
- Lubrication parameters include type of lubricant, lubricant stability, type of fluid lubrication, etc.
- Presence or absence of wear-in (or break-in).

It is therefore concluded that no clearly defined threshold values can be developed for PWR internals materials.

There also are no quantitative screening criteria that can be identified for wear concerns. Therefore, it is concluded that for screening purposes, PWR internals locations be identified where wear is likely to occur, based on the following criteria:

- a. Locations where relative motion may occur between component items (such as control rod guide tubes)
- b. Locations where clamping force is required (such as the mating ledge between the internals and the RV).
- c. All bolted or spring locations where irradiation-enhanced stress relaxation/creep has been screened as applicable.

C.5 Wear References

- C-1 D.J. DePaul, Corrosion and Wear Handbook, TID 7006, March 1957.
- C-2 AuYang, M.K., Flow-Induced Vibration of Power and Process Plant Components, ASME Press, 2001, New York.
- C-3 Clark, R.W., and Gregory, FM., “Demonstration of the Management of Aging Effects for the Reactor Vessel Internals,” Framatome ANP Document BAW-2248A, March 2000.
- C-4 Forsyth, D.R., et al., “License Renewal Evaluation: Aging Management for Reactor Internals,” WCAP-14577, Revision 1-A, October 2000.
- C-5 Nuclear Regulatory Commission Information Notice No. 87-44: Thimble Tube Thinning in Westinghouse Reactors, September 16, 1987.
- C-6 Nuclear Regulatory Commission Bulletin No. 88-09, Thimble Tube Thinning in Westinghouse Reactors, July 26, 1988.
- C-7 Lowe, A.L., et al., “Integrated Reactor Vessel Material Surveillance Program for Babcock & Wilcox 177-FA Plants,” Effects of Radiation on Materials, Twelfth International Symposium, American Society for Testing and Materials, Volume II, ASTM STP 870, 1985.

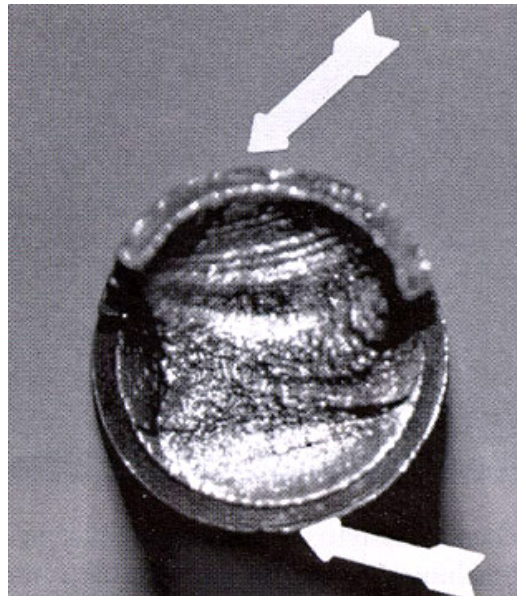
- C-8 Luk, K.H., “Pressurized-Water Reactor Internals Aging Degradation Study,” NUREG/CR-6048, September 1993.
- C-9 ASME Boiler and Pressure Vessel Code, Section XI, Rules for Inservice Inspection of Nuclear Power Plant Components, 2004 Edition, American Society of Mechanical Engineers.

D

APPENDIX D: FATIGUE

D.1 General Description of Fatigue

Fatigue of metals is a metallurgical degradation process involving the evolution of persistent slip bands at the surface and subsequent crack formation and propagation during exposure to cyclic stresses. Fatigue failures may occur in structures due to exposure to cyclic stresses with magnitudes well below the monotonic tensile fracture stress. The forms of fatigue that can (generally) occur include low-cycle fatigue (LCF) associated with significant plastic strains, and high-cycle fatigue (HCF) that occurs at stresses below the elastic limit (cyclic lives $> 10^5$ or 10^6 cycles, depending on the material). Figure D-1 provides a classic example of a bolting HCF failure. Also, for both cases, the environment can have an impact on the final fatigue results. This is known as environmentally-enhanced or corrosion fatigue.



(Arrows denote the fatigue initiation sites)

Figure D-1
Classical Fatigue Failure of a Bolt by Reverse Bending

The source of cyclic stresses may arise from one or more of a combination of mechanical, thermal or flow-induced sources. The process is often described as occurring in four stages:

- a. Nucleation of localized plastic damage (formation of persistent slip bands)

- b. The growth of micro-cracks with sizes typically of the same order as the material grain size
- c. The formation and growth of micro-cracks to one or more cracks of critical size, and
- d. The subsequent growth of a macro-crack, which is often expressed in terms of the Paris equation, $da/dN = C\Delta K^n$.

The percentage of total fatigue life varies among the forms of fatigue, e.g., in HCF, stages 1, 2 and 3 can occupy from 70% to 90% of the total fatigue life. In LCF, the formation of a detectable crack may occur much earlier in life, and its growth – in general – predicted using fracture mechanics. The theories of fatigue in metals are well documented in countless periodicals and text books.^[D-1] LCF and HCF are briefly described below in terms of how they might occur (or have occurred in LWR component items). Of potential importance with regard to the PWR internals is environmentally-enhanced fatigue that can significantly affect fatigue lives in either the low or high cycle regimes.

D.1.1 Low-Cycle Fatigue (LCF)

LCF is due to relatively high stress range cycling where the number of cycles to failure is less than about 10^4 to 10^5 . To induce cracking at this number of cycles, the stress/strain range causes plastic strains that exceed the yield strength of the material. The cycling causes local plasticity concentration in persistent slip bands leading to rapid material fatigue degradation. The stress cycling that contributes to LCF is generally due to the combined effects of pressure and temperature changes that result from normal operation particularly during plant heat-up and cool-down cycles and for which the design procedures of Section III of the ASME B&PV Code have to date been very successful in avoiding failures due to this cause. Generally, as noted above, cracks are initiated early in the fatigue life (approx. 10% of life) and propagate to critical size over the remaining life (approx. 90% of life).

D.1.2 High-Cycle Fatigue (HCF)

HCF may be:

- Mechanical in nature, i.e., vibration or pressure pulsation or due to FIV. FIV can induce HCF in otherwise normally passive component items merely through the interaction of flow adjacent to the component item or within the system, establishing a cyclic resonant stress response in the component item. Thus, attention has to be directed to bolted connections subject to relaxation, particularly by irradiation-enhanced creep. Additionally, power uprates are also of concern as an increase in flow may change the acoustical characteristics of the system and excite an HCF mode where a resonant frequency is achieved.
- Thermally-induced due to mixing of cold and hot fluids where local instabilities of mixing lead to low-amplitude, high-cycle thermal stresses at the component item surfaces exposed to the fluid; this is generally referred to as thermal striping. Often, the damage (cracking) is self limiting in depth due to the attenuation of the local temperature variations at a short distance below the surface.

D.1.3 Environmental or Corrosion Fatigue

The terms “environmental fatigue” or “corrosion fatigue” refer to the reduction in fatigue “life” in an aqueous or gaseous environment compared to the air environment. Environmental fatigue is potentially an issue for LWR Owners, the NRC and stakeholders and has been the subject of considerable research and rules making activities throughout the world for over 20 years.

Environmental fatigue, in the context of these activities, involves two primary elements: (1) the effects of a PWR environment on the overall fatigue life (as represented by either multiplying the fatigue usage factor by a penalty factor to account for environment or use of an environment-adjusted fatigue design curve), and (2) the potential accelerated growth of an identified defect due to the PWR environment. Environmental acceleration of fatigue crack growth is important in dispositioning detected/postulated flaws in a component item to permit continued operation. Of course the environment present for the PWR internals also involves consideration of the effects of neutron irradiation. The work of several researchers suggest that neutron irradiation does not result in a further reduction in fatigue properties and in some cases suggest an improvement.^[D-2 – D-4]

However, minimal data on the combined effects of the PWR water chemistry and neutron fluence currently exist in the literature.

The current industry situation and evolving consensus process involves the adoption of specific rules for addressing environmental fatigue in the materials used in the PWR internals. Basically, the rules to address operating plants, either during the current license or license renewal, or for new plants are in the formative stage and agreements are evolving among the affected organizations. There are many key references in this regard including References D-5 through D-11.

D.2 Application of ASME B&PV Code Rules

At the time most PWR internals were designed, no specific fatigue design rules existed in the ASME B&PV Code. Later, the ASME B&PV Code began work on Subsection NG, “Core Support Structures” and a draft version was available for guidance in some cases. Subsection NG was first issued in the Winter 1973 Addenda to the 1971 Edition of the ASME B&PV Code.^[D-12]

As a result, the methodologies employed by the designers varied in assessing fatigue on PWR internals. In the case of the B&W-designed plants, calculated cyclic stress levels were compared with “endurance limit values” from projections (extrapolations) of the then existing “in air” fatigue data to 10^{12} cycles for 40 years of operation.^[D-13] These calculations, to determine fatigue usage factors (a.k.a., cumulative usage factors [CUFs]), were then reassessed in terms of actual plant transients for license renewal purposes. The original calculations were determined to be very conservative. The other NSSS designers used various approaches to basically make similar conclusions regarding the conservative nature of the original calculations. In the various license renewal submittals, the PWR internals designers identified the component items with the most significant usage factors.^[D-14,D-15] Significant usage factors were calculated in some cases, including baffle-to-former and other forms of bolting. The challenge in the future will be to apply any fatigue reduction environmental factors to establish revised fatigue usage factors if such an approach is adopted.

D.3 Fatigue Summary and Discussion

The understanding of environmental fatigue is still evolving and is under considerable discussion in the technical community,^[B-15] Code bodies, and regulatory agencies. Laboratory data indicate that the fatigue resistance of austenitic stainless steels and nickel-base alloys is lower in deoxygenated primary water environments dependent on the cyclic frequency or rising load strain rate than in room-temperature air. Code safety factors may not bound this difference in all cases in the LCF region.

The PWR internals are also exposed to neutron irradiation of very low to extremely high values. Limited results suggest that these exposures do not result in a further reduction in fatigue properties and in some cases an improvement is suggested. The HCF life should be expected to increase by irradiation due to the increase in the yield strength of the material. For LCF, however, since the stresses are high, if the time at stress is sufficiently long it is expected that IASCC will initiate and reduce the fatigue life.^[D-16] However, the combined effects of the PWR coolant and neutron fluence are not documented.

Difficulty often arises in evaluating fatigue when the total comprises both HCF and LCF. In theory, a particular CUF calculation can be expressed as a summation of LCF and HCF component items. However, a simple summation is not always appropriate. A component item that is subject to LCF prior to being subject to HCF is not equivalent to the reverse order of fatigue loading. Therefore, for component items subjected to both LCF and HCF, transient tracking may not be appropriate to monitor damage due to fatigue.

A number of parameters are important to the fatigue of a material. These include stress amplitude, mean and maximum stress, surface roughness, and temperature. As each of these increases in magnitude, the number of cycles required for failure decreases. Geometry also affects fatigue because of stress concentrations. It has been dealt with pragmatically and apparently successfully to date by the current ASME B&PV Code Section II design rules. In addition, the occurrence of other degradation mechanisms may affect fatigue life. For instance, SCC may initiate a flaw and HCF may propagate it to failure rather rapidly.

D.4 Fatigue Threshold and Screening Criteria

The development of PWR internals threshold and screening criteria for fatigue are based on the following assumptions:

- a. Water chemistry conditions, in accordance with EPRI guidelines, are maintained.
- b. Fatigue can occur within all PWR materials, subjected to cycling (mechanical or thermal).
- c. Fatigue can occur at all PWR internals temperatures. However, temperature gradients are of concern (e.g., those occurring during transients).

The threshold values for fatigue depend on the HCF usage factors and cyclic stresses for LCF. As material aging concerns with IE, IASCC, etc. occur, LCF and/or HCF may become an issue. It will most likely be required to consider each load or stress pair in terms of yet to be formalized

threshold values. The current industry thinking on appropriate threshold values (for the environmental effects on fatigue) are contained in Reference D-11. This document includes the following threshold values for 300-series stainless steel for license renewal (but not limited to):

- Strain range $\leq 0.20 \%$
- Strain rate $\geq 0.4 \%/second$
- Temperature $\leq 356 \text{ }^{\circ}\text{F}$ ($180 \text{ }^{\circ}\text{C}$)
- Dissolved Oxygen no threshold

In case any one of these thresholds is met, the fatigue penalty factor $F(en)$ is equal to 1.0 for that particular load or stress pair. This means that the particular load or stress pair is not impacted by the environmental effects on fatigue.

The threshold values listed above can also be found in the latest Welding Research Council (WRC) Bulletin on the subject of the environmental effects on fatigue. They are listed in the Article X-2000 of Section 7.0 (Code Implementation) of WRC Bulletin 487, dated December 2003.^[D-6]

Other threshold values under evaluation include the R value and hold time while in tension. There are currently differences between the industry and the NRC on the magnitude of the threshold environmental factors to consider (this subject must be addressed at a later date). Therefore, no clear threshold criteria can be developed at this time.

For screening purposes, in lieu of clear codified guidelines regarding the effects of environmentally-enhanced fatigue (including irradiation effects), the following criteria are suggested:

- a. All bolted connections or springs where irradiation-enhanced stress relaxation/creep is screened as applicable.
- b. Locations where the CUF values are > 0.10 (calculated for a 40-year life) should be identified.³

Follow-on evaluations for functionality may include engineering judgment or the use of the currently NRC-accepted methods described in Reference D-8; however, as noted above, there is currently no clear industry consensus for addressing environmental fatigue concerns.

D.5 Fatigue References

D-1 American Society of Metals Handbook, "Fatigue and Fracture," Volume 19, 1996.

³ In some instances fatigue life was alternatively qualified through testing. These component items should be initially screened in for potential fatigue concerns and evaluated.

- D-2 Shahinian, P., “Fatigue Crack Propagation in Fast Neutron Irradiated Stainless Steels and Welds,” *Properties of Reactor Structural Alloys After Neutron or Particle Irradiation*, ASTM STP 570, American Society for Testing and Materials, 1975.
- D-3 Michel, D.J., “Irradiation Effects on Fatigue Crack Propagation in Austenitic Stainless Steels,” NRL Memorandum Report 3610, September 1977.
- D-4 Shahinian, P., “Effect of Neutron Irradiation on Fatigue Crack Propagation in Types 304 and 316 Stainless Steels at High Temperature,” NRL Report 7446, July, 1972.
- D-5 “Guidelines for Environmental Fatigue Evaluation for LWR Components,” Thermal and Nuclear Power Engineering Society (TENPES), June 2002 (Translated into English in November 2002).
- D-6 Van der Sluys, W.A., “PVRC’s Position on Environmental Effects on Fatigue Life in LWR Applications,” Welding Research Council, Inc. Bulletin No. 487, 2003.
- D-7 NUREG/CR-5999 (ANL-93/3), “Interim Fatigue Design Curves for Carbon, Low-Alloy, and Austenitic Stainless Steels in LWR Environments,” April 1993.
- D-8 NUREG/CR-6260 (INEL-95/0045), “Application of NUREG/CR-5999 Interim Fatigue Curves to Selected Nuclear Power Plant Components,” March 1995.
- D-9 NUREG/CR-5704 (ANL-98/31), “Effects of LWR Coolant Environments on Fatigue Design Curves of Austenitic Stainless Steels,” April 1999.
- D-10 Stevens, G.L., and Davis, J.M., “Guidelines for Addressing Fatigue Environmental Effects in a License Renewal Application (MRP-47 Revision 1),” Industry Guidance Document, TR-1012017, May 18, 2005 Draft 1G.
- D-11 Mehta, H.S., “An Update on the Consideration of Reactor Water Effects in Code Fatigue Initiation Evaluations for Pressure Vessels and Piping,” PVP-Volume 410-2, American Society of Mechanical Engineers, 2000.
- D-12 Winter 1973 Addenda, 1971 Edition of Subsection NG of the ASME B&PV Code.
- D-13 Fyffitch, S., et al., “Oconee Nuclear Power Station Unit 1 Reactor Vessel Internals Life Extension Project,” BAW-2060, October 1988.
- D-14 Clark, R.W., and Gregory, FM., “Demonstration of the Management of Aging Effects for the Reactor Vessel Internals,” Framatome ANP Document BAW-2248A, March 2000.
- D-15 Forsyth, D.R., et al., “License Renewal Evaluation: Aging Management for Reactor Internals,” WCAP-14577, Revision 1-A, March 2001.

- D-16 Conermann, J., et al., "Irradiation Effects in a Highly Irradiated Cold Worked Stainless Steel Removed from a Commercial PWR," Proc. of the 12th Int. Symp. on Environmental Degradation of Materials in Nuclear Power Systems - Water Reactors, TMS, August 2005 (to be published).

E

APPENDIX E: THERMAL AGING EMBRITTLEMENT

E.1 General Description of Thermal Aging Embrittlement

Thermal aging embrittlement (TE), sometimes simply known as thermal embrittlement, is a time and temperature dependent process whereby a material undergoes microstructural changes leading to decreased ductility, and degradation of toughness and impact properties. MRP-80^[E-1] is a document that was prepared for the MRP to summarize the available TE data for materials utilized in PWRs and to identify those materials potentially susceptible to TE. Much of the information utilized in this section is contained in that summary report.

This phenomenon is usually accompanied by an increase in yield strength, ultimate tensile strength, and hardness. Wrought austenitic stainless steels and nickel-base alloys are not subject to TE at PWR operating temperatures.^[E-2] For the PWR internals, the only materials that are potentially susceptible to TE are cast austenitic stainless steels (CASS), austenitic stainless steel welds, martensitic stainless steels, and martensitic precipitation-hardenable (PH) stainless steels.^[E-3, E-4] CASS and PH materials are typically embrittled in the temperature range of 700 to 1000°F (371 to 538°C) within a short time.^[E-5] For example, Charpy impact test data show that CASS TE reaches saturation after 2,600 hours at 752°F (400°C).^[E-6] In addition for Type 17-4PH, Charpy impact test data show severe TE after 250 hours at 427°C (800°F).^[E-7]

There are no known published studies of the stress corrosion resistance of CASS, welded CASS, or austenitic stainless steel weld materials in the thermally aged and embrittled condition when exposed to primary coolant although there are some instances of SCC propagating into stainless steel weld metals in BWRs, apparently along the delta-ferrite, after long periods of service. However, a number of studies have shown that martensitic PH stainless steels (e.g., Type 17-4 PH) become more susceptible to SCC in the embrittled condition (e.g., Reference E-8). There are also no known published studies of the influence of the primary water environment compared to air on fracture resistance.

E.1.1 CASS

The most commonly used CASS materials in PWR internals are ASME SA-351 or ASTM A 296 Grades CF-3M and CF-8. They have a duplex microstructure consisting of austenite (gamma phase) and ferrite (delta phase). The delta-ferrite phase is susceptible to TE at long times at reactor internal temperatures. The volume fraction of ferrite is typically 10 to 20%, but may attain 25%.

The mechanisms of TE that cause embrittlement in CASS have been reviewed and evaluated extensively by Chopra and Chung ^[E-9 – E-16] of Argonne National Laboratory (ANL). Embrittlement or loss of toughness in CASS during elevated-temperature exposure is related to (1) the formation of the Cr-rich alpha-prime phase and the Ni-rich and Ti-rich silicide (G phase) in the delta-ferrite, and (2) the precipitation of carbides at the austenite-ferrite phase boundaries. The phase-boundary carbides play a significant role in embrittlement for exposure at temperatures $\geq 400^{\circ}\text{C}$ (752°F), but have less effect on the embrittlement at exposure temperatures $< 400^{\circ}\text{C}$ (752°F).

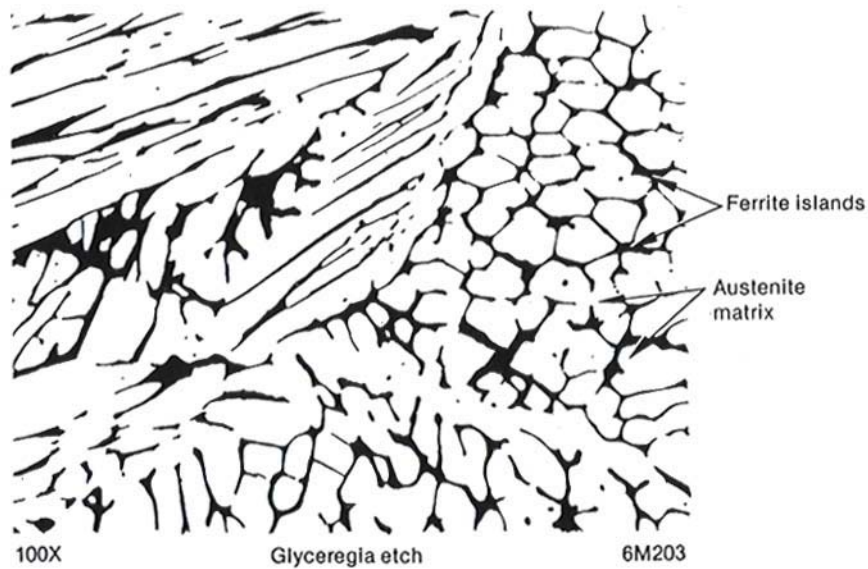
Different heats of CASS may exhibit different degrees of property degradation depending on the amount, size, and distribution of ferrite in the duplex austenitic/ferrite structure and the presence of carbides at the grain boundaries. ^[E-3] When the ferrite tends to be interconnected (rather than being present as isolated islands), the potential loss of toughness is increased. ^[E-17] Low ferrite CASS alloys typically exhibit isolated islands of ferrite and therefore show less thermal aging susceptibility. ^[E-18] Figure E-1 shows examples of two ferrite levels.

For typical PWR internals temperatures [$< 350^{\circ}\text{C}$ (662°F)], the formation of the alpha-prime phase and the G phase in the ferrite are the primary factors involved in embrittlement. Also, Chopra and Chung report that the kinetics of the formation of these phases appears to be different at temperatures $< 400^{\circ}\text{C}$ (752°F). Because of these differences in formation and precipitation behavior, the results of tests on material subjected to accelerated aging at temperatures $\geq 400^{\circ}\text{C}$ (752°F) are recommended not to be extrapolated to the lower temperatures.

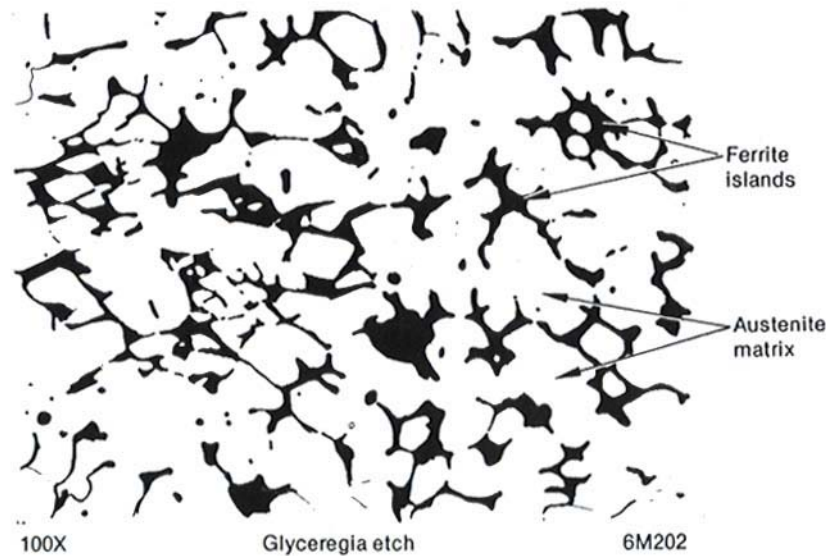
The alpha-prime phase typically forms by the process of spinodal decomposition. Spinodal decomposition refers to the reaction whereby two phases of the same crystal lattice type, but different compositions and properties, form because a miscibility gap exists in the alloy system. In the iron-chromium system, these immiscible phases are known as the iron-rich alpha phase and the chromium-rich alpha-prime phase. This phase separation process occurs at a very fine scale (on the order of only a few nanometers) in the ferrite regions of cast stainless steel, and use of an atom probe field ion microscope is required to resolve the presence of the alpha-prime phase. ^[E-19] After long-term aging at PWR internals temperatures, there are indications that alpha-prime phase also can form by means of a nucleation and growth process (in addition to spinodal decomposition). ^[E-12] Whether one or both of these mechanisms occurs seems to depend on the composition of the ferrite and the exposure temperature.

G phase forms in the ferrite by a nucleation and growth process. Its rate of formation is enhanced by increased levels of carbon and molybdenum. ^[E-12] When the G phase is present, it appears to mitigate the degree of embrittlement caused by the alpha-prime phase. A CF-8 stainless steel pump cover material was found to be embrittled (with a room temperature Charpy impact energy of 131 J/cm^2 [77 ft-lbs]) after 8 years of service at a temperature of 284°C (543°F) in a BWR. ^[E-16] Annealing for one hour at 550°C (1022°F) dissolved the alpha-prime phase and restored the Charpy impact resistance to the level expected for unaged material (232 J/cm^2 [137 ft-lbs]), but had no effect on the G phase that was present. Thus, the G phase had no significant effect on the degree of embrittlement, and the alpha-prime embrittlement was easily reversed by a short heat treatment at a moderate temperature. This annealing treatment was used in the laboratory to

verify that embrittlement was primarily caused by the alpha-prime, but it would not be practical to apply it to component items in the field.



a. Grade CF-8 stainless steel (16% ferrite)



b. Grade CF-8M stainless steel (30% ferrite)

Figure E-1
Typical Microstructures Of Centrifugally Cast Austenitic Stainless Steel, With Islands Of Ferrite In An Austenite Matrix^[E-35]

Because only the ferrite phase is embrittled by long-term service at operating temperature, the overall TE of a CASS component item depends on the amount and morphology of the ferrite that is present. In addition, molybdenum, being influential in the amount of ferrite and G phase

formed, is considered the most important chemical element to TE. Therefore threshold and screening criteria can be developed based on temperature, molybdenum content, and ferrite levels. In the case of a CASS component item that is welded, evidence has been shown that the heat-affected zone (HAZ) is potentially more susceptible to TE.^[E-20]

CASS materials are not normally subjected to high neutron fluence, although some CASS component items located at the edge of the reactor core may reach fluence levels on the order of 10^{20} n/cm² ($E > 1.0$ MeV). The Nuclear Regulatory Commission (NRC) Staff has proposed the existence of a potential synergistic⁴ effect of neutron irradiation on TE. There are currently no data to prove or disprove this proposal. The Westinghouse Owners Group (WOG) Materials Subcommittee (in collaboration with the MRP RI-ITG) is sponsoring tests to obtain PWR and test reactor irradiated material fracture toughness data from CASS component item materials and austenitic SS welds with different amounts of TE. These material samples will yield data in the near future that will shed light on the postulated synergistic effect.

E.1.2 Austenitic Stainless Steel Welds

The austenitic stainless steel weld deposits used in PWR internals, typically Types 308 or 308L, have a similar duplex microstructure to CASS material, but with a lower volume fraction of delta-ferrite (in the range of 5 to 15%, by ASME B&PV Code specifications but typically 5 to 10%) and notably lower chromium contents. The ferrite content is beneficial in preventing hot cracking and stress corrosion cracking, but it is a potential source of TE for austenitic stainless steel weldments.

The TE of austenitic stainless steel welds has been investigated by several researchers and the results are summarized in MRP-80.^[E-1] Fracture toughness of austenitic stainless steel welds is found to be dependent on the weld process, but insensitive to filler metal.^[E-21] Figure E-2 shows the room temperature J_{Ic} of several commonly used stainless steel welds by five different weld processes including gas-tungsten-arc (GTA), shielded metal-arc (SMA), submerged-arc (SA), gas-metal-arc (GMA) and flux-cored-arc (FCA).^[E-22] Welds produced by the GTA process obtain the highest toughness values while welds produced by the SA process consistently have the lowest toughness values. This is mainly due to the fact that GTA welds have the lowest inclusion density due to the inert gas protecting the molten pool from oxygen and to the absence of a flux. No statistical difference is found between J-R curves for SA and SMA welds. The J_{Ic} fracture toughness data for GMA and SMA weld processes are intermediate.

⁴ The word synergistic, in this case, refers to the possibility that the effects of neutron irradiation and thermal aging could be greater than the sum of the effects from each mechanism considered individually.

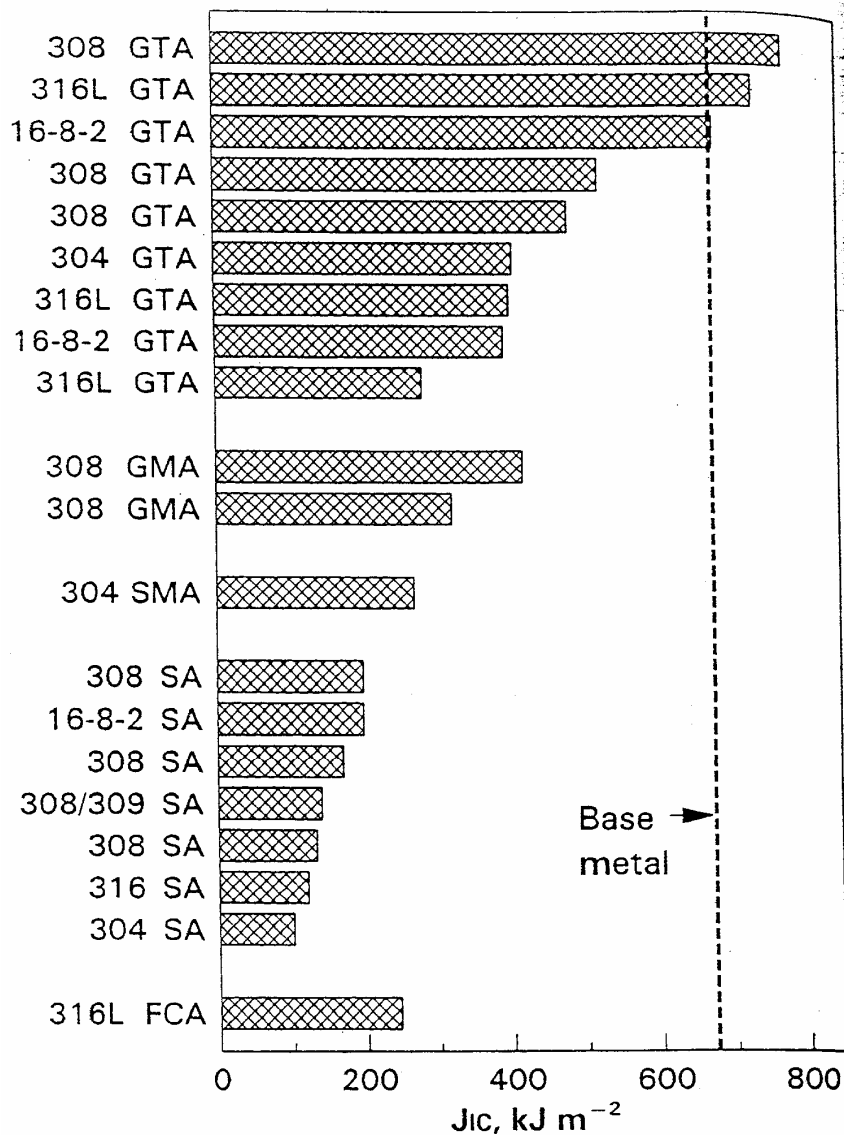


Figure E-2
Comparison Of J_{IC} Of Unirradiated Stainless Steel Weld By Different Processes^[E-19]

Mills^[E-23] performed a study where he investigated the TE of Type 308 welds fabricated using the GTA welding process. The ferrite content of the weld metal was about 10 ferrite number (FN).⁵ Mills' results indicate that the fracture toughness of the welds was not affected by aging at 427°C (800°F) for 10,000 hours. However, other research results show that thermal aging may cause a reduction in both the impact energy and fracture toughness of SMA welds. Hale and Garwood^[E-24] investigated the thermal aging of Type 19-9-L austenitic welds made by a manual-metal-arc (MMA) welding process. The ferrite content of the weld metal was in the range of 5 to 9

⁵ Ferrite number (FN) is the currently accepted designation for ferrite measurement and refers to a magnetically determined scale of ferrite measurement. It is related to ferrite volume (%) as shown in the constitution diagram relating nickel equivalent and chromium equivalent values (see ASME Code, Section III). A FN of 10 is approximately 9.2% ferrite by volume.

FN. Their results show that aging at 400°C (730°F) for 10,000 to 20,000 hours had little effect on the room temperature tensile properties and Charpy impact energy of these welds, but resulted in a significant increase in the ductile-to-brittle transition temperature measured at the 27-J energy level, which was increased from -158 to -75°C (-252 to -103°F), an increase of 83°C (150°F). The results also show that TE at 400°C (752°F) for up to 10,000 hours reduces the J-R fracture toughness of the weld metal. The lower bound fracture toughness, J_{IC} , measured at 300°C (572°F) was reduced from 67 to 32 kJ/m². Most of this reduction in fracture toughness took place in the first 1,000 hours.

Alexander et al.^[E-25] also investigated the TE of Type 308 weld material fabricated using the SMA welding process. The ferrite content of these welds was 12% (by volume). Their results also show that aging of these welds at 343°C (650°F) for 20,000 hours resulted in a minimal effect on the room temperature tensile properties but caused a significant increase in the ductile-to-brittle transition temperature measured at the 68-J energy level, an increase from -25 to 60°C (572°F) or 85°C (153°F). However, O'Donnell et al.^[E-22] have argued that a significant reduction in fracture toughness is likely when the ferrite volume fraction exceeds 10%. It appears that there may be a synergistic interaction between the embrittled ferrite phase and inclusions in the SMA welds. Further investigation is needed of the thermal aging behavior of SMA welds having a ferrite content representative of that in production welds.

Some austenitic stainless steel weldments located close to the reactor core may reach relatively high fluence levels on the order of several dpa. As noted above, the WOG Materials Subcommittee (in collaboration with the MRP RI-ITG) is sponsoring tests to obtain PWR and test reactor irradiated material fracture toughness data from CASS component item materials and austenitic SS welds with different amounts of TE. These material samples will yield data in the near future that will shed light on the NRC Staff postulated synergistic effect.

In summary, although no significant TE is anticipated for the typical delta-ferrite levels (5-10%) in austenitic stainless steel weld deposits, a significant reduction in fracture toughness is likely if the ferrite volume fraction exceeds a threshold of ~10%. However, because of the potential concern with a synergistic effect between neutron dose and TE, TE may become significant for some austenitic stainless steel weld locations.

E.1.3 Martensitic Stainless Steel

Martensitic stainless steels (Types 403 and 410) have mainly been used for component items in PWR internals and control rod drive mechanisms, and for valve stems and pump shafts. Martensitic stainless steels are most commonly used in the quenched and tempered (950-1250°F [510-677°C]) condition. Available embrittlement data are mostly related to Type 410 material. TE of Type 403 is expected to be similar to or bounded by Type 410.

It is interesting to note that TE of Type 410 during service was not investigated or even suspected as a possible cause for past failures in PWRs. This may be due to the fact that embrittlement of martensitic stainless steels is less pronounced than CASS and martensitic PH stainless steels and, in part, due to the misconception that thermal aging embrittlement is always accompanied by a hardness increase. Meyzaud and Wagner, et al.,^[E-26, E-27] investigated thermal

aging embrittlement of both martensitic stainless steels and martensitic PH stainless steels. The materials were austenitized at 1805°F (985°C) for 1 hour followed by oil-quenching, and tempering at 1112°F (600°C) for 4 hours and then air cooled. These heats were aged at 572, 662, 752, and 842°F (or 300, 350, 400, and 450°C, respectively) from 1000 hours up to 10,000 hours. As shown in Figure E-3, there is no significant effect from aging on the measured hardness of the 13%Cr (Type 410) and the 13%Cr-1%Ni, except some softening at 842°F (450°C) for 10,000 hours.^[E-26]

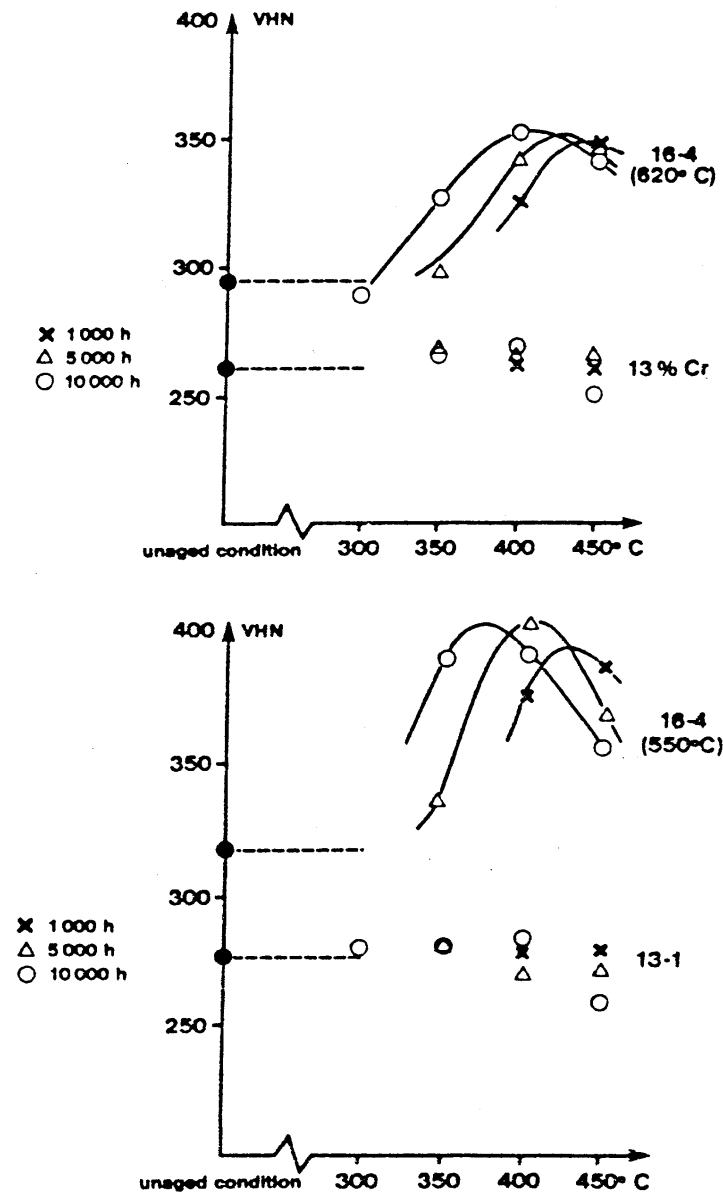


Figure E-3
Variation In Hardness As A Function Of Aging Time And Temperature For 13%Cr (Type 410), 13%Cr-1%Ni, And 16%Cr-4%Ni^[E-26]

Despite a lack of hardening, aging has produced noticeable embrittlement in the tempered Type 410 stainless steel. Wagner, et al., performed Charpy impact tests on the un-aged and aged materials at 752°F (400°C) for 5000 and 10,000 hours.^[E-27] As shown in Figure E-4, aging produced a noticeable embrittlement effect on the 13%Cr material, where the ductile-brittle transition temperature (DBTT) shifted toward a significantly higher temperature. The embrittlement effect is more pronounced for the 13%Cr-1%Ni material, where the DBTT shifted by ~135°F (75°C) after 10,000 hours at 752°F (400°C). The upper-shelf and lower-shelf are not greatly affected by aging. Figure E-5 shows typical Charpy impact energy curves of unaged Type 410 tempered at 1100, 1225, and 1450°F (593, 663, and 788°C).^[E-28] Figure E-6 shows the Izod impact data of Type 410 quenched from 1800°F and tempered at 1150°F (621°C) to a hardness of HB 228.^[E-29] The measured DBTTs range from -100 to 200°F (-73 to 93°C). Because the DBTT of un-aged Type 410 is near room temperature, the room temperature fracture toughness can potentially be sensitive to TE. Wagner, et al. performed fracture toughness tests at room temperature for materials aged at 752°F (400°C) for 5,000 hours. For the 13%Cr, J_{Ic} decreased from ~265 to ~230 kJ/m² and dJ/da from ~400 to ~250. No valid values were obtained for the 13%Cr-1%Ni alloy due to brittle fracture of the test specimens.

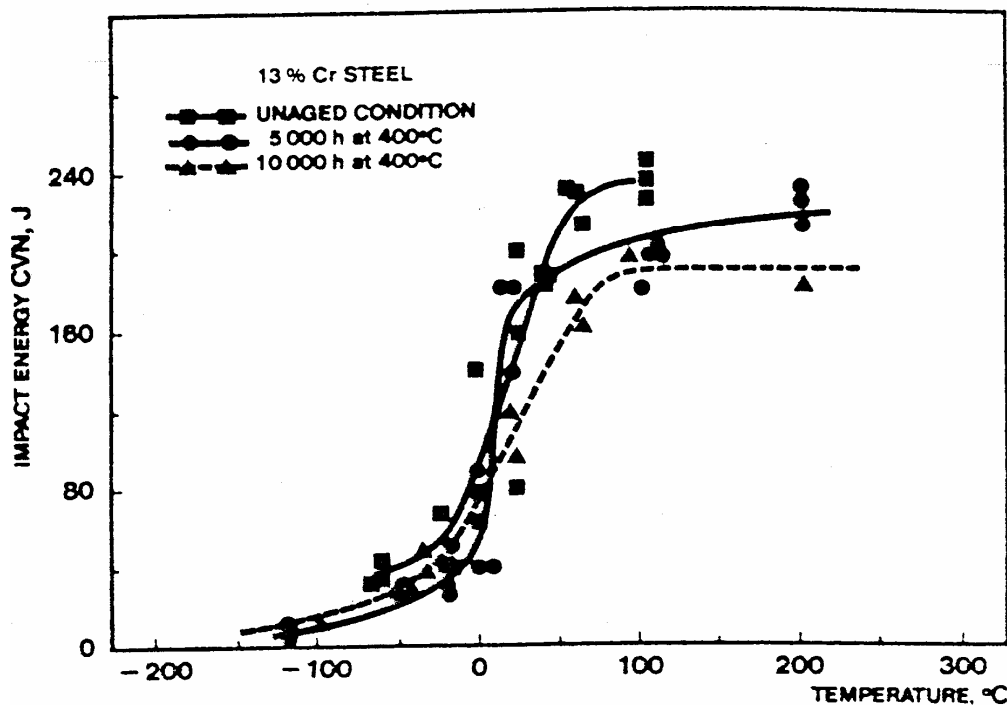
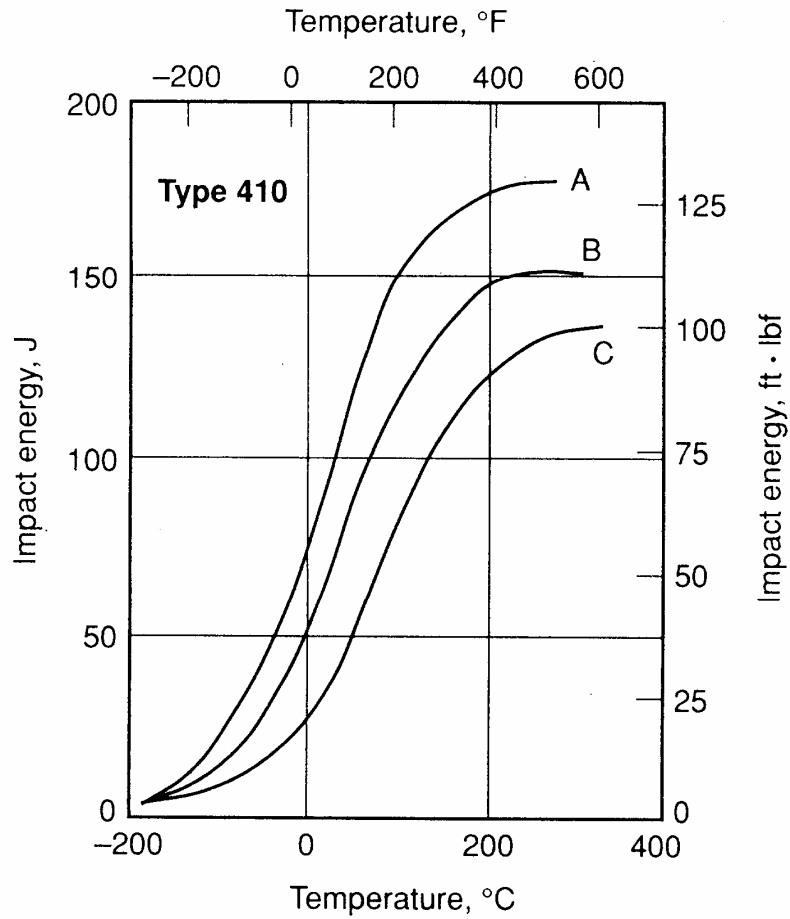


Figure E-4
Charpy V-Notch Impact Energy Transition Curves In The Unaged And Aged Conditions Of 13%Cr (Type 410) And 13%Cr-1%Ni (Longitudinal Orientation)^[E-27]



A is tempered at 1450°F with final hardness 95 HRB;
 B is tempered at 1225°F with final hardness 24 HRC
 C is tempered at 1100°F with final hardness 30 HRC.

Figure E-5
Typical Charpy V-Notch Transition Behavior of Unaged Type 410 Martensitic Stainless Steel^[E-28]

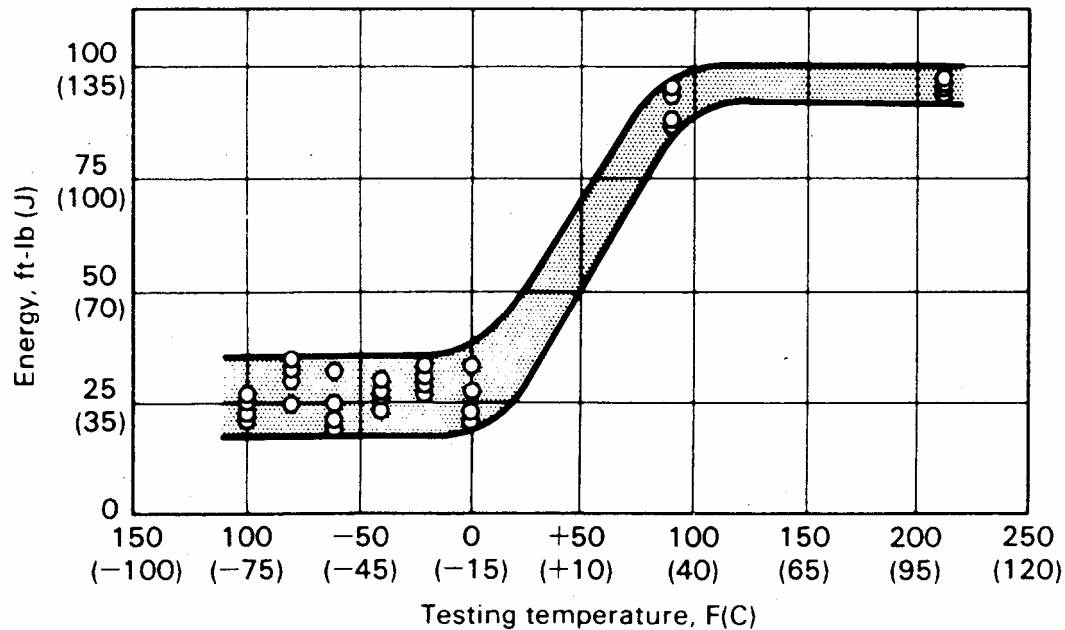


Figure E-6
Izod Data for Unaged Type 410 after Quenching From 1800°F and Tempering At 1150°F (HB 228)^[E-29]

Although TE is believed to be due to grain boundary segregation of impurities such as antimony, phosphorous, tin, arsenic to the prior austenite grain boundaries (which occurs during temper embrittlement of these alloys), a literature review has not revealed any definitive underlying causes of the TE of martensitic stainless steels. The TE of martensitic stainless steel is likely linked to grain boundary segregation of impurities while hardness is controlled by the post-quench heat treatment temperature. Aging at PWR internals temperatures for long periods of time could cause significant grain boundary segregation of impurities. Even a minor increase in the DBTT can result in a drastic deterioration of the room temperature impact energy because the initial un-aged DBTT of martensitic stainless steel material is near room temperature.

E.1.4 Martensitic Precipitation-Hardenable Stainless Steel

Type 17-4 PH material is the most commonly used martensitic precipitation-hardenable stainless steel used in LWRs. As noted in Appendix A, Type 15-5 PH is used in some PWR internals designs, and it is a delta-ferrite-free compositional modification of the Type 17-4 PH alloy. Long-term exposure to temperatures between about 600-900°F (288-482°C) is known to result in reduced toughness in martensitic precipitation-hardenable stainless steels through a secondary aging process. Although no known studies of TE with Type 15-5 PH material have been found in the open literature, what is known about Type 17-4 PH material is assumed to be directly applicable and is detailed below.

The secondary thermal aging (or TE) of martensitic PH stainless steels (such as Type 17-4 PH and Type 15-5 PH) at temperatures above 600°F was recognized by Armco Steel Corporation

(Armco), the original developer of these alloys. For the Type 17-4 PH material aged to the H-1100 condition, Armco reported values of room temperature Izod impact (ft-lb.) after being aged at 700, 800 and 900°F for 1000 or 2000 hours as listed in Table 2.5-1.^[E-30] This indicates that, for the three temperatures investigated, the TE kinetics for Type 17-4 PH (H-1100) are the fastest around 800°F. This was reflected in Armco's recommendation for parts requiring corrosion resistance and high strength at service temperatures not higher than 600°F. As the aging rate has an inverse exponential dependency on temperature, the time required to achieve significant TE would take longer than a few thousand hours. Hence, these short-term low temperature aging data could not settle the question of the long-term aging effect of Type 17-4 PH (H-1100) at or below 600°F. The 1989 ASME B&PV Code Section III mentioned that Type 17-4 PH in the H-1100 condition has reduced toughness at room temperature after exposure for about 5000 hours (~7 months) at 600°F and after shorter exposure above 650°F.^[E-31] All these observations and test results indicate the significant loss of ductility and impact strength of Type 17-4 PH (H-1100) from relatively short-term exposure at 600°F.

Table E-1
Temperature Izod Impact Values of Type 17-4 PH (H-1100) ^[E-24]

The initial room temperature Izod impact value is 56 ft-lbs

Aging Temperature	1000 hours Exposure time	2000 hours Exposure time
700 °F	7 ft-lb.	4 ft-lb.
800 °F	3 ft-lb.	2 ft-lb.
900 °F	6 ft-lb.	11 ft-lb.

The potential TE of Type 17-4 PH (H-1100) for BWR applications at 550°F was a concern in the early 1960s.^[E-32] The metallurgical basis of TE of Type 17-4 PH (H-1100) was also studied in the early 1960s.^[E-33] The TE at 800°F was accompanied by increases in hardness and tensile strengths. The low temperature TE and hardening was a surprise at the time from the following three considerations: (1) little additional decrease in copper solubility below 1100°F to allow additional precipitation hardening; (2) diminishing precipitation hardening from continued overaging of copper precipitates; and (3) continued tempering of the martensitic matrix. Hence, it was reasoned that the TE of Type 17-4 PH (H-1100) must be caused by precipitation of a second phase, not related to the primary Cu-rich precipitates. Due to their similar embrittlement characteristics, the TE of Type 17-4 PH (H-1100) was linked to the 885°F embrittlement of ferritic stainless steels. The generally accepted mechanism for the 885°F embrittlement of ferritic stainless steels is associated with the precipitation of an alpha-prime phase, which is a very fine, coherent, chromium-rich body centered cubic phase. With X-ray diffraction and X-ray fluorescence analysis, Antony identified the existence of alpha-prime in aged Type 17-4 PH (H-1100).^[E-33] The alpha-prime precipitation cause of TE of Type 17-4 PH is also supported by studies of TE of CASS in a similar temperature range (Section E.1.2) Clarke later showed that variation in Type 17-4 PH chemical composition has a significant influence on the initial room

temperature Charpy impact properties and the embrittlement kinetics (see Figure E-7 and Figure E-8).^[E-34]

Compared to the martensitic stainless steels such as Type 403 and 410 (Section E.1.3), Type 17-4 PH is more susceptible to TE due to its higher content of chromium and other alloying elements. The degree of TE with Type 15-5 PH material may be similar to the martensitic stainless steels, but data are unavailable to confirm this presumption. The effect of thermal aging on Charpy impact properties is shown in Figure E-9.^[E-34] The DBTT of unaged Type 17-4 PH (H-1100) is similar to unaged Type 410 martensitic stainless steel, i.e., around room temperature.^[E-29] The transition temperature of aged Type 17-4 PH (H-1100) can approach ~500°F as compared to 75-200°F for Type 410 from comparable exposure to elevated temperature.^[E-26] In addition, TE of Type 17-4 PH (H-1100) is accompanied by a severe decrease in upper shelf energy (USE), unlike Type 410 steel whose USE is only moderately decreased by aging at similar temperatures.

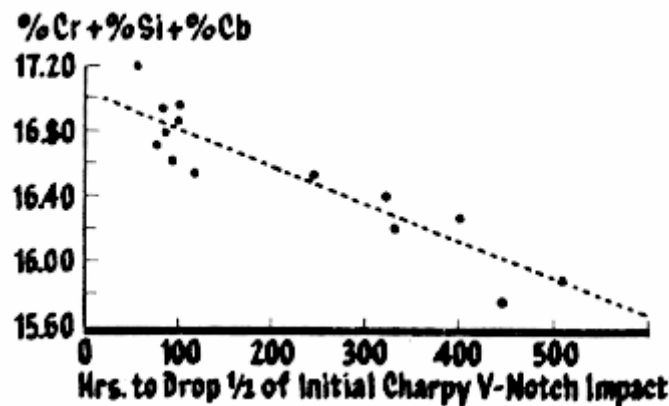


Figure E-7
Type 17-4 PH (H-1100), Effect Of %Cr + %Si + %Cb On Exposure Time At 800°F To Cause A 50% Drop In Initial Room Temperature Charpy Impact Energy^[E-28]

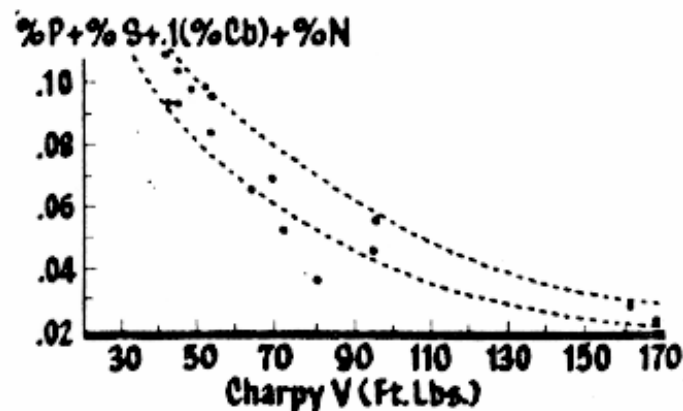


Figure E-8
Type 17-4 PH (H-1100), Effect Of %P + %S + 0.1%Cb + %N On The Initial Room Temperature Charpy Impact Energy^[E-28]

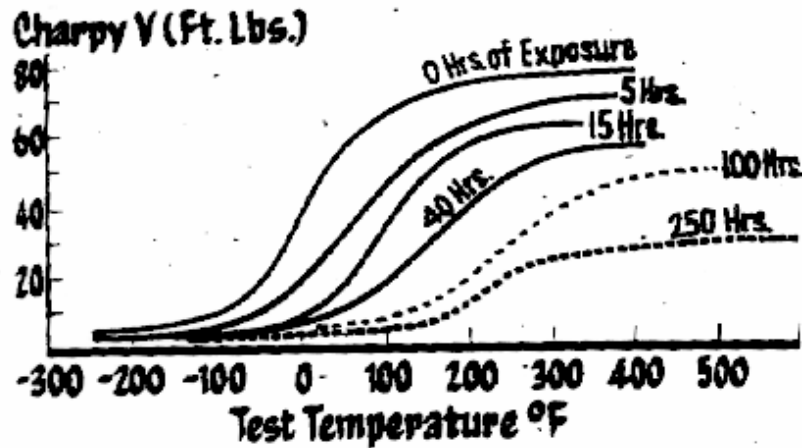


Figure E-9
Effect Of Exposure On Charpy V-Notch Impact Properties At 800°F For Type 17-4 PH (H-1100)^[E-28]

Because TE of CASS and martensitic PH stainless steels is accompanied by an increase in hardness, embrittlement is often characterized by the hardness increase. Yrieix et al. found that the decline in Charpy impact properties is linearly correlated with hardening.^[E-35] Empirical correlations were also made to link the hardness increase with exposure temperature and time based experimental test results.^[E-35, E-36] Based on these studies, an embrittlement model for Type 17-4 PH (H-1100) in PWRs has been developed by Xu and Fyitch.^[E-4] The hardness increase of Type 17-4 PH (H-1100) component items removed from service was found to be in good agreement with the model. Based on the model, Figure E-10 shows the increase in the fracture appearance transition temperature (FATT₅₀) and decrease in USE as a function of exposure time at 600°F. The increase in DBTT and loss of USE is in agreement with studies by Clarke, Meyzaud and Cozar, and Wagner, et al. Although the embrittlement kinetics are sensitive to heat-to-heat differences in composition, severe thermal hardening and embrittlement would be reached for Type 17-4 PH (H-1100) near 600°F during a 60-year PWR internals lifetime.

E.2 TE Summary and Discussion

Thermal aging embrittlement is an aging degradation mechanism that is dependent upon time and temperature. TE manifests itself by an increase in a materials yield strength, ultimate tensile strength, and hardness along with decreased ductility and degradation of toughness and impact properties. [Note: However, depending upon the specific material, each of these material properties is not always affected, as is the case noted above for martensitic SS.]

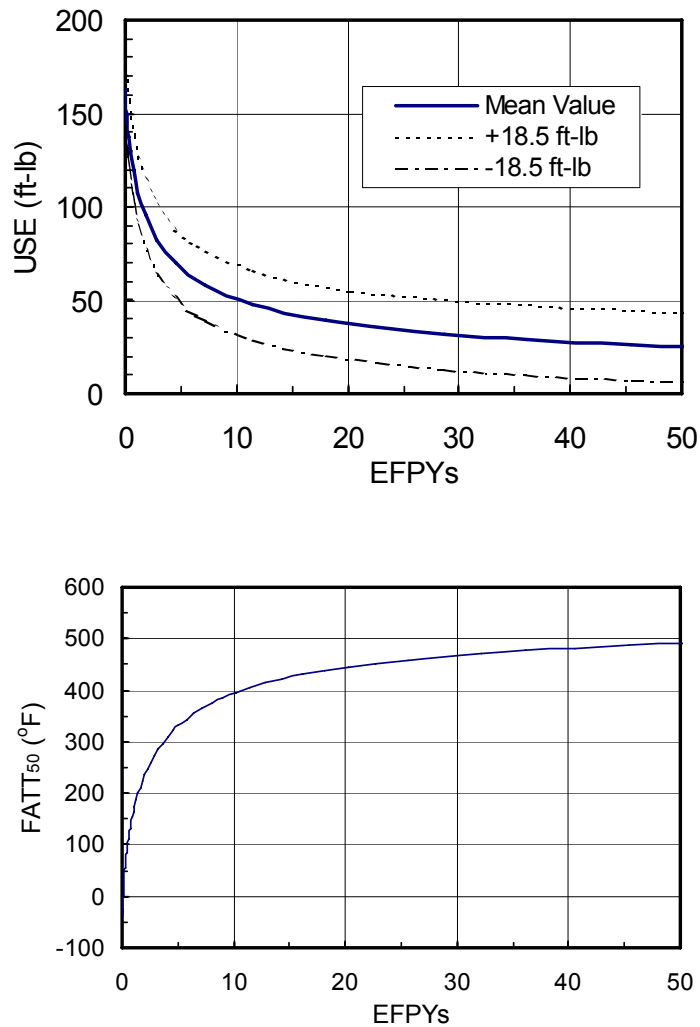


Figure E-10
Predicted Embrittlement of Type 17-4 PH (H-110) FATT₅₀-vs.-EFPYs and USE-vs.-EFPYs as a Function of Exposure Time at 600°F^[E-3]

Materials in the PWR internals that are potentially susceptible to TE include CASS, martensitic stainless steels, martensitic PH stainless steels, and austenitic stainless steel weldments. The following have been identified as the major parameters for developing threshold and screening criteria:

- The ferrite phase in CASS materials becomes embrittled by long-term service at PWR internals operating temperatures. Threshold and screening criteria can be developed based on the type of casting, the material composition (particularly molybdenum content), and ferrite level.
- Data exist showing martensitic stainless steels to be susceptible to TE. However, inadequate data exist to develop threshold or screening criteria; therefore, all martensitic stainless steels are considered susceptible to TE.

- Martensitic PH stainless steels are well known to be susceptible to TE. Threshold and screening criteria can be developed based on temperature. Material composition appears to have an effect on the degree of TE, but inadequate data are available for developing criteria for screening purposes.
- Austenitic stainless steel weld materials show a wide range of tensile and fracture toughness properties in the as-welded and un-aged condition. Their microstructure and aging susceptibility are superior to static stainless steel castings with low molybdenum contents because of their lower Cr and delta-ferrite content. Thus, utilizing the same screening criteria as suggested for statically-cast CASS materials, no weld metal will fall above the ferrite screening level (i.e., >20%) due to the lower ferrite content.

As noted above, CASS materials are not normally subjected to high neutron fluence, although some CASS component items located at the edge of the reactor core may reach fluence levels on the order of 10^{20} n/cm² ($E > 1.0$ MeV). There are currently no data to prove or disprove the existence of a potential synergistic effect of neutron irradiation on TE. However, samples from CASS component items and austenitic SS welds with different amounts of TE are currently in a test program designed to shed light on the postulated synergistic effect.

E.3 TE Threshold and Screening Criteria

Temperature and time at temperature are the overriding parameters controlling TE. Significant TE during the PWR operating life is possible for some materials (e.g., Type 17-4 PH material at temperature above approximately 500°F (260°C)).^[E-37] Therefore, a reasonable threshold temperature for all TE susceptible materials is ~ 500°F (260°C).

Since the ferrite content is one of the major parameters for TE of CASS and austenitic stainless steel weld materials, a reasonable threshold criterion for CASS and austenitic stainless steel welds is suggested as ferrite volume contents > 10%.

All martensitic and martensitic PH stainless steel materials are considered potentially susceptible to TE. Therefore, no screening criteria have been developed.

Based on recognized industry efforts, the following CASS alloys have been determined to be susceptible to loss of toughness and are suggested to be screened for TE:^[E-38, E-39]

- Centrifugal castings with > 20% ferrite
- Static castings with molybdenum content $\leq 0.50\%$ and ferrite > 20%
- Static castings with molybdenum content > 0.50% and ferrite > 14%

Also, it is suggested that a screening criterion of $\geq 6.7 \times 10^{20}$ n/cm² ($E > 1.0$ MeV) [≥ 1 dpa], which is the screening criterion for IE (Appendix F) be utilized for those CASS materials located at the edge of the reactor core that may potentially be susceptible to a synergistic effect between accumulated dose and TE.

In addition, austenitic stainless steel welds (e.g., Types 308 and 308L) are similar to statically-cast CASS with low molybdenum contents and it is suggested that the same screening criteria be used. Provided that the levels of ferrite and molybdenum contents are low in these welds, it is expected that the effects of TE will be insignificant.

E.4 TE References

- E-1 Materials Reliability Program: A Review of Thermal Aging Embrittlement in Pressurized Water Reactors (MRP-80), EPRI 1003523, 2003.
- E-2 Yukawa, S., "Review and Evaluation of the Toughness of Austenitic Steels and Nickel Alloys After Long-Term Elevated Temperature Exposures," WRC Bulletin 378, Welding Research Council, New York, January 1993.
- E-3 Chopra, O.K., "Estimation of Fracture Toughness of Cast Stainless Steels During Thermal Aging in LWR Systems," NUREG/CR-4513, U.S. Nuclear Regulatory Commission, Washington, D.C., June 1991.
- E-4 Xu, H. and Fyfe, S., "Aging Embrittlement Modeling of Type 17-4 PH at LWR Temperatures," The 10th International Conference on Environmental Degradation of Materials in Nuclear Power Systems – Water Reactors, NACE International, Houston, Texas (2001).
- E-5 Peckner, D., and Bernstein, I. M., Eds., Handbook of Stainless Steels, McGraw-Hill, New York, 1977.
- E-6 Chopra, O.K. and Chung, H.M., "Aging Degradation of Cast Stainless Steels: Effects on Mechanical Properties," The 3rd International Conference on Environmental Degradation of Materials in Nuclear Power Systems – Water Reactors, TMS 1987.
- E-7 Clarke, Jr., W. C., "A Study of Embrittlement of a Precipitation Hardening Stainless Steel and Some Related Materials," Transactions of the Metallurgical Society of AIME, 245, 2135-2140, (October 1969).
- E-8 Suss, H., "Stress Corrosion and Hydrogen Embrittlement Properties of 17-4 PH in 600°F Waters." KAPL-M-6580, April, 1967.
- E-9 Chopra, O.K., and Chung, H.M., "Aging of Cast Duplex Stainless Steels in LWR Systems," Nuclear Engineering and Design, Vol. 89, 1985, pp. 305-318.
- E-10 Chopra, O.K., and Chung, H.M., "Aging of Cast Stainless Steel," Thirteenth Water Reactor Safety Research Information Meeting, Vol. 2, NUREG/CP-0072, February, 1986, pp. 387-407.

- E-11 Chopra, O.K., and Chung, H.M., “Long-Term Embrittlement of Cast Duplex Stainless Steels in LWR Systems: Semiannual Report October 1985-March 1986,” NUREG/CR-4744 Vol. 1, No. 1, ANL-86-54, September, 1986.
- E-12 Chopra, O.K., and Chung, H.M., “Long-Term Embrittlement of Cast Duplex Stainless Steels in LWR Systems: Semiannual Report April-September 1986,” NUREG/CR-4744 Vol. 1, No. 2, ANL-87-16, March, 1987.
- E-13 Chung, H.M., and Chopra, O.K., “Long-Term Aging Embrittlement of Cast Austenitic Stainless Steels – Mechanism and Kinetics,” Properties of Stainless Steels in Elevated Temperature Service, MPC-Vol. 26, PVP-Vol. 132, The American Society of Mechanical Engineers, New York, 1987, pp. 17-34.
- E-14 Chopra, O.K., and Chung, H.M., “Effect of Low-Temperature Aging on the Mechanical Properties of Cast Stainless Steels,” Properties of Stainless Steels in Elevated Temperature Service, MPC-Vol. 26, PVP-Vol. 132, The American Society of Mechanical Engineers, New York, 1987, pp. 79-105.
- E-15 Chopra, O.K., and Chung, H.M., “Initial Assessment of the Processes and Significance of Thermal Aging in Cast Stainless Steels,” Presented at 16th Water Reactor Safety Information Meeting, National Institute of Standards and Technology, Gaithersburg, MD, October 24-27, 1988.
- E-16 Chopra, O.K., and Shack, W.J., “Mechanical Properties of Thermally Aged Cast Stainless Steels from Shippingport Reactor Components,” NUREG/CR-6275, ANL-94/37, April 1995.
- E-17 “Cast Stainless Steels,” M. Blair, Metals Handbook, Vol. 1, Selection of Iron and Steel, 10th Edition, ASM International, Materials Park, OH, 1990.
- E-18 Shah, V.N., and Macdonald, P.E., editors, “Aging and Life Extension of Major Light Water Reactor Components,” Chapter 5, Figure 5-8, Elsevier, 1993, p. 164.
- E-19 Sassen, J.M., et al., “Kinetics of Spinodal Decomposition in the Ferrite Phase of a Duplex Stainless Steel,” Properties of Stainless Steels in Elevated Temperature Service, MPC-Vol. 26, PVP-Vol. 132, the American Society of Mechanical Engineers, New York, 1987, pp. 65-78.
- E-20 Mimura, H., et al., “Thermal Embrittlement of Simulated Heat-Affects Zone in Cast Austenitic Stainless Steels,” Welding Research Supplement, August 1998, pp. 350-s – 360-s.
- E-21 “Effects of Thermal Aging on Fracture Toughness and Charpy-Impact Strength of Stainless steel Pipe Welds,” NUREG/CR-6428, Argonne National Laboratory for U.S. Nuclear Regulatory Commission, 1996.

- E-22 O'Donnell, I.J., Huthmann, H., and Tavassoli, A.A., "The Fracture Toughness Behavior of Austenitic Steels and Weld Metal Including the Effects of Thermal Ageing and Irradiation," International Proceedings of Vessel & Piping 65, 1996, pp. 209-220.
- E-23 Mills, W.J., "Fracture Toughness of Type 304 and 316 Stainless Steels and Their Welds," International Materials Reviews, 1997, Vol. 42, No. 2, pp. 45-82.
- E-24 Hale, G.E., and Garwood, S.J., "Effect of Aging on Fracture Behavior of Cast Stainless and Weldments," Material Science and Technology, 6, March 1990, pp. 230-235.
- E-25 Alexander, K.B., et al., "Microscopical Evaluation of Low Temperature Aging of Type 308 Stainless Steel Weldments," Materials Science and Technology, 6, March 1990, pp. 314-320.)
- E-26 Y. Meyzaud and R. Cozar, "Design of Aging-Resistant Martensitic Stainless Steels for Pressurized Water Reactors," Proceedings of Topical Conference on Ferritic Alloys for Use in Nuclear Energy Technologies, Snowbird, Utah, June 19-23, 1984.
- E-27 Wagner, D., Chavaillard, J-P., Meyzaud, Y. et. al, "Toughness and Fatigue Properties of Martensitic Stainless Steels for Nuclear Applications," 1984 ASM International Conference on New Developments in Stainless Steel Technology, Detroit, Michigan, September, 1984.
- E-28 "Properties and Selection: Iron, Steels, and High Performance Alloys," Metals Handbook, Vol. 1, Tenth Edition, ASM International, p. 859.
- E-29 R. A. Lula, Stainless Steel, 1986, American Society for Metals, Metals Park, OH.
- E-30 "Armco 17-4 PH Stainless Steel Bar and Wire," 1969, Armco Product Literature, Armco Steel Corporation, Middletown, OH.
- E-31 ASME Boiler and Pressure Vessel Code, Section III, Rules for Construction of Nuclear Power Plant Components, Division I – Appendices, Table I-1.1, p. 20, 1989, The American Society of Mechanical Engineers, New York, NY.
- E-32 S. Naymark, "Materials for Dresden and Other Boiling Water Reactors," Nuclear Metallurgy, Vol. III, American Institute of Mining, Metallurgical, and Petroleum Engineers, Inc., 1962.
- E-33 K. C. Antony, "Aging Reactions in Precipitation Hardenable Stainless Steel," Journal of Metals, December, 1963.
- E-34 W. C. Clarke, Jr. "A Study of Embrittlement of a Precipitation Hardening Stainless Steel and Some Related Materials," Transactions of the Metallurgical Society of AIME, Vol. 245, October 1969, pp. 2135-2140.

- E-35 B. Yrieix and M. Guttman, "Aging Between 300 and 450°C of Wrought Martensitic 13-17 wt-% Cr Stainless Steels," Materials Science and Technology, Vol. 9, pp. 125-134, Feb. 1993
- E-36 C. E. Jaske and V. N. Shah, "Life Assessment Procedure for LWR Cast Stainless Steel Components," Proc. 4th Int. Symp. on Environmental Degradation of Materials in the Nuclear Power Systems – Water Reactors, August 6-10, 2001, Jekyll Island, Georgia.
- E-37 "Materials Handbook for Nuclear Plant Pressure Boundary Applications," TR-109668-S1-R1, Electric Power Research Institute, December 1998.
- E-38 "PWR Reactor Coolant System License Renewal Industry Report," Project RP-2643-32, Electric Power Research Institute, Palo Alto, California, May 1992.
- E-39 "License Renewal Issue No. 98-0030, 'Thermal Aging Embrittlement of Cast Austenitic Stainless Steel Components,'" Letter from C.I. Grimes (NRC) to D.J. Walters (NEI), May 19, 2000.

F

APPENDIX F: IRRADIATION EMBRITTLEMENT

F.1 General Description of Irradiation Embrittlement

Irradiation embrittlement (IE) refers to the phenomenon of loss of ductility and fracture toughness from exposure to high-energy neutrons ($E > 1.0$ MeV). The loss of ductility and fracture toughness is usually accompanied by marked increases in yield and ultimate tensile strength. Mechanistically, irradiation embrittlement results from lattice defects from neutron bombardment. High-energy neutrons displace atoms from their normal lattice positions and create point defects. Although most point defects (called interstitials and vacancies) are annihilated by recombination, surviving point defects form various irradiated microstructures consisting of dislocations, precipitates, and cavities. Cavities, which are three-dimensional clusters of vacancies, gas atoms (bubbles), or a combination of the two, can be associated with other microstructural features such as precipitates, dislocations, and grain boundaries. These defects and precipitates from irradiation are obstacles to dislocation movement and result in an increased yield and tensile strengths and decreased work hardening capacity and ductility, and loss of fracture toughness.

The detrimental effect of irradiation embrittlement (also called radiation embrittlement) has long been recognized for the low alloy steel PWR and BWR reactor pressure vessel materials. However, until recently, irradiation embrittlement had not been considered to be a concern for PWR internals. This is partly because the PWR internals are constructed of austenitic stainless steels, which possess high levels of ductility and fracture toughness even after neutron exposure levels that would have caused significant embrittlement in low alloy steel reactor vessels. However, the proximity to the core means that the neutron flux for many lower PWR internals component items is one to three orders of magnitude higher than for the low alloy steel PWR reactor vessel. A large reduction in fracture toughness of stainless steels due to neutron irradiation can significantly increase the sensitivity to flaws that are either pre-existing during PWR construction or flaws developed during service due to SCC, IASCC, or fatigue. Decreasing toughness values correlate to decreasing critical crack lengths that can be tolerated by the structure. This affects inspection requirements and procedures.

In September 1999, EPRI published TR-112718^[F-1] “Evaluation of Neutron Irradiation Embrittlement for PWR Stainless Steel Internal Component Supports,” to provide a generic evaluation of the effects of reduced ductility and fracture toughness due to neutron irradiation for austenitic stainless steel PWR internals. However, the PWR reactor vessel internal supports evaluated in TR-112718 are based on a fracture toughness value to a moderate fluence level of 8

$\times 10^{20}$ n/cm², $E > 1.0$ MeV (~ 1.2 dpa⁶). In September 2004, EPRI published MRP-79 – Revision 1, “A Review of Radiation Embrittlement of Stainless Steels for PWRs,”^[F-2] that reviewed the fracture toughness value of austenitic stainless steels irradiated up to ~ 80 dpa, which is approximately the maximum expected fluence level of highly irradiated PWR internal component items during a PWR lifetime including life extension up to 60 years (~ 100 dpa). In September 2005, EPRI published MRP-160 that documented fracture toughness data of 304 SS baffle plate and former plate samples harvested from a decommissioned PWR.^[F-6] These samples experienced radiation up to about 13 dpa. Also reported therein are fracture toughness data of highly irradiated 316 SS thimble tube up to 65 dpa. Recently, in parallel with the preparation of this report, a synthesis of fracture toughness testing in the JOBB program has also been documented.^[B-15]

In the present discussion of irradiation embrittlement, the affected materials are limited to wrought austenitic stainless steels, austenitic stainless steel welds, and cast austenitic stainless steel (CASS). This is because all lower PWR internals next to the core, where degradation due to irradiation embrittlement is considered, are fabricated from these materials. Other PWR internals component items that are made of martensitic stainless steels, austenitic or martensitic precipitation-hardenable stainless steels, austenitic nickel-base alloys, austenitic precipitation-hardenable nickel-base alloys, and cobalt-base alloys usually do not reach significant neutron exposures during the PWR lifetime to be a concern for irradiation embrittlement.

F.2 Fracture Toughness of Irradiated Austenitic Stainless Steels

Conventional design criteria for engineering structures are based on tensile strength, yield strength, and buckling stress. However, for a structure containing pre-existing flaws or developing cracks during operation, failure could occur at stresses below the highest design service stress. To prevent unexpected and often catastrophic failures of engineering structures, fracture mechanics has been increasingly used to provide a methodology for design basis, material testing, service inspection, and safety analysis. The two most commonly used methodologies in fracture mechanics are linear elastic fracture mechanics (LEFM) and elastic-plastic fracture mechanics (EPFM) using appropriate fracture toughness values taking into account in-service degradation where necessary. Fracture toughness is a measure of a material's ability to resist crack extension. Therefore, the most useful measure of irradiation embrittlement in austenitic stainless steels is the reduction in fracture toughness.

F.2.1 Type 304 and Type 316 in Fast Reactors

The EPRI MRP-79 report^[F-2] reviewed literature data on the fracture toughness of highly irradiated austenitic stainless steels in fast reactors up to 80 dpa and in light water reactors (LWRs) up to 18 dpa, excluding the most recent MRP-160 304 SS fracture toughness data and the flux thimble data up to 65 dpa reported therein. The fracture toughness data of irradiated stainless steels and welds from various fast reactors indicate that the effect of irradiation at 370-

⁶ The dpa conversion used in this report is based on an estimated conversion factor for PWRs of 10^{22} n/cm², $E > 1.0$ MeV = 15 dpa. Note however that this factor will vary with fuel design, vendor design, and location within the PWR internals.^[F-3]

430°C (698-806°F) can be divided into three regions (0 to 80 dpa): a threshold neutron exposure between 0 and 0.5 dpa below which there is no significant loss in fracture toughness, intermediate exposures between 0.5 and 10 dpa where toughness decreases rapidly with neutron dose, and a saturation exposure (10 to 40 dpa) above which increasing irradiation damage produces little additional reduction in fracture toughness provided swelling does not occur. The rapid initial decrease in fracture toughness corresponds to a transition in fracture mechanism from dimpled rupture to channel fracture. The convergence of fracture toughness reflects the saturation of irradiation defect microstructure, which is observed to be largely independent of the starting conditions of austenitic stainless steels. The saturation of fracture toughness with increasing fluence is due to the saturation of the irradiation defect microstructure.

Figure F-1 is a summary of the elevated temperature fracture toughness K_{Jc} for Type 304, Type 304L, and Type 316 austenitic stainless steel irradiated in fast reactors. It shows that the reduction in fracture toughness occurs mostly between 0.5 and 10 dpa. No statistically significant difference in toughness has been observed between highly irradiated solution-annealed (SA) Type 304 and cold-worked (CW) Type 316 stainless steels. The minimum K_{Jc} fracture toughness in Figure F-1 is estimated to be 71 MPa√m (65 Ksi√in).

F.2.2 Type 347 and Type 348 in Fast Reactors

The MRP-79^[F-2] report has found some studies indicating a lower fracture toughness value for highly irradiated Type 347 and Type 348 austenitic stainless steels in fast reactors. In addition, the fracture toughness of Type 347 and Type 348 was further reduced by irradiation creep. The fracture toughness results of Type 347 and Type 348 irradiated at 260–399°C (500–750°F) are summarized in Table F-1. The reported K_{Jc} is about 60 MPa√m (55 Ksi√in). The minimum K_{Jc} fracture toughness was 38 MPa√m (35 Ksi√in) after 89 dpa with 0.6% irradiation creep. No embrittlement mechanism by irradiation creep was postulated by the studies. To date, there have been no other studies linking irradiation creep and fracture toughness of austenitic stainless steels or their weldments.

F.2.3 Austenitic Stainless Steel Weld Metals in Fast Reactors

The MRP-79^[F-2] report has reviewed Types 308 and 316 austenitic stainless weld metals irradiated in fast reactors. The irradiation embrittlement of weld metals is similar to that for wrought austenitic stainless steels, i.e., fracture toughness deteriorates rapidly with the first few dpa of exposure and then gradually levels off. Fracture toughness is seen to saturate after 10 dpa; however, the maximum fluence for the weld metal data points is limited to about 15 dpa. The minimum elevated temperature K_{Jc} fracture toughness is estimated to be 40 MPa√m (36 Ksi√in), which is lower than the minimum fracture toughness for highly irradiated wrought austenitic stainless steels in fast reactors.

Figure F-1

Elevated Temperature Fracture Toughness K_{Jc} as a Function of dpa for Type 304 and Type 316 Irradiated in Fast Reactors (Based on Reference F-2)

Table F-1
Fracture Toughness of Type 347/348 Irradiated in Fast Reactors ^[F-2]

F.2.4 Austenitic Stainless Steel and Weld Metals in PWRs and BWRs

The MRP-79 report^[F-2] provided elevated temperature fracture toughness data of austenitic stainless steels and welds irradiated in BWRs or PWRs. The results are summarized in Figure F-2. The reduction of fracture toughness with increasing neutron dose in BWRs and PWRs is consistent with that observed in fast reactors. However, a significant number of data points seem to fall below the scatter band for stainless steels irradiated in fast reactors. Figure F-2 includes the only PWR fracture toughness data points from baffle bolts. It should be noted that the baffle bolt test specimen was not a standard ASTM fracture toughness specimen. The MRP-160 304 SS fracture toughness data and the flux thimble data up to 65 dpa reported therein published subsequent to MRP-79 are enveloped by the lower bound curve shown in Figure F-2.^[F-6] These LWR results suggest that the minimum fracture toughness of stainless steels irradiated in BWRs and PWRs may be lower than the minimum fracture toughness shown in Figure F-1 from fast reactors. Recent BWR data suggest that a minimum of $\sim 55 \text{ MPa}\sqrt{\text{m}}$ ($50 \text{ Ksi}\sqrt{\text{in}}$) should be adopted for LWR spectrum irradiated materials.^[F-4] There are good grounds for believing that the

difference may be linked to the formation of large numbers of nanometer size gas bubbles (due to the insolubility of helium in metals) during LWR neutron irradiation, which occurs to a much lesser extent in Fast Reactors.

Figure F-2
Elevated Temperature Fracture Toughness K_{Jc} of Austenitic Stainless Steels and Welds
Irradiated in BWRs or PWRs as a Function of $dpa^{[F-2]}$

F.3 Tensile Properties of Irradiated Austenitic Stainless Steels

The MRP-79 report^[F-2] has reviewed the tensile properties of highly irradiated austenitic stainless steels in fast reactors and light water reactors in the literature, excluding the 304 SS baffle plate and former plate data published after the publication of MRP-79. These data documented in MRP-129 came from testing samples harvested from a decommissioned PWR.^[F-7] The fast reactor data show that the dependence of tensile properties on fluence parallels that of fracture toughness shown in Figure F-1. Such an irradiation embrittlement dependence on neutron exposure has been confirmed by the tensile data from the Joint Owners Baffle Bolt (JOBB) Program,^[F-8] which is specifically designed to represent the neutron doses encountered in PWR internals, and the decommissioned 304 data.^[F-7] The JOBB program includes testing of irradiated tensile specimens fabricated from stainless steels and welds representative of internals materials used in the French and U.S. PWRs. The reduction of total elongation of JOBB materials with increasing neutron exposure at elevated temperature is summarized in Figure F-3, Figure F-4, and Figure F-5. The total elongation is seen to decrease rapidly in the first 10 dpa and gradually levels off at ~8% at high dpa while the uniform elongation is typically less than 1%. The weld metals and castings have a larger scatter than the wrought products due to greater variability in welds and castings.

F.4 IE Threshold and Screening Criteria

Significant scatter is observed in the loss of fracture toughness between 0 and 0.5 dpa for austenitic stainless steels, austenitic stainless steel welds, and cast austenitic stainless steels. This scatter in the initial onset of irradiation embrittlement, reflecting the differences in initial thermomechanical conditions and heat-to-heat variations, makes it difficult to define a threshold for IE. Therefore, it is concluded that no threshold neutron exposure for irradiation embrittlement can be established.

Fracture toughness decreases rapidly with increasing neutron dose for neutron exposures between 0 and 10 dpa as shown in Figure F-1. The following equation has been developed to bound all available fracture toughness data from fast reactors, BWRs, and PWRs. This lower bound fracture toughness line is included in a plot of all the available data in Figure F-2.

(F-1)

No statistically significant difference between solution-annealed Type 304 and cold-worked Type 316 materials appears to exist. Even though some studies suggest that the stabilized Type 347 and Type 348 stainless steels may have lower fracture toughness, Table F-1 and Figure F-2 show that the fracture toughness of highly irradiated Type 347 and Type 348 is also bounded by Eq. F-1.

Figure F-3
Elevated Temperature Total Elongation as a Function of dpa for Type 304, Type 304L, and Type 347^[F-2]

Figure F-4
Elevated Temperature Total Elongation as a Function of dpa for Type 316^[F-2]

Figure F-5
Elevated Temperature Total Elongation as a Function of dpa for Type 308 and 308L Weld, Type 304 HAZ, and Type CF-8 CASS^[F-2]

References F-4 and F-5, also confirmed by References and F-6 and F-9, indicate that for austenitic stainless steel component items with neutron exposures $> 3 \times 10^{21} \text{ n/cm}^2$ ($E > 1.0 \text{ MeV}$) [$> 4.5 \text{ dpa}$] LEFM (in place of EPFM) should be considered for design and operational analyses. In addition, a number of material properties (e.g., yield strength and tensile strength)

plateau when exposed to doses in the range of 5-10 dpa. Thus, based on equation F-1 and Figure F-2, at 5 dpa (3.3×10^{21} n/cm², $E > 1.0$ MeV) the corresponding lower bound fracture toughness is about 40 MPa√m (36 Ksi√in), which should be adequate toughness for functionality. Also, as shown in Figure F-2, there is a reasonable database available to establish this minimum value. However, for added assurance in performing the screening, 30% of the 5 dpa value (or 1.5 dpa) is suggested. Therefore, for wrought austenitic stainless steel, a screening neutron exposure for irradiation embrittlement is conservatively established to be ≥ 1.5 dpa, or 1×10^{21} n/cm², $E > 1.0$ MeV.

Because the austenitic stainless steel weld metals and CASS show much greater variability in initial values, their screening neutron exposure is conservatively established to be somewhat lower at ≥ 1 dpa or 6.7×10^{20} n/cm², $E > 1.0$ MeV. In addition, this screening criterion is suggested for use in evaluation of the potential synergistic effect of dose on thermal aging embrittlement (Appendix E).

F.5 IE References

- F-1 “Evaluation of Neutron Irradiation Embrittlement for PWR Stainless Steel Internal Component Supports,” EPRI TR-112718, 1999.
- F-2 Materials Reliability Program: A Review of Radiation Embrittlement of Stainless Steels for PWRs (MRP-79) –Revision 1, EPRI Report 1008204, 2004.
- F-3 Garner, F.A., Greenwood, L.R., and Reid, B.D., “An Assessment of the Possible Role of Transmutation on Development of Irradiation-Assisted Stress Corrosion Cracking in Light Water Reactors,” EPRI TR-107159, “Critical Issue Reviews for the Understanding and Evaluation of Irradiation Assisted Stress Corrosion Cracking,” Final Report, November 1996.
- F-4 Carter, R.G., and Gamble, R.N., “Assessment of the Fracture Toughness of Irradiated Stainless Steel for BWR Core Shrouds,” Contribution of Materials Investigation to the Resolution of Problems Encountered in Pressurized Water Reactors, Fontevraud 5, September 2002.
- F-5 Mills, W.J., “Fracture Toughness of Type 304 and 316 Stainless Steels and Their Welds,” International Materials Reviews, 1997, Vol. 42, No. 2, pp. 45-82.
- F-6 Materials Reliability Program: Fracture Toughness Testing of Decommissioned PWR Core Internals Samples (MR-160), EPRI 1012079, 2005.
- F-7 Materials Reliability Program: Characterization of Decommissioned PWR Vessel Internals Material Samples – Tensile and SSRT Testing (MR-129), EPRI 1008205, 2004.
- F-8 Joint Owners Baffle Bolt Program, JOBB-CD, Version 05.12, EPRI 1012083, 2005.

- F-9 Materials Reliability Program: Inspection and Flaw Evaluation Strategies for Managing Aging Effects in PWR Internals (MRP-153), EPRI 1012082, 2005.

G

APPENDIX G: VOID SWELLING

G.1 General Description of Void Swelling

Irradiation-induced void swelling, hereafter called void swelling (VS), occurs under some conditions in all structural alloys used in various reactor types, but is especially prevalent in austenitic stainless steels and nickel-base alloys. The common feature of these alloys is their face-centered cubic crystal structure, which is more prone to swelling earlier and at an eventually higher rate than that of body-centered cubic and hexagonal close-packed crystal structured metals.^[G-1]

Void swelling is a potential concern for PWRs and other reactor types operating at elevated temperatures in that it produces volume and thus dimensional changes, and when acting in concert with irradiation creep, it produces distortions of structural components.^[G-2] However, if swelling passes ~5% an additional concern begins to develop. Whereas the radiation-induced changes in mechanical properties typically saturate at relatively low neutron exposures, a new form of embrittlement associated with void swelling arises with increasing swelling. Based on fast reactor data available to date, when ~10% volume change is exceeded, the tearing modulus at PWR operating temperatures of 300-series stainless steels is dramatically reduced and falls to zero at room temperature, producing severe embrittlement with little energy required to propagate any crack.^[G-3]

Swelling arises during neutron or charged particle bombardment of metals at elevated temperatures, leading to a pronounced evolution of the dislocation and precipitate microstructure in response to radiation-induced displacement of atoms from their lattice sites. Exposure doses are best quoted in displacements per atom (dpa) in order to divorce the data from differences in their flux-spectral origins.^[G-4]

Depending on the reactor type and the threshold energy chosen to count the neutrons, the conversion factor for dpa per neutron fluence can vary significantly. A typical value for stainless steel in the metal-fueled EBR-II core is ~5 dpa per 10^{22} n/cm² ($E > 0.1$ MeV) or actually 4.8 to 5.2 over the usable core volume. Outside the core the conversion factor is significantly lower. The conversion values are significantly lower in oxide-fueled cores of Fast Flux Test Facility (FFTF) and various other reactors in Russia, England, Japan and France.

While frequently used for light water reactor applications, a threshold energy of $E > 1.0$ MeV is not used for fast reactor cores. For typical PWR and BWR spectra the conversion values are ~ 7 and ~ 15 dpa per 10^{22} n/cm² for $E > 0.1$ and $E > 1.0$ MeV,⁷ respectively.^[G-4, G-5]

During this displacement-induced evolution, small cavities called voids can appear under some conditions of temperature and dose rates due to the migration and condensation of vacancies to form high densities of void embryos, the nucleation of which can be stabilized by residual (N, O) or transmuted gas atoms (H, He). Eventually these embryos grow to larger sizes that do not require additional gas, and then develop crystallographically-faceted faces. The macroscopic consequence of these microscopic voids is an increase in material volume.

The volume changes associated with void swelling are normally isotropically distributed in three dimensions if there are no physical restraints that resist swelling in a given direction. In general, however, there are external restraints associated with interaction of swelling component items with neighboring component items and there are also internal restraints associated with swelling gradients within a component item. Such restraints generate stress fields that activate irradiation creep and direct the swelling toward unrestrained directions, producing anisotropic swelling and much lower stress levels than those that would develop in the absence of irradiation creep. In situations where two component items interact via differential swelling, such as bolts and the plates in which they are embedded, the stress state can be driven by rather low levels of swelling.^[G-6]

Void swelling was first observed using transmission electron microscopy (TEM) by Cawthorne and Fulton at relatively low levels ($< 1\%$) in irradiated fuel cladding removed from the Dounreay Fast Reactor (DFR) in 1967.^[G-7] Subsequent examination of Type 304 stainless steel ducts from the EBR-II fast reactor showed that swelling levels of 5 to 10 % were possible at ~ 50 dpa.^[G-8] Later studies showed that at very high doses and temperatures that swelling of austenitic alloys in a fast reactor environment did not saturate, and that swelling could approach levels as high as 100% and possibly more under some conditions.^[G-2, G-9]

While the majority of void swelling studies were conducted in sodium-cooled fast reactors in the USA, France, England, Japan and several former Soviet states, other studies conducted by these same countries in water-moderated reactors showed that void swelling was not confined to fast neutron spectra. In order to compile swelling data from various neutron spectra of different types of reactors it is traditional to specify the neutron exposure in displacements per atom or dpa, as mentioned above. This practice is valid as long as there are no large differences in transmutation resulting from the differing spectra, which is a suitable assumption for austenitic alloys as long as differences in helium and hydrogen generation rates are taken into account. Although there are other differences with respect to burn-out of Mn and formation of V, these differences appear to have no large impact on void swelling.^[G-10, G-11]

Swelling is known to exhibit a strong sensitivity to irradiation temperature, which in fast reactors usually spans a much higher range than found in PWRs. While the water temperature in PWRs does not exceed 345°C (653°F), gamma heating of thick near-core component items can drive

⁷ Note however that these factors will vary with fuel design, vendor design, and location within the PWR internals.

local internal temperatures higher, sometimes exceeding 400°C (752°F), and into a temperature regime where void swelling occurs more easily.^[G-12]

In the limited number of internal components extracted from PWRs, significant void swelling has not been detected in austenitic stainless steels to date, with the largest documented swelling of ~0.2%.^[G-13] Similar low swelling levels have been observed in internal component items removed from Russian PWRs, called VVERs.^[G-14] In some cases, very high densities of very small cavities, thought to be helium gas bubbles, have been observed, but the associated volume change is again < 0.1%.

Voids and/or helium bubbles are not generally observed below an irradiation temperature of 300°C (572°F), although two Russian steels irradiated in the BN-350 fast reactor have clearly developed voids at ~280°C (536°F).^[G-15]

Fine dispersions of helium bubbles (2-3 nm diameter or less) have been detected in austenitic stainless steels in various light water reactor (LWR) component items operating at 300-340°C (572-644°F) after 7-56 dpa.^[G-16, G-17] More recent studies on PWR thimble tubes at ~70 dpa have shown that bubble densities can increase significantly, but may also contain hydrogen as well as helium.^[G-18, G-19] None of these bubble distributions involves a significant amount of volume increase, however.

A potentially important aspect of swelling in PWRs arises from transmutation to produce helium and hydrogen at much higher levels than generated in fast reactors. While most previous studies focused on helium, more recent studies focus on both hydrogen and helium.

Helium is chemically inert and virtually insoluble in metals and is essentially immobile at PWR-relevant temperatures of 290-400°C (554-752°F). For austenitic stainless steels in LWRs, helium arises from transmutation by several routes. One is the $^{10}\text{B} (n, \alpha) ^7\text{Li}$ reaction at low (primarily thermal) neutron energies, arising from small trace amounts of boron found in most austenitic stainless steels although it is often localized on grain boundaries. After a relatively low neutron exposure ($\sim 10^{21}$ n/cm² thermal), almost all ^{10}B (20% of natural boron) will have been converted to helium and lithium.

The second source of helium arises from high energy threshold-type (n, α) reactions, primarily with the various isotopes of nickel, with smaller contributions from iron and chromium. This type of neutron reaction occurs only above a threshold energy of ~6 MeV and the helium production rate is almost in direct proportion to the nickel content.^[G-5]

The third and predominant source of helium in LWR spectra arises from the two-step reaction sequence $^{58}\text{Ni} (n, \gamma) ^{59}\text{Ni} (n, \alpha) ^{56}\text{Fe}$ with thermal neutrons.^[G-20] The ^{59}Ni isotope does not occur naturally. The helium generation rate is directly proportional to the ^{59}Ni content and the thermal neutron flux. The generation rate therefore increases strongly with time as the ^{59}Ni is accumulated. This reaction sequence is only a small contribution to the helium production in fast reactor spectra.

Hydrogen likewise arises primarily from the various isotopes of nickel via two major reactions, high energy (n, p) reactions with threshold energy on the order of 1 MeV and the two-step reaction sequence $^{58}\text{Ni} (n, \gamma) ^{59}\text{Ni} (n, p) ^{59}\text{Co}$ with thermal neutrons.^[G-21] More importantly, however, hydrogen arises from many non-transmutation sources in water moderated reactors. These sources are radiolytic decomposition of water, corrosion, hydrogen overpressure maintained on the water and recoil injection from neutron collisions with hydrogen of the water molecule.

Hydrogen is rather mobile in austenitic stainless steels at PWR-relevant temperatures and therefore would not be expected to accumulate like helium. However, recent studies show that significant amounts of hydrogen are being stored when cavities develop in the microstructure. The only reasonable explanation can be an increase in trap density and trap effectiveness, rather than an increase in hydrogen fugacity. It appears that these increased traps are helium-nucleated bubbles and voids.^[G-22, G-23]

G.2 Descriptions of Void Swelling of Austenitic Stainless Steels Irradiated in EBR-II

G.2.1 Earlier Published Equations

Void swelling data (>1%) of irradiated austenitic stainless steels relevant to US PWRs is limited to studies from fast breeder reactors such as EBR-II and FFTF or in mixed spectrum reactors such as ORR (Oak Ridge Research Reactor) and HFIR. Essentially all of the data for annealed Type 304 stainless steel were developed in EBR-II, however. After early studies showed that Type 304 swelled much more than cold-worked Type 316 stainless steel, all irradiation programs shifted to Type 316 in both EBR-II and FFTF. The early studies clearly showed that Type 304 swelled faster than Type 316, and that cold-working led to a reduction in swelling for both steels while preserving the relative swelling vs. composition behavior.^[G-2, G-24, G-25]

Over the years, there have been a number of published empirical equations proposed from regression fitting of void swelling data generated in such reactors. The predominant empirical swelling equations based on fast reactor data have the following power-law form.

$$\% \frac{\Delta V}{V_0} = A(dpa)^n \quad (\text{G-1})$$

Where:

A = temperature dependent parameter

n = temperature dependent or independent parameter.

This equation form is particularly appropriate for annealed austenitic alloys that swell rather easily, especially for annealed Type 304. These materials exhibit continuous curvature in swelling rate as they rise toward the terminal swelling rate of 1%/dpa.^[G-25] Later equations for

cold-worked Type 316 steels adopted a linear-after-incubation format that was consistent with the long incubation transient characteristic of cold-worked 316.^[G-26] For PWR purposes the power law description appears to be more appropriate, especially for the bulk of the baffle-former assembly which is comprised primarily of annealed Type 304 material.

Six published empirical swelling equations from References G-8 and G-27 to G-32 have been reviewed. The form of the temperature dependence of “A” or “n” is usually in the form of a polynomial expression. Table G-1 lists the temperature and dpa range of the underlying void swelling data for each equation evaluated. The parameters “A” and “n” for these models have been calculated from 300°C (572°F) to 400°C (752°F) in 20°C (36°F) increments. It should be emphasized that the database for validating these proposed equations at the lower temperature, lower neutron flux and mixed spectrum conditions of PWRs for the austenitic stainless steels of interest here is extremely limited. The predicted swelling as a function of dpa is plotted in Figure G-1. The following considerations pertaining to the swelling predictions plotted in Figure G-1 should be noted:

Table G-1
Irradiation Conditions for the Empirical Equations Plotted in Figure G-1

Equation Code	Equation Author(s) and Reference	Material	Temp. Range	dpa Range ^a
C-B-F	T.T. Claudson, R.W. Barker, and R.L. Fish in Ref. G-27.	304 SA & 316 SA	Not stated	Not stated
Claudson	T.T. Claudson in Ref. G-28.	316 CW20%	Not stated	Not stated
B-S-H-B	H.R. Brager, J.L. Straalsund, J.J. Holmes and J.F. Bates in Ref. G-29.	304 SA & 316 SA	370-600°C	18-32.5
B-S	J. F. Bates and J. L. Straalsund in Ref. G-8 and Ref. G-30.	304 SA	370-580°C	Up to 34
F-F	J.P. Foster and J.E. Flinn in Ref. G-31.	304L SA	388-542°C	Up to 42
A-C	T.R. Allen and J.I. Cole in Ref. G-32.	316 CW12%	372-386°C	9-47
Yilmaz	Yilmaz et al, Russian stainless steel irradiated in BN-350, See Section G.3.2.	1Cr18Ni10Ti (MTO) and 08Cr16Ni11Mo3 (MTO) in BN-350	See Section G.3.2	

Notes:

a. Based on a conversion factor of 10^{22} n/cm², $E > 0.1$ MeV = 4.5 dpa for EBR-II.^[G-5]

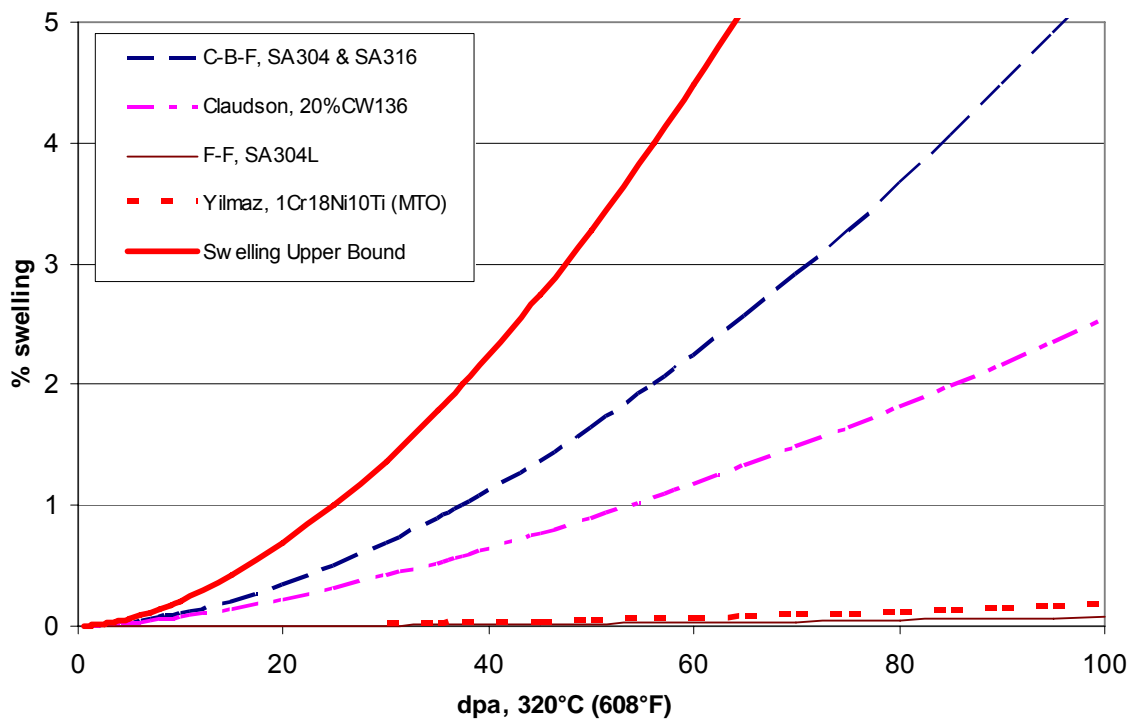
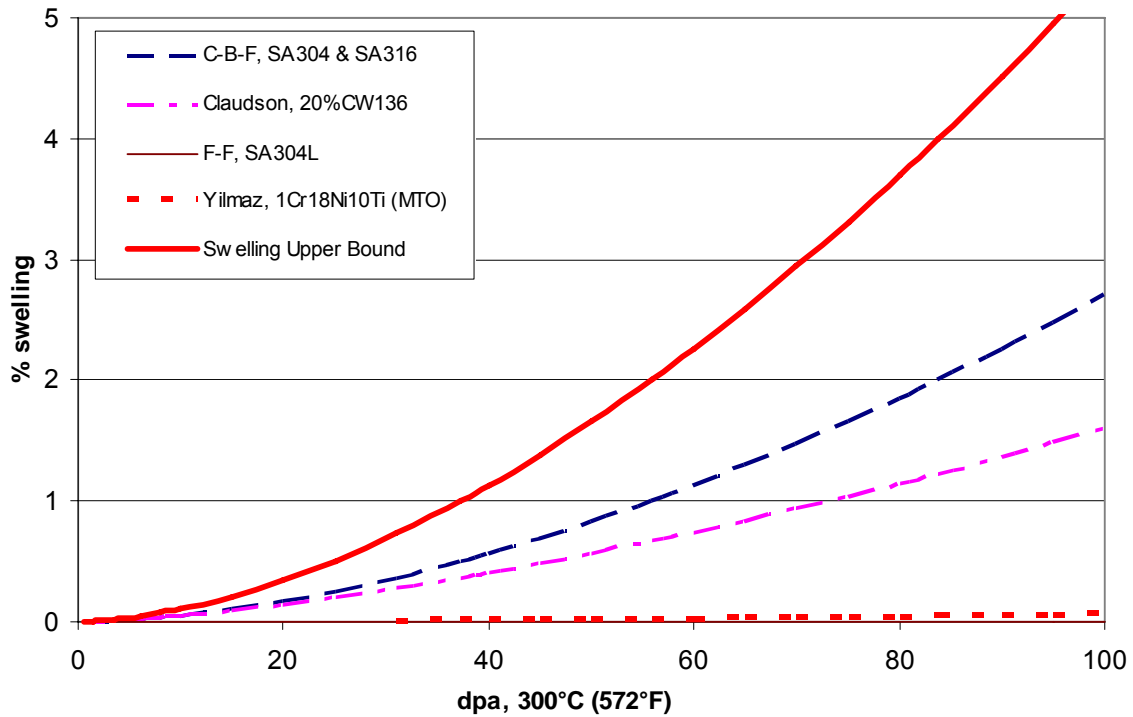


Figure G-1
Swelling-vs.-dpa at Different Irradiation Temperatures for Several Empirical Swelling
Equations (Based on Austenitic Stainless Steel Swelling Data From EBR-II, Except
1Cr18Ni10Ti(MTO) From BN-350 (The Bounding Swelling Line is Also Indicated)

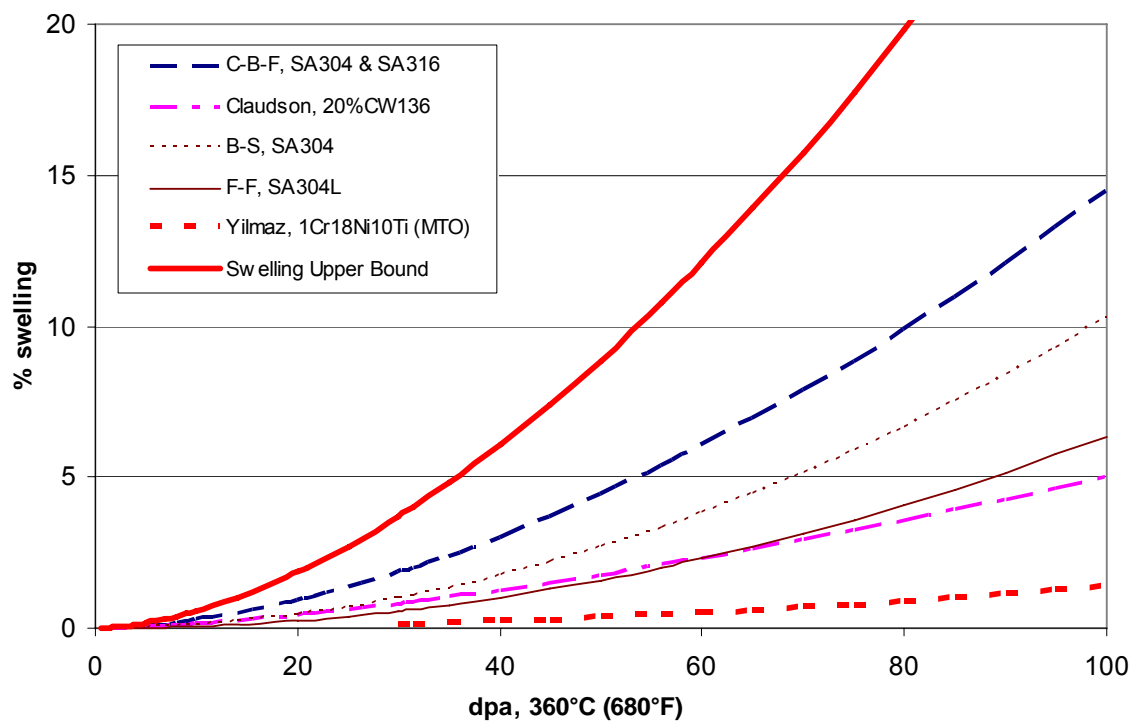
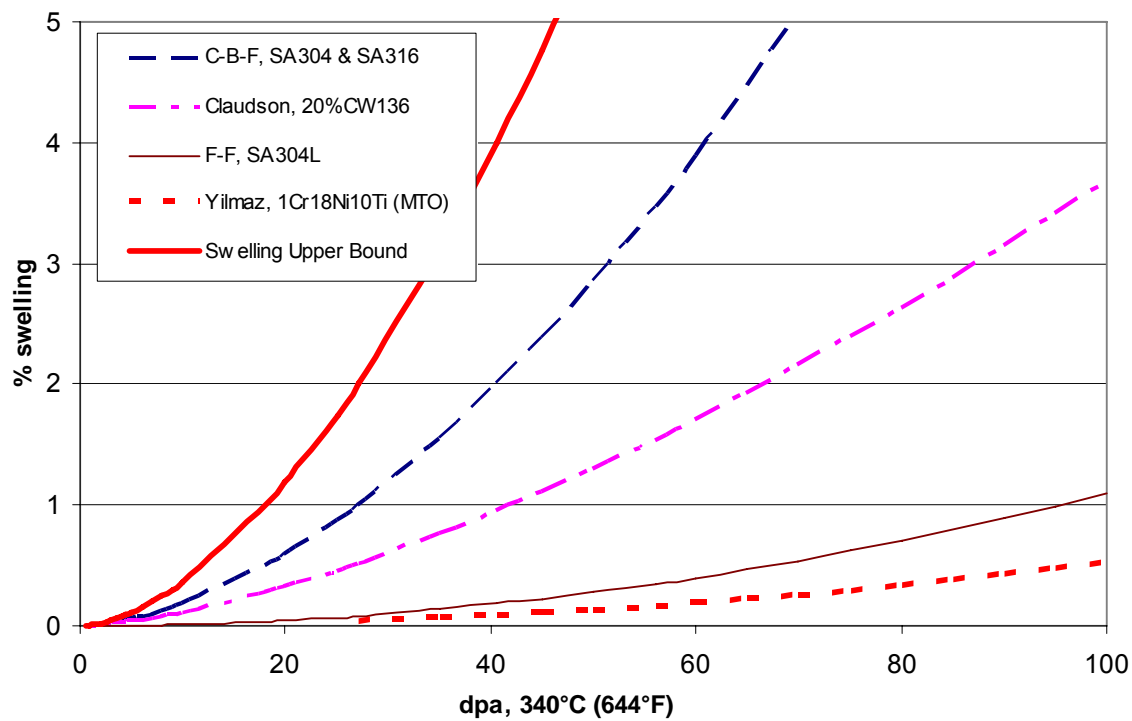


Figure G-1 (continued)

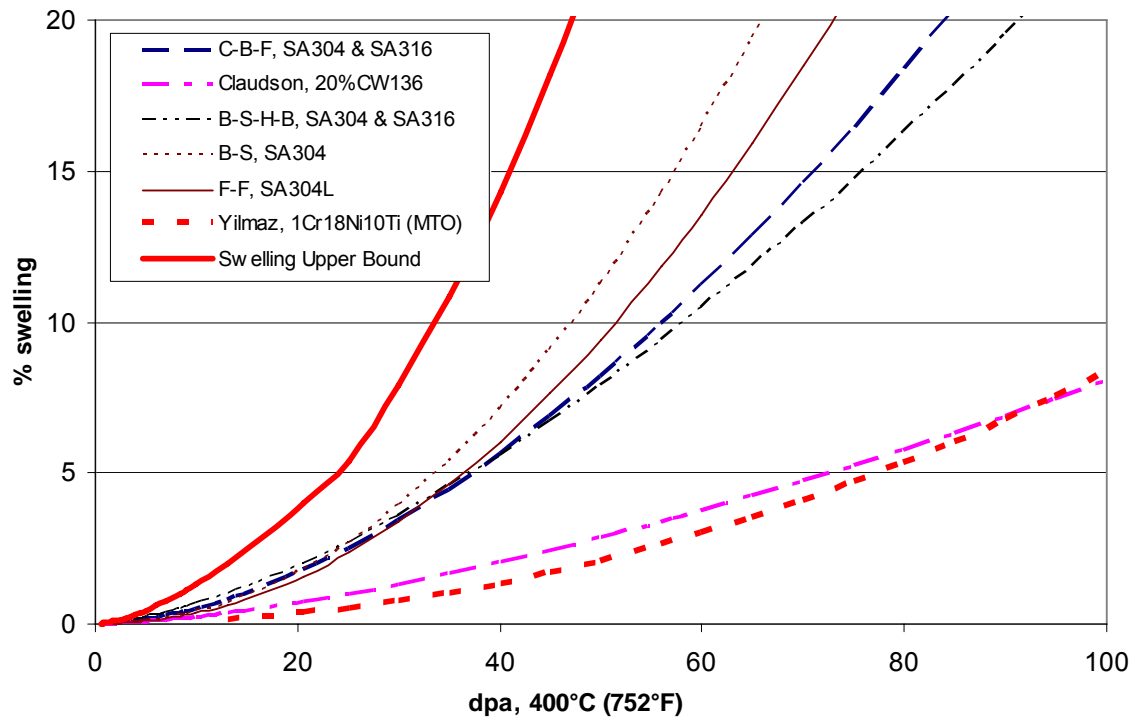
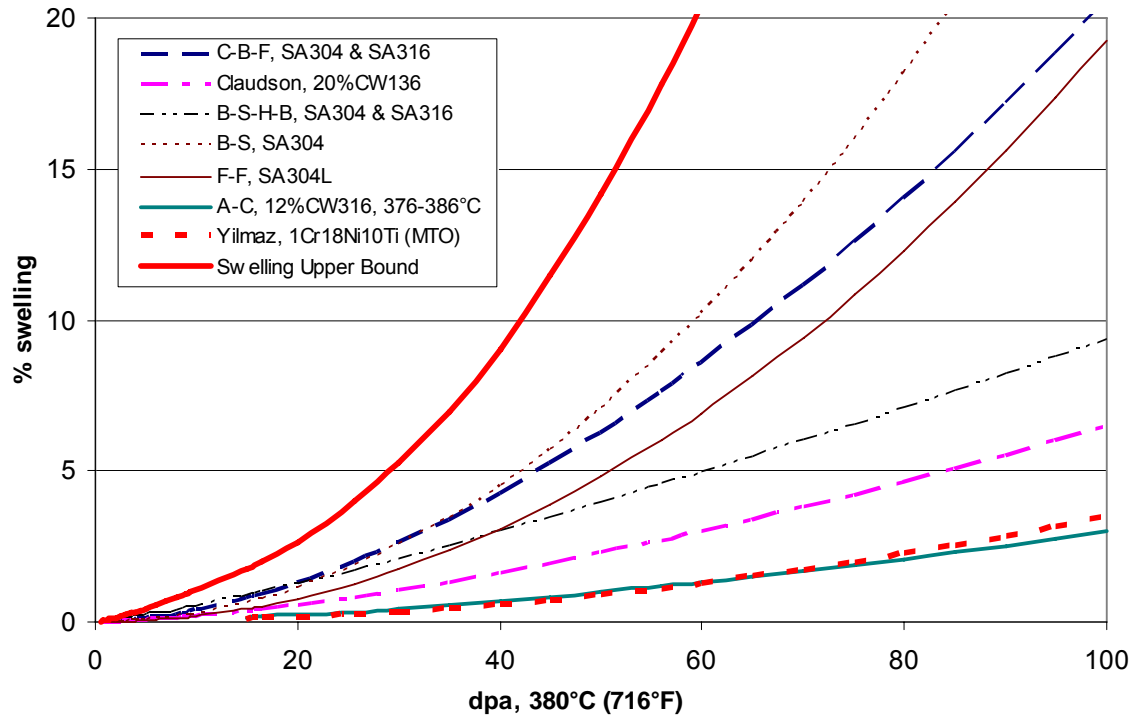


Figure G-1 (continued)

- a. The empirical void swelling equations developed from EBR-II are based on data collected only above 370°C (698°F), which is the EBR-II core inlet temperature. The EBR-II core is also rather small with significant gradients in neutron flux-spectra across both the core axial and radial directions. However, most of the volume of PWR internals experience temperatures that are significantly below 370°C (698°F). Extrapolation of these equations to temperatures below 370°C (698°F) is therefore very problematic for several reasons. First, the potential flux dependence of swelling (see next subsection) was ignored during equation development and thus inadvertently folded into the temperature dependence. Second, and most importantly, there are insufficient PWR data to validate extrapolation of these equations not only to lower temperatures and lower dpa rates characteristic of PWRs, but also to the significantly higher helium and hydrogen generation rates characteristic of LWR spectra.
- b. The maximum temperature plotted in Figure G-1 is 400°C (752°F), which is expected to approximately bound the highest irradiation temperature locations anticipated in the PWR internals; for example, the hot spots in the former plates behind the re-entrant corners of baffle plates.^[G-33] The lowest temperature plotted is 300°C (572°F), below which swelling has not yet been observed in PWR irradiated components.
- c. The maximum fluence plotted is 100 dpa, which is approximately the highest 60-year lifetime dose anticipated in the internals of some PWRs for the re-entrant corners of the baffle-former assembly. It should be emphasized that 100 dpa is well beyond the dose limits of the currently available swelling database. Therefore, even greater uncertainties are expected in the extrapolated swelling at >50 dpa. Furthermore, the highest temperature location and the highest fluence (flux) location on the baffle and former plates in the PWR internals do not coincide, but are offset by several centimeters, which moves the peak swelling away from the highest dose position and into the assembly.^[G-33]

These equations do not incorporate the effect of applied stresses, which after temperature and displacement rate is one of the most important environmental variables. It is the shear components of any applied stress state that accelerate the onset of void swelling, but for PWR applications the applied stresses are relatively low, except for the preloading of bolts. The possibility that large shear strains might develop under the heads of bolts as baffle plates accumulate swelling is still an open question.

The action of internal stresses arising from swelling gradients will be to reduce the steepness of the predicted swelling gradient and thereby spreading the swelling profile to larger areas than predicted by stress-free swelling equations.

To accommodate the above-listed uncertainties, a bounding swelling curve is also shown in Figure G-1, which is based on a factor of two times the highest swelling predicted by the EBR-II empirical equations at any given temperature and dpa level. This bounding curve can be used for rough scoping studies to determine whether swelling should be considered as an issue to address for a particular component location and exposure history.

G.2.2 New Type 304 Stainless Steel Equation

Based on a soon-to-be published experiment conducted in EBR-II, a new stress-free swelling equation has been developed for annealed Type 304.^[G-34] This equation explicitly addresses the

strong flux dependence of swelling observed in the experiment, which covered the full range of PWR-relevant dpa rates. However, the experiment did not overcome the earlier-cited limitation of 370°C (698°F) as the lower temperature limit in EBR-II. By decoupling the flux and temperature dependencies, it is expected that extrapolation to lower PWR-relevant temperatures might be more appropriate for the major portions of the baffle-former assembly experiencing temperatures below 370°C (698°F). In the hot spots expected behind re-entrant corners, the swelling prediction should be more correct. However, it is important to note that regardless of the equation being used, the underlying assumption is that the differences in helium and hydrogen generation rate can be ignored; this is an assumption that requires testing as more data become available from PWRs.

The annealed Type 304 equation developed for PWR use has the following form:

While the A-coefficient was explicitly derived from Type 304 data, coefficients for cold-worked Type 316 are more difficult to specify due to the well-known strong sensitivity of swelling of cold-worked Type 316 to every environmental and material parameter.^[G-2]

In Reference G-6 an equation for cold-worked Type 316 was developed to assist in analysis of bolt-plate interactions. This equation was chosen to retain the same form as that of Type 304 and to fit the few available cold-worked Type 316 data, unfortunately from various heats of material. The cold-worked Type 316 equation was designed primarily to reflect the fact that the smaller volumes of this material in bolts will experience substantially less swelling and therefore did not require extensive and unjustified separate correlation development for the problem being addressed, especially from such a limited and divergent database. Nevertheless, the uncertainty in this and any cold-worked Type 316 equation is substantially larger than that of the Type 304 equation, even though the absolute swelling values will be much smaller. For the development of screening criteria it does not appear to be feasible to confidently develop an improved equation to describe the swelling of cold-worked Type 316 stainless steel.

Figure G-2 compares predicted swelling values as a function of dpa using Eq. G-2 for several dpa rates (fluxes) relevant to the baffle-former region of a PWR internals design (1.4E-7 to 1.4E-8 dpa/sec). Included in Figure G-2 are predictions using the correlation developed by Foster-Flinn.^[G-31]

Figure G-2
Swelling Predictions versus DPA Using the Stress-Free Swelling Equation Developed by
Garner[G-34] [Note: F-F indicates predictions using the Foster-Flinn Equation[G-31] for
Comparison]

Figure G-2 (continued)

Figure G-2 (continued)

There are several effects resulting from this equation compared to use of the dpa-rate insensitive equations of the previous section. First, in general the predicted swelling is higher at the lower dpa rates characteristic of PWRS when compared to that of rate-insensitive equations. Second, predicted swelling gradients arising from dpa gradients are not be as steep as predicted by rate-insensitive equations, as declining dpa rates tend to counteract the effects of declining dpa exposure. This will have an impact on the interaction of swelling and irradiation creep, and the resultant swelling-driven distortion. It should be noted that no effect of stress on swelling has been incorporated in any of the published equations or this new unpublished equation. This will

tend to lead to some degree of under-prediction, but it is anticipated to not be very large for most PWR applications.

G.3 Void Swelling of Russian Stainless Steels in Other Fast Reactors

Void swelling is known to be sensitive to elemental composition and thermal-mechanical starting state, but most overall trends of void swelling have been shown to be exceptionally generic to the austenitic stainless steels.^[G-2] The swelling behavior of one stainless steel usually is representative of all steels and conditions, with the primary variation expressed only in the duration of the transient regime of swelling.

Therefore, it is instructive to review the results of studies on various Russian austenitic stainless steels irradiated in fast reactors located in Russia and Kazakhstan, especially those reactors having lower inlet temperatures of ~280°C (536°F).

G.3.1 Void Swelling Reported in BN-350, BOR-60 and BR-10

Void swelling was not considered to be a potential concern for the major portion of PWR internals operating at relatively low temperature. However, the recent reports of void swelling of Russian stainless steels irradiated in BN-350 show significant swelling under low temperature conditions. This now-decommissioned, sodium-cooled fast reactor was located on the Caspian Sea at Aktau, Kazakhstan, which was part of the former Soviet Union. The swelling observations fell into two major categories: 1) high swelling at high dose and PWR-relevant temperatures and 2) extension of the swelling regime to lower PWR-relevant temperatures and also to earlier swelling as the dpa rate decreased.

In 1998, Garner et al. reported >10% void swelling and resultant severe void-induced embrittlement of a Russian stainless steel at PWR-relevant operating temperatures in BN-350.^[G-35, G-36] The EI-847 niobium-stabilized stainless steel (16Cr-15Ni-3Mo-Nb, used by Russians for applications where Type 316 would be used in the West) tubes were irradiated in the BN-350 to 73-82 dpa at 335-365°C (635-689°F). The composition of this alloy is listed in Table G-2.

Table G-2
Chemical Composition of Russian EI-847 Stainless Steel in BN-350^[G-35, G-36]

Wt%	C	Si	Mn	S	P	Cr	Ni	Mo	Nb	B	N
Solution-annealed	0.050	0.29	0.78	0.009	0.011	15.74	15.32	2.95	0.54	0.001	0.035
18% Cold-worked	0.060	0.20	0.73	0.004	0.012	15.61	14.90	2.96	0.59	0.001	0.022

Some of the stainless steel tubes in this experiment were pressurized by argon to produce hoop stresses up to 196 MPa (28.4 ksi). The total irradiation time was 14,400 hours (600 days), corresponding to dpa rates of 1.41 and 1.58 x 10⁻⁶ dpa/s, rates typical of in-core regions of fast

reactors. For 18% cold-worked EI-847 irradiated to 82 dpa at 365°C (689°F), the reported swelling was 10.3-15.5% by density measurement and 11.7-14.5% from TEM observations. For stress-free solution-annealed tubes irradiated to 73 dpa at 335°C (635°F), the reported swelling was ~6.2%.

So far, this is the only known report of significantly large swelling of austenitic stainless steel at 335-365°C (635-689°F) irradiated in a fast reactor. Such high swelling in an austenitic stainless steel at the reported temperature range was very surprising in view of the current understanding of void swelling developed from the many studies in Western fast reactors, but it must be recognized that the lower inlet temperature (280°C) (536°F) of BN-350 allows measurements at doses and temperatures that could never be made in Western fast reactors that operate at >370°C (698°F). This observation demonstrates the difficulty of extrapolating downward in temperature even in the absence of differences in neutron flux-spectra.

In 1999, Garner et al. reported swelling measurement of yet another Russian stainless steel 12X18H10T (Fe-18.5Cr-9.5Ni-1.5Mn-0.7Si-0.65Ti-<0.12C), which is the Russian equivalent of Type 321 and is used for applications where Type 304 would be used in the West. This alloy was also irradiated in the BN-350 fast reactor.^[G-37] This solution-annealed austenitic stainless steel was irradiated up to 56 dpa at 280-332°C (536-630°F) in the BN-350. Irradiation at 321°C (610°F) and 332°C (630°F) and 4×10^{-8} dpa/s produced 0.17 and 0.28% swelling after ~15 dpa, respectively. The data showed that 56 dpa (at 10^{-7} dpa/s) at 310°C (590°F) produced less than 0.1% swelling from TEM observations. A later update by Garner^[G-38] indicated even higher swelling than previously reported in Reference G-37, with the swelling at a given temperature and dose increasing strongly with lower dose rate.

In a number of recent studies conducted in BN-350, BR-10 and BOR-60, Garner and various Russian and Kazakh coworkers have shown that the onset of swelling in the various Russian stainless steels is indeed accelerated at lower dpa rates,^[G-38, G-39, G-40, G-41, G-42] and that the lower temperature limit of swelling moves to temperatures as low as 280°C (536°F).^[G-15] One comparison of swelling of the 12X18H10T material in BR-10 and BN-350 showed clearly that earlier perceptions of the lower temperature limit of swelling were dictated by the inlet temperature of the reactor and the flux gradient near the bottom of the core, and not the inherent swelling behavior of the stainless steel.^[G-40]

G.3.2 BN-350 Void Swelling Database Analyzed by Yilmaz et al.

In 2003, Yilmaz et al. published a study that analyzed the swelling database of Russian stainless steels irradiated as hexagonal ducts in BN-350.^[G-43] Details of the void swelling database were not provided but review of the original publications in Russian showed that these ducts were irradiated in-core at typical fast reactor dpa rates.

The study led to the following empirical swelling expression:

$$\% \frac{\Delta V}{V_0} = A(dpa - dpa_{incub})^n \quad (\text{G-3})$$

Where

$$A = k \cosh^{-1} \left[p \left(\frac{1}{T} - \frac{1}{T_m} \right) \right] \quad (\text{G-4})$$

The power law form of Eq. G-3 adopted by Yilmaz et al. is identical to Eq. G-1, except for the inclusion of an abruptly ending incubation period. Such an equation form is only valid for austenitic stainless steels that initially resist swelling strongly, especially cold-worked austenitic stainless steels, and will not replicate the gradual onset of swelling toward the end of the transient regime.

The reported data fitting parameters for Eq. G-3 and Eq. G-4 are listed in Table G-3. Based on Eq. G-3 and Eq. G-4, the swelling curve for the Russian 1Cr18Ni10Ti (MTO) material is plotted as a function of dpa between 300 and 400°C (572 and 752°F) in Figure G-1 for comparison with the U.S. stainless steels from EBR-II.

Table G-3
Swelling Parameters for Russian Stainless Steels by Yilmaz et al. ^[G-43]

Russian Designation ^a	Closest AISI ^b	k	n	p	T _m (K) ^c	dpa _{incu} _b
1Cr18Ni10Ti (MTO)	Type 321 or Type 304Ti	6.1x10 ⁻³	2.0±0.2	1.918x10 ⁴	743	0
08Cr16Ni11Mo3 (MTO)	Type 316	5.5x10 ⁻⁴	2.4±0.4	9.0x10 ³	723	20

(a) MTO stands for 20% cold work followed by annealing at 800°C (1472°F) for 1 hour.

(b) Closest AISI equivalent based on chemical composition.

(c) T_m (K) indicates the peak swelling temperature in Kelvin.

Figure G-1 shows that swelling of the Russian stainless steel 1Cr18Ni10Ti in BN-350 is actually lower than the swelling of the U.S. stainless steels in EBR-II, reflecting the known effect of titanium addition to reduce swelling at some higher temperatures. Swelling of the Russian stainless steel 08Cr16Ni11Mo3 was also evaluated but was not plotted in Figure G-1. The swelling of this latter alloy was lower than that of the 1Cr18Ni10Ti (MTO) material, reflecting primarily the well-known effect of nickel content on swelling.

Based on the chemical composition, it is evident that the 1Cr18Ni10Ti (MTO) material listed in Table G-3 is the same type Russian stainless steel reported by Garner et al. as 12X18H10T in Section G.3.1. However, Figure G-1 shows that the swelling of the 1Cr18Ni10Ti (MTO) material was within the band of the results from materials irradiated in EBR-II. Yilmaz's study was conducted on much earlier data produced in Kazakhstan and published only in Russian. Therefore it did not mention the newer work on Russian niobium-stabilized stainless steel EI-847, which showed ~10% swelling at higher exposure reported by Garner et al. in Section G.3.1. This latter work was conducted not in Kazakhstan but in Russia at a different institute (i.e., Institute of Physics and Power Engineering in Obninsk).

The only significant PWR-relevant conclusion to draw from the study of Yilmaz is that the generic behavior of Russian stainless steels is not significantly different in their swelling behavior compared to those of comparable Western stainless steels.

G.4 JOBB Void Swelling Data

G.4.1 JOBB BOR-60 Density Measurement

The JOBB (Joint Owners Baffle Bolt) program was initiated during the 1990s after baffle bolts in EDF's (Electricité de France) CP0 plants were found to have cracked with symptoms characteristic of irradiation-assisted stress corrosion cracking (IASCC).

Specimens of typical French and U.S. PWR austenitic stainless steels with and without welds, as well as candidate replacement materials, were irradiated in both the BOR-60 fast and SM-2 thermal reactors located in Russia. As part of the JOBB program, density measurements were performed on some tensile specimens irradiated at 320°C (608°F) up to 125 dpa at high, in-core dpa rates in the BOR-60 fast breeder reactor in Russia.^[G-44] Density measurements were made on two French heats of solution-annealed Type 304L and two heats of cold-worked Type 316. The chemical compositions and thermal-mechanical starting state are listed in Tables G-4 and G-5.

The measured volumetric changes of the tensile specimens are plotted in Figure G-3 against dpa. A significant amount of scatter in density measurements is seen in Figure G-3. The scatter was attributed to inadequate wetting of the density specimens by the immersion fluid. For example, the density of the four unirradiated specimens was measured three times each. The difference between the maximum and minimum measured value for the same specimen ranges from 0.30% to 0.89%. For the solution-annealed Type 304, the volumetric change ranged from -0.9% to 1.3%, with negative values indicating densification strains as being dominant.

Non-wetting of the fluid usually means that there were tiny air bubbles or thin air films adhering to the specimens. This in general causes the density increase to be overestimated. Thus the higher swelling values should be discounted somewhat in favor of the lower values. This conclusion needs to be confirmed by microscopy examination, however, since the onset of swelling, especially for cold-worked Type 316, is notoriously heterogeneous on both the microscopic and macroscopic level. There is also some heterogeneity associated with the densification process.

Table G-4
Chemical Composition of JOBB Specimens ^[G-44]

Table G-5
Thermomechanical History of JOBB Specimens ^[G-44]

The negative density change numbers indicate that densification has occurred that is attributable to lattice parameter changes accompanying precipitation of carbides during the early stage of neutron irradiation.^[G-2, G-44, G-45] For the cold-worked Type 316, densification (up to 1.2%) dominated the early irradiation period in BOR-60. With increasing fluence, swelling gradually started to offset the initial densification effect. After 125 dpa, swelling gradually overcomes the densification effect due to precipitation. This densification will generally obscure the early development of void swelling. No evidence of voids was found in the TEM specimens irradiated to 40 dpa in BOR-60.

However, the JOBB density data as plotted appear to show swelling in progress at ~60 dpa. TEM observation for specimens irradiated up to 125 dpa should be performed in the future to overcome uncertainties associated with data scatter and densification.

It should be noted that while densification is controlled primarily by time-at-temperature with some possible effect of radiation to accelerate or homogenize the precipitation, the swelling will probably be strongly influenced by the high dpa rate of the BOR-60 experiment as has been observed in a number of studies cited earlier. Therefore the swelling measured in this BOR-60 experiment may be an underestimate of swelling compared to that which would occur at PWR-relevant displacement rates.

G.4.2 JOBB TEM Measurement of EBR-II Specimens

As a part of the JOBB program, specimens from various heats of austenitic stainless steels, including one heat of solution-annealed Type 304L (304L-1) and one heat of cold-worked Type 316 (316-1), were irradiated at 375°C (707°F) in EBR-II at relatively high dpa rates in 1994. The maximum dose achieved in EBR-II was 10 dpa just prior to permanent shutdown of the reactor in September 1994. These are some of the same heats of Type 304L and Type 316 irradiated in BOR-60 (see Table G-5 and Table G-6).

TEM specimens were taken from the head of the tensile specimens. The void size and density are listed in Reference G-46 (Table 7). The estimated swelling is only 0.02% for the solution-annealed Type 304L. No voids were observed for the cold-worked Type 316 after 10 dpa, a behavior consistent with the known relative swelling behavior of these two stainless steel alloys (Table G-6). Because the estimated swelling does not take into account the densification due to carbide precipitations, the overall change in volume could be near-zero or more likely, slightly negative.

Table G-6
Swelling of JOBB Specimens Irradiated in EBR-II at 375°C (707°F)^[G-46]

Figure G-3
Volumetric Change from Density Measurements of JOBB Tensile Specimens Irradiated in BOR-60 at 320°C (608°F)

G.5 Void Swelling in Removed PWR Baffle Bolts

To date, the only PWR void swelling data comes from the baffle-to-former bolts removed due to IASCC concerns. Minor void concentrations were observed with TEM in some baffle bolts removed from Point Beach Unit 1, Farley Unit 1, and Tihange 1. Table G-7 is a summary of the operating parameters of these three plants.^[G-47, G-48]

Table G-7
Plants with Baffle Bolts Removed and Inspected for Void Swelling^[G-47, G-48]

Fluence and temperature gradients exist along the length of these bolts, with the bolt heads experiencing the highest fluence due to being closer to the core. The highest calculated temperature was usually in the shank or threads arising from gamma heating and heat transfer considerations. The amount of void swelling in each case was estimated from the void size distribution and density in the TEM specimens.

The locations with observable void swelling coincided with the position having the highest irradiation temperature. The void swelling results and the local irradiation conditions are summarized in Table G-8, where a maximum calculated swelling value of 0.24% is noted for a bolt from Tihange 1.

The U.S. bolts examined experienced a deliberate operational change in temperature during irradiation. The high temperature period specified in Table G-8 corresponds to the period involving a high leakage core and/or a down-flow configuration, i.e., before conversion to a low leakage core and/or an up-flow configuration. These conditions may have a bearing on swelling measured in these bolts.

The baffle bolt swelling data derived from TEM evaluations shows a very minor amount of void swelling (0.24% or less) at 340-363°C (644-685°F) after ~20 EFPYs of plant operation. Considering the densification effect arising from carbide precipitation, the actual overall volumetric swelling was likely somewhat lower or even slightly negative.

Table G-8
Void Swelling in PWR Baffle-to-Former Bolts

It is important to recognize that significant uncertainties existed in the estimated swelling by counting void density and size with TEM. Considering the densification effect arising from carbides precipitation, the actual overall volumetric swelling was likely lower or could be even slightly negative.

It is also important to note that voids were observed at their highest levels in the shanks of the bolts, regions which were under stress and therefore likely to have experienced stress-enhancement of swelling.

G.6 Factors Affecting Void Swelling

From the above discussion, it is evident that swelling of any particular austenitic stainless steel is rather sensitive to temperature and dpa rate. Other factors have also been reported to affect void swelling, some of which have been mentioned above. An expanded summary is given in the following paragraphs to guide the establishment of screening criteria.

1. Solution-Annealed vs. Cold-Worked

Swelling data from EBR-II and other reactors demonstrate that cold-work is effective in prolonging the swelling incubation period for austenitic stainless steel. The temporary suppression effect of cold-work is usually attributed to the elevated dislocation density, which provides additional recombination sites for interstitials and vacancies. This reduces the vacancy supersaturation, delaying void nucleation, and also interferes with diffusion of minor solutes thereby influencing the various precipitation processes that occur thermally or that are stimulated by radiation.

2. Major Differences in Chemical Composition

The duration of the transient regime of swelling is known to be strongly sensitive to the nickel and chromium content.^[G-49, G-50] These elements strongly change the effective vacancy diffusivity and therefore the vacancy supersaturation, affecting the duration of the transient regime^[G-51] but not the steady state swelling rate.

On this basis alone, Type 304 always swells more than Type 316 in the same thermal-mechanical starting state. The combined effect of cold-work and alloy composition insure that the incubation period for solution-annealed Type 304 is significantly shorter than that of cold-worked Type 316 in fast reactors at the same irradiation temperature and dpa rate. It is assumed, but not yet conclusively demonstrated, that this relationship will be preserved under PWR-relevant temperature conditions.

3. Minor Differences in Chemical Composition

In 1974, Bates presented results of a comprehensive study aimed at determining how minor changes in alloying constituents would affect the swelling behavior of Type 316 stainless steel.^[G-52] Later, more comprehensive studies by Brager and Garner confirmed

and extended the results of Bates. These studies showed that, atom-for-atom, phosphorus, silicon, titanium and carbon in solid solution, in that order, were most effective in delaying the onset of swelling.^[G-50, G-53, G-54, G-55] However the influence of carbon with elements such as titanium, niobium, and zirconium, which determine the distribution and precipitation of carbides, often is reversed with temperature, sometimes increasing swelling.

Phosphorus and silicon strongly change the effective vacancy diffusivity and therefore the vacancy supersaturation, affecting the duration of the transient regime but not the steady state swelling rate.^[G-56]

It is important to note that minor heat-to-heat differences are usually expressed in the minor compositional elements, especially phosphorus, both in their concentration and microscopic distribution as a result of differences in thermal-mechanical treatment during production. Thus, essentially identical heats of stainless steel material can sometimes exhibit large differences in swelling behavior as a result of relatively small differences in thermal-mechanical preparation.^[G-57]

4. Stress and Stress History

Stress is generally regarded as a factor that accelerates swelling.^[G-2, G-58] Much of the swelling data used to generate the empirical correlations in Section G.2 were derived from various thimbles in the EBR-II with only a minor pressure difference across the tube wall. In general there will be stresses imposed by gradients in temperature and swelling, but these are quickly relaxed by irradiation creep during irradiation. If the temperature gradient is very large, such as across the thin cladding of high power fuel pins, then the initial stresses are large enough to strongly accelerate swelling of the cladding,^[G-59, G-60] but such situations are not expected in PWR internals.

Interestingly, it is the shear components of the stress state that accelerate swelling, not the hydrostatic components. Therefore the sign of the stress state is not relevant.^[G-61, G-62]

Another facet of stress-enhanced swelling is that swelling gradients will generate short-lived stresses on adjacent lower swelling volumes, forcing them to try to catch up with adjacent faster-growing volumes. Thus predictions of stress-free swelling will project steeper swelling gradients than will actually develop and swelling footprints of hot spots behind reentrant corners will be wider than predicted using stress-free swelling equations.

As mentioned earlier, swelling can be anisotropic in the presence of both external and internal constraints. For the hot corner in the former plate behind the reentrant baffle plate corner, significant internal constraints will occur. One consequence will be that the swelling will tend to be redirected vertically, producing a bulge in the plate, most likely with no deleterious consequences for continued functionality.

Stresses are often very time-dependent in their development, decreasing via stress relaxation or increasing as components swell and interact. The cumulative effect of such histories has only been examined for fast reactor fuel pins, which are not relevant to the

PWR internals situation. The changing stress state associated with baffle bolts was addressed in an earlier report.^[G-6] In such case, the stress state is driven by stress-relaxation via irradiation creep and by differential swelling.

5. Displacement Rate

Garner and various coworkers have compiled a number of data from fast reactors suggesting that a dpa rate effect on void swelling will occur in the PWR-relevant temperature range, i.e., the lower dpa rate in PWR internals would result in higher swelling than in fast reactors when irradiated to the same dpa at the same temperature.^[G-40, G-41, G-42, G-63, G-64] The dpa rate effect on PWR-induced swelling is still not completely defined, however, with a few studies^[G-33, G-65] not observing a strong effect. The implication of such a dpa rate effect on void swelling, if it indeed exists, would make a PWR void swelling prediction based on high-flux fast reactor swelling data non-conservative.

6. Temperature History

A number of studies have shown that austenitic stainless steels, especially those that resist swelling, are particularly prone to accelerated swelling as a result of certain temperature histories inherent in fast reactor operation.^[G-66, G-67] These temperature histories involve prolonged persistent decreases in temperature during irradiation and are not thought to be relevant to PWR operation.

PWRs do experience one form of temperature history that is atypical of any fast reactor situation. This history is associated with gamma heating variations arising from the burnout of the boron in the primary coolant and the periodic refreshment of the boron.^[G-4, G-33] This induces a periodic saw-tooth variation in the thermal neutron population, local gamma heating rates and finally the temperature history in the internals. The oscillations are only on the order of 15-20°C (27-36°F), but since this oscillation occurs in the temperature range where the boundary of the lower temperature limit of void swelling occurs there may be some significant impact on the onset of void nucleation and subsequent swelling. The potential, but unknown, influence of such history on void nucleation and growth adds to the uncertainty associated with prediction of swelling in PWR internals.

As mentioned earlier there were sometimes major operational changes in temperature arising from changes to a low leakage core and/or to up-flow cooling. There are no data to assess the impact of such variations on void swelling, especially for PWR-relevant temperatures.

7. Helium Production

Some studies have shown^[G-68, G-69] that a very high helium content or production rate can prolong the incubation period of void swelling under certain conditions, especially during

ion bombardment conditions at very high dpa rates. For neutron irradiation this situation is not so clearly manifested, with various studies giving conflicting results.

In this proposed scenario, the presence of a large number of helium gas bubbles early in life is thought to increase the vacancy sink density and the point defect recombination rate. This decreases the vacancy supersaturation level, and hence, increases the critical cavity size for the biased void growth, delaying the onset of rapid swelling. Once the steady state swelling condition has been reached, it appears that high bubble densities generated in LWRS can coexist with voids without decreasing the steady state swelling rate.^[G-70]

The presence of bubbles reflects gas production, especially that of helium. Helium production is higher in Type 316 than in Type 304 due to a roughly 50% higher Ni content, but the difference is insufficient in itself to cause either a prolongation or shortening of incubation via changes in vacancy supersaturation. The higher nickel content of Type 316 is by itself sufficient to drop the vacancy supersaturation by a much larger amount.^[G-51]

As discussed earlier, the recently rediscovered issue of helium and hydrogen cogeneration in LWR environments and the subsequent storage of hydrogen in voids and bubbles add an additional level of uncertainty to swelling prediction.

In summary, void swelling is a complex phenomenon that is highly dependent on the material (chemical composition and thermal-mechanical treatment) and on the irradiation conditions (temperature history, flux-spectrum, dpa rate and gas production). These factors are often highly interactive and synergistic in determining the path taken by the swelling phenomenon. All of these contribute to the difficulty of confidently forecasting the level and distribution of void swelling and its associated strains in PWR internals. However, there are sufficient data and insight developed from fast reactor experience to provide a path forward to establishing initial screening criteria.

G.7 VS Threshold and Screening Criteria

To date, there have been no reports of PWR internals component items showing significant distortion or failures as a direct or contributing consequence of void swelling. However, in practice, this may be a poor indicator because of the lengthy incubation period that is often observed prior to the onset of steady state swelling. On the other hand, if swelling does manifest itself in PWR internals component items, it is highly likely that significant swelling will be localized in relatively small and isolated volumes due to the factors cited above. Since there are few data available derived from irradiation conditions in PWRs in the temperature range where the risk of void swelling is greatest, the possibility of swelling-induced problems requires attention.

Based on the above discussion, void swelling depends primarily on temperature, flux, stress and many other factors, although stress is thought not to be as important for most PWR applications. Other factors such as minor heat-to-heat differences are probably secondary for stainless steel

materials compared to temperature and flux but more importantly, these variables cannot be quantified separately based on the current swelling database. As discussed earlier it appears that a swelling-based screening criterion for cold-worked Type 316 may not be necessary based on the anticipated much lower swelling of this material.

Therefore, at this point the suggested threshold and screening criteria for austenitic stainless steel materials (wrought and weld) should depend primarily upon the temperature, accumulated dpa and dpa rate that the PWR internals component item will experience during operation. However, the screening criteria should focus not on the irradiation conditions themselves, but on well-defined potential consequences. For swelling, the consequences are: a) volume and dimensional changes, and b) swelling-induced embrittlement.

Since the onset of void-induced embrittlement is ~5% swelling, it is deemed to be prudent that swelling of one half that level should trigger examination. Since the swelling rate will never exceed 1%/dpa this gives a minimum of 2.5 years and probably much longer to clear the 5% criterion, allowing time for analysis and examination. Total embrittlement occurs at ~10% swelling, allowing even more time to assess consequences and initiate examination, remediation or replacement.

Isotropic swelling of 2.5% swelling implies maximum linear strains of ~0.8%, a number comparable to uncertainties in production tolerances of most in-core components and probably not observable during inspection. Even for completely anisotropic swelling, which is quite improbable in PWR application, linear strains of 2.5% are most probably within the envelope of continued component functionality. Certainly by ~4% isotropic swelling or 2.5% anisotropic swelling there will be measurable strains possibly observable upon inspection or measurement via non-destructive ultrasonic or electro-resistivity techniques.^[G-71, G-72]

As documented in earlier sections all swelling predictions for PWR-relevant conditions will be very uncertain, but some estimate can be made based on data derived from fast reactor irradiation.

Therefore it is suggested that the best currently available predictive swelling equation (based on Type 304 stainless steel) be used to calculate the predicted potential for void swelling. If the predicted swelling approaches 2%, then some evaluation of the specific stainless steel material and estimate of the stress state should be made to ascertain whether the 2.5% criterion will be reached, triggering a requirement for further assessment.

It is important to note that the largest predicted swelling will most probably occur in regions that are not easily accessed, such as the hot spots within the former plates behind reentrant baffle plate corners. When these locations exceed 2.5%, the overwhelming remainder of the baffle-former assembly will be very much below even 1%. This statement will probably remain valid even when the hot spot regions exceed the 10% criterion.

It should also be noted that component items such as baffle bolts will have their behavior determined by lesser amounts of swelling, primarily via differential swelling with the plates in

which they are embedded. Establishment of a screening criterion is harder for such situations and requires further data and discussion.

Given the demonstrated sensitivity of void swelling to dpa rate, it is recommended that the new flux-dependent equation presented in Section G.2.2 be employed. It will most certainly predict the largest conservative swelling for most situations. As additional data accumulate the equation should be updated and the consequences reassessed.

In summary, based on currently available PWR data it appears that for austenitic stainless steel alloy and austenitic stainless steel weld metal locations below 320°C (608°F) and less than 20 dpa (1.3×10^{22} , $E > 1.0$ MeV) no significant swelling is expected. Therefore no screening is required. It is also concluded that austenitic stainless steel alloy and austenitic stainless steel weld metal locations achieving temperatures $\geq 320^\circ\text{C}$ (608°F) and neutron exposure ≥ 20 dpa (1.3×10^{22} , $E > 1.0$ MeV) are to be initially screened in for further evaluation.

A procedure for follow-on evaluations might use the following logic sequence:

Locations with temperatures $< 320^\circ\text{C}$ (608°F) and neutron exposure < 20 dpa (1.3×10^{22} , $E > 1.0$ MeV) are below the screening criteria and no calculations or further evaluation is needed.

For locations with temperatures $\geq 320^\circ\text{C}$ (608°F) and neutron exposure ≥ 20 dpa (1.3×10^{22} , $E > 1.0$ MeV), estimate the void swelling using the best currently available predictive equation (e.g., Eq. G-2). If void swelling predictions are $< 2.5\%$, no further evaluation is required.

For locations with temperatures $\geq 320^\circ\text{C}$ (608°F) and neutron exposure ≥ 20 dpa (1.3×10^{22} , $E > 1.0$ MeV), estimate the void swelling using the best currently available predictive equation (e.g., Eq. G-2). If void swelling predictions are $\geq 2.5\%$, further functionality evaluations are necessary.

G.8 VS References

- G-1 Sniegowski, J. J., and Wolfer, W. G., Proceedings of Topical Conference on Ferritic Alloys for Use in Nuclear Energy Technologies, Edited by J. W. Davis and D. J. Michel, TMS-AIME, 1983, pp. 579-586.
- G-2 Garner, F. A., Chapter 6: "Irradiation Performance of Cladding and Structural Steels in Liquid Metal Reactors," Vol. 10A of Materials Science and Technology, A Comprehensive Treatment, VCH Publishers, 1994, pp. 419-543.
- G-3 Hamilton, M. L., Huang, F. H., Yang, W. J. S., and Garner, F. A., "Mechanical Properties and Fracture Behavior of 20% Cold-Worked 316 Stainless Steel Irradiated to Very High Exposures," Effects of Radiation on Materials: Thirteenth International Symposium (Part II) Influence of Radiation on Material Properties, ASTM STP 956, F. A. Garner, N. Igata and C. H. Henager, Jr., Eds., ASTM Philadelphia, PA, 1987, pp. 245-270.

- G-4 Garner, F. A., and Greenwood, L.R., "Survey of Recent Developments Concerning the Understanding of Radiation Effects on Stainless Steels Used in the LWR Power Industry," 10th International Conference on Environmental Degradation of Materials in Nuclear Power Systems – Water Reactors, 2003, pp. 887-909.
- G-5 Garner, F.A., Greenwood, L.R., and Reid, B.D., "An Assessment of the Possible Role of Transmutation on Development of Irradiation-Assisted Stress Corrosion Cracking in Light Water Reactors," EPRI TR-107159, "Critical Issue Reviews for the Understanding and Evaluation of Irradiation Assisted Stress Corrosion Cracking," Final Report, November, 1996, Electric Power Research Institute (EPRI), Palo Alto, CA.
- G-6 Simonen, E. P., Garner, F. A., Klymyshym, N. A. and Toloczko, M. B., "Response of PWR Baffle-Former Bolt Loading to Swelling, Irradiation Creep and Bolt Replacement As Revealed Using Finite Element Modeling", Proc. 12th International Conference on Environmental Degradation of Materials in Nuclear Systems-Water Reactors, 2005, issued in CD format with no page numbers.
- G-7 Cawthorne, C. and Fulton, J. E., Nature 216, 515-517.
- G-8 Fish, R.L., Straalsund, J.L., Hunter, C.W., and Holmes, J.J., "Swelling and Tensile Property Evaluations of High-Fluence EBR-II Thimbles," Effects of Radiation on Substructure and Mechanical Properties of Metals and Alloys, ASTM STP 529, American Society for Testing and Materials 1973, pp. 149-164.
- G-9 Garner, F. A., and Gelles, D. S., "Neutron-Induced Swelling of Commercial Alloys at Very High Exposures," Proceedings of Symposium on Effects of Radiation on Materials: 14th International Symposium, ASTM STP 1046, N. H. Packan, R. E. Stoller and A.S. Kumar, eds., American Society for Testing and Materials, Philadelphia, 1990, Vol. II, pp. 673-683.
- G-10 Bates, J. F., Garner, F. A., and Mann, F. M., "The Effects of Solid Transmutation Products on Swelling in AISI 316 Stainless Steel," Journal of Nuclear Materials, 103 and 104 (1981), p. 999.
- G-11 Garner, F. A., Heinisch, H. L., Simons, R. L. and Mann, F. M., "Implications of Neutron Spectrum and Flux Differences on Fission-Fusion Correlations at High Neutron Fluence," Radiation Effects and Defects in Solids, 113, 1990, 229-239.
- G-12 Garner, F. A., Greenwood, L. R. and Harrod, D. L., "Potential High Fluence Response of Pressure Vessel Internals Constructed from Austenitic Stainless Steels", Proc. Sixth International Symposium on Environmental Degradation of Materials in Nuclear Power Systems - Water Reactors, San Diego, CA. August 1-5, 1993, pp. 783-790.
- G-13 Edwards, D. J., Simonen, E. P., Garner, F. A., Oliver B. M. and Bruemmer, S. M., "Sensitivity of Microstructural Evolution Due to Temperature and Dose Gradients in Neutron-Irradiated 316SS", Journal of Nuclear Materials 317 (2003) 32-45.

- G-14 Neustroev, V. N., Dvoretzky, V. G., Ostrovsky, Z. E., Shamardin, V. K. and Shimansky, G. A., "Investigation of the Microstructure and Mechanical Properties of 18Cr-10Ni-Ti Steel Irradiated in the Core of VVER-1000 Reactor," Effects of Radiation on Materials, 21st International Symposium, ASTM STP 1447, 2004, pp. 32-45.
- G-15 Maksimkin, O. P., Tsai, K. V., L. G. Turubarova, L. G. , Doronina, T. and Garner, F. A., "Characterization of 08Cr16Ni11Mo3 Stainless Steel Irradiated in the BN-350 Reactor," Journal of Nuclear Materials, 329-333 (2004) 625-629. Also "Void Swelling of AISI 321 Analog Stainless Steel Irradiated at Low dpa Rates in the BN-350 Reactor", Submitted for Publication in Journal of Nuclear Materials as proceedings of ICFRM-12.
- G-16 Maziasz, P.J., "Overview of Microstructural Evolution In Neutron-Irradiated Austenitic Stainless Steels," Journal of Nuclear Materials, 205 (1993), 118-145.
- G-17 Foster, J.P., Porter, D.L., Harrod, D.L., Mager, T.R., Burke, and M.G., "316 Stainless Steel Cavity Swelling in a PWR," Journal of Nuclear Materials 224 (1995) 207-215.
- G-18 Fujimoto, K., Yonezawa, T., Wachi, E., Yamaguchi, Y., Nakano, M., Shogan, R. P., Massoud, J. P. and Mager, T. R., "Effect of Accelerated Irradiation and Nuclear Transmuted Gas on IASCC Characteristics for Highly Irradiated Austenitic Stainless Steels", 12th International Conference on Environmental Degradation of Materials in Nuclear Systems – Water Reactors, in press.
- G-19 Edwards, D. J., Bruemmer S. M. and Efsing, P., "Microstructural Evolution in Neutron-Irradiated Stainless Steels: Comparison of LWR and Fast-Reactor Irradiations", 12th International Conference on Environmental Degradation of Materials in Nuclear Systems – Water Reactors, in press.
- G-20 Garner, F. A., Hamilton, M. L. , Greenwood, L. R., Stubbins, J. F. and Oliver, B. M. , "Isotopic Tailoring with ⁵⁹Ni to Study the Effect of Helium on Microstructural Evolution and Mechanical Properties of Neutron Irradiated Fe-Cr-Ni Alloys", Proceedings of 16th ASTM International Symposium on Effects of Radiation on Materials, ASTM STP 1175, Denver, CO, June 22-24, 1992, pp. 921-939.
- G-21 Greenwood L. R., and Garner, F. A., "Hydrogen Generation Arising from the ⁵⁹Ni (n , p) Reaction and its Impact on Fission-Fusion Correlations", Journal of Nuclear Materials, 233-237 (1996) 1530-1534.
- G-22 Garner, F. A., Simonen, E. P., Oliver, B. M., Greenwood, L. R., Grossbeck, M. L., Wolfer, W. G. and Scott, P. M., "Retention of Hydrogen in FCC Metals Irradiated at Temperatures Leading to High Densities of Bubbles or Voids, with Implications for Accelerator Driven Systems", accepted for publication in Journal of Nuclear Materials as part of proceedings of IWSMT-7.
- G-23 Tolstolutsкая, G. D., Ruzhytskiy, V. V., Kopanets, I. E., Karpov, S. A., Bryk, V. V., Voyevodin, V. N. and Garner, F. A., "Displacement and Helium-induced Enhancement

of Hydrogen and Deuterium Retention in Ion-Irradiated 18Cr10NiTi Stainless Steel”, accepted for publication in Journal of Nuclear Materials as part of proceedings of IWSMT-7.

- G-24 Garner, F. A. and Porter, D. L., "A Reassessment of the Swelling Behavior of AISI 304L Stainless Steel," Proceedings International Conference on Dimensional Stability and Mechanical Behavior of Irradiated Metals and Alloys, April 11-13, 1983, Brighton, England, Vol. II, pp. 41-44.
- G-25 Garner, F. A., "Recent Insights on the Swelling and Creep of Irradiated Austenitic Alloys," Invited Paper, Journal of Nuclear Materials, 122 and 123, (1984), pp. 459-471.
- G-26 Garner, F. A., Laidler J. J. and Guthrie, G. L., "Development and Evaluation of a Stress-Free Swelling Correlation for 20% Cold-Worked 316 Stainless Steel," in "Irradiation Effect on the Microstructure and Properties of Metals," ASTM STP 611, (1976) pp. 208-276.
- G-27 Bement, A.L. "Void Formation In Irradiated Austenitic Stainless Steels," Advances in Nuclear Science and Technology, Vol. 7, edited by E.J. Henley and J. Lewis, 1973, pp.14-17 Academic Press, Inc., New York.
- G-28 Claudson, T.T., "Irradiation Induced Swelling and Creep In Fast Reactor Materials," Proc. Karlsruhe Conf. Fast Reactor Fuel and Fuel Elements, 1970, pp. 637-670.
- G-29 Brager, H.R., Straalsund, J.L., Holmes, J.J. and Bates, J.F., "Irradiation-Produced Defects In Austenitic Stainless Steel," Metallurgical Transactions, 1971, pp. 1893-1904.
- G-30 Bates, J. F. and Straalsund, J. L., "An Empirical Representation of Irradiation-Induced Swelling of Solution Treated Type 304 Stainless Steel," Nuclear Technology 14, 1972, pp. 292-298.
- G-31 Foster, J.P. and Flinn, J.E., "Residual Stress Behavior in Fast Neutron Irradiated SA AISI 304L Stainless Steel Cylindrical Tubing," Journal of Nuclear Materials 89 (1980) 99-112.
- G-32 Allen, T.R., Cole, J.I., "The Effect of Low Dose Rate Irradiation on the Swelling of 12% Cold-Worked 316 Stainless Steel," Proc. 9th International Symposium on Environmental Degradation of Materials in Nuclear Power Systems – Water Reactors, TMS, 1999, pp. 1035-1042.
- G-33 Tang, H. T. and Gilreath, J. D, "Aging Research and Management of PWR Vessel Internals", Proceedings Fontevraud 5, Contribution of Materials Investigation to the Resolution of Problems Encountered in Pressurized Water Reactors, 23-27 September, 2002, paper #19, on CD format, no page numbers.
- G-34 Battelle Pacific Northwest Laboratories Letter from Garner, F.A., to Tang, H.T., "New Swelling Equation for Annealed 304 Stainless Steel," November 11, 2005.

- G-35 Porollo, S.I., Vorobjev, A.N., Konobeev, Yu.V., Dvoriashin, A.M., Krigan, V.M., Budylkin, N.I., Mironova, E.G., and Garner, F.A., "Swelling and Void-Induced Embrittlement Of Austenitic Stainless Steel Irradiated to 73-82 dpa at 335-365°C," *Journal of Nuclear Materials* 258-263 (1998) pp. 1613-1617.
- G-36 Porollo, S.I., Dvoriashin, A.M., Vorobjev, A.N., Krigan, V.M., Konobeev, Yu.V., Garner, F.A., Budylkin, N.I., and Mironova, E.G., "Neutron-Induced Swelling And Embrittlement Behavior of Two Russian Stainless Steels at PWR-Relevant Temperatures and 65-85 dpa," *Proc. Ninth International Symposium on Environmental Degradation of Materials in Nuclear Power Systems – Water Reactors, The Minerals, Metals, and Materials Society (TMS)*, 1999, pp. 1060-1067.
- G-37 Garner, F.A., Porollo, S.I., Vorobjev, A.N., Konobeev, Yu.V., and Dvoriashin, A.M., "Void Swelling At Low Displacement Rates In Annealed X18H10T Stainless Steel at 30-56 dpa and 280-332°C," *Proc. Ninth International Symposium on Environmental Degradation of Materials in Nuclear Power Systems – Water Reactors, The Minerals, Metals, and Materials Society (TMS)*, 1999, pp. 1051-1058.
- G-38 "Determination of the Lower Temperature Limit of Void Swelling of Stainless Steels at PWR-Relevant Displacement Rates," by Porollo, S.I. et al., RI-ITG/JOBB Meeting Minutes, Baltimore, Maryland, May 20-22, 2002, available from the Electric Power Research Institute (EPRI), Palo Alto, California.
- G-39 Porollo, S. I., Dvoriashin, A. M., Konobeev, Yu. V., Ivanov, A. A. and Shulepin, S. V. and Garner, F. A., "Microstructure and Mechanical Properties of Austenitic Stainless Steel 12X18H9T after Neutron Irradiation in the Pressure Vessel of BR-10 Fast Reactor at Very Low Dose Rates", submitted to *Journal of Nuclear Materials* and published in *Fusion Reactor Materials Semiannual Progress report*, 2005.
- G-40 Garner, F. A., Budylkin, N. I., Konobeev, Yu. V., Porollo, S. I., Neustroev, V. S. Shamardin, V. K. and Kozlov, A. V., "The Influence of DPA rate on Void Swelling of Russian Austenitic Stainless Steels," *10th International Conference on Environmental Degradation of Materials in Nuclear Power Systems – Water Reactors*, 2003, pp. 647-656.
- G-41 Budylkin, N. I., Bulanova, T. M., Mironova, E. G., Mitrofanova, N. M., Porollo, S. I. , Chenov, V. M., Shamardin, V. K. and Garner, F. A., "The Strong Influence of Displacement Rate on Void Swelling in Variants of Fe-!6Cr-15Ni-3Mo Austenitic Stainless Steel in BN-350 and BOR-60," *Journal of Nuclear Materials*, 329-333 (2004) 621-624.
- G-42 Neustroev, V. S., Shamardin, V. K., Ostrovsky, Z. E., Pecherin, A. M. and Garner, F. A., "Temperature-Shift of Void Swelling Observed at PWR-Relevant Temperatures in Annealed Fe-18Cr-10Ni-Ti Stainless Steel Irradiated in the Reflector Region of BOR-60", *Effects of Radiation on Materials: 19th International Symposium*, ASTM STP 1366,

- M. L. Hamilton, A. S. Kumar, S. T. Rosinski and M. L. Grossbeck, Eds., American Society for Testing and Materials, 2000, pp. 792-800.
- G-43 Yilmaz, F., Hassan, Y.A., Porter, D.L., Romanenko, O., "Swelling and Mechanical Property Changes in Russian and American Austenitic Steels in EBR-II and BN350," Nuclear Technology, Vol. 144, December 2003. pp 369-378.
- G-44 Massoud, J-P., and Dubuisson, PH., "Irradiation in Bor-60 Reactor, Results of Post Irradiation Tests and Investigations," Draft Report EDF HT-27/03/018/A, August 2003, JOBB-CD, Version 03.12, available from the Electric Power Research Institute (EPRI), Palo Alto, California.
- G-45 Garner, F. A., Cummings, W. V., Bates, J. F. and Gilbert, E. R., "Densification-Induced Strains in 20% Cold-Worked 316 Stainless Steel During Neutron Irradiation," Hanford Engineering Development Laboratory, HEDL-TME-78-9, June 1978.
- G-46 Pokor, C., Dubuisson, PH., and Massoud, J-P., "Task B4: EBR-II Irradiation, Task B5: Characterization of Irradiated Materials, Progress Report on the Idaho TEM Observations," Progress Report, JOBB-CD, Version 03.12, available from the Electric Power Research Institute (EPRI), Palo Alto, California.
- G-47 "Inspection and Replacement of Baffle to Former Bolts at Point Beach-2 and Ginna, Processes, Equipment Design, and Equipment Qualification," TR-114779, Final Report, February 2000, EPRI, Palo Alto, CA.
- G-48 "Materials Reliability Program, Determination of Operating Parameters of Extracted Bolts (MRP-52)," 1003076, Final Report, October 2001, EPRI, Palo Alto, CA.
- G-49 Garner, F. A. and Brager, H. R., "Swelling of Austenitic Fe-Cr-Ni Ternary Alloys During Fast Neutron Irradiation," Effects of Radiation on Materials: Twelfth International Symposium, ASTM STP 870, F. A. Garner and J. S. Perrin, Eds., ASTM, Philadelphia, PA, 1985, pp. 187-201.
- G-50 Garner, F. A. and Kumar, A. S., "The Influence of Both Major and Minor Element Composition on Void Swelling on Simple Austenitic Steels," Effects of Radiation on Materials: Thirteenth International Symposium (Part 1) Radiation-Induced Changes in Microstructure, ASTM STP 955, F. A. Garner, N. H. Packan and A.S. Kumar, Eds., ASTM, Philadelphia, PA, 1987, pp. 289-314.
- G-51 Coghlan, W. A. and Garner, F. A., "Effect of Nickel Content on the Minimum Critical Void Radius in Ternary Austenitic Alloys," Effects of Radiation on Materials: Thirteenth International Symposium (Part 1) Radiation-Induced Changes in Microstructure, ASTM STP 955, F. A. Garner, N. H. Packan and A.S. Kumar, Eds., ASTM, Philadelphia, PA, 1987, pp. 315-327.

- G-52 Bates, J.F., "Irradiation-Induced Swelling Variations Resulting from Compositional Modifications of Type 316 Stainless Steel," Properties of Reactor Structural Alloys after Neutron or Particle Irradiation, ASTM STP 570, American Society for Testing and Materials, 1974, pp. 369-387.
- G-53 Garner, F. A. and Brager, H. R., "The Role of Phosphorus in the Swelling and Creep of Austenitic Alloys," Journal of Nuclear Materials, 133 & 134, (1985), pp. 511-514.
- G-54 Garner, F. A., Brager, H. R. and Puigh, R. J., "Swelling Behavior of Titanium-Modified AISI 316 Alloys," Journal of Nuclear Materials, 133 & 134, (1985), pp. 535-539.
- G-55 Garner, F. A. and Brager, H. R., "The Influence of Mo, Si, P, C, Ti, Cr, Zr and Various Trace Elements on the Neutron-Induced Swelling of AISI 316 Stainless Steel," Journal of Nuclear Materials, 155-157 (1988), pp. 833-837.
- G-56 Esmailzadeh, B., Kumar, A. S. and Garner, F. A., "The Influence of Silicon on Void Nucleation in Irradiated Alloys," Journal of Nuclear Materials, 133 & 134, (1985), pp. 590-593.
- G-57 Garner, F. A., Bates, J. F. and Mitchell, M. A., "The Strong Influence of Temper Annealing Conditions on the Neutron-Induced Swelling of Cold Worked Austenitic Steels", Journal of Nuclear Materials, 189 (1992), pp. 201-209.
- G-58 Garner, F. A., Gilbert, E. R. and Porter, D. L., "Stress-Enhanced Swelling of Metals During Irradiation," in Proceedings, ASTM 10th International Symposium on Effects of Radiation on Materials, ASTM STP 725, Savannah, GA, (June 3-5, 1980), pp. 680-697.
- G-59 Seran, J. L., Tournon, H., Maillard, A., Dubuisson, P., Hugot, J. P., Le Boulbin, E., Blanchard, P. and Pelletier, M., "The Swelling Behavior of Titanium-Stabilized Austenitic Stainless Steels Used as Structural Materials of Fissile Assemblies in Phenix", Effects of Radiation on Materials: 14th International Symposium (Vol. II), 1990, pp. 739-752.
- G-60 Akasaka, N., Yamagata, I. and Ukai, S., "Effect of Temperature Gradients on Void Formation in Modified 316 Stainless Steel Cladding", Journal of Nuclear Materials, 283-287 (2000)169-173.
- G-61 Sahu, H. K. and Jung, P., "Void Swelling and Irradiation Creep in Stainless Steel Under Compressive and Tensile Stress", Journal of Nuclear Materials, 136 (1985) 154-158.
- G-62 Lauritzen, T., Vaidyanathan, S., Bell, W. L. and Yang, W. J. S., "Irradiation-Induced Swelling in AISI 316 Steel: Effect of Tensile and Compressive Stresses", 13th International Symposium on Radiation-Induced Changes in Microstructure, ASTM STP 955, 1987, pp. 101-113.

- G-63 Garner, F.A. and Toloczko, M.B., "Irradiation Creep And Void Swelling Of Austenitic Stainless Steels At Low Displacement Rates In Light Water Energy Systems," *Journal of Nuclear Materials*, 251 (1997) pp. 252-261.
- G-64 Bond, G.M., Spencer, B.H., Garner, F.A., Hamilton, M.L., Allen, T.R., and Porter, D.L., "Void Swelling Of Annealed 304 Stainless Steel at ~370-385°C and PWR-Relevant Displacement Rates," *Proc. Ninth International Symposium on Environmental Degradation of Materials in Nuclear Power Systems – Water Reactors*, The Minerals, Metals, and Materials Society (TMS), 1999, pp. 1045-1050.
- G-65 Makenas, B.J., Bates, J.F., and Jost, J.W., "The Swelling Behavior of 20% Cold Worked Stainless Steel Cladding Irradiated With And Without Adjacent Fuel," *Effects of Radiation on Materials*, 11th conference, ASTM 782, American Society for Testing and Materials, 1982, pp. 17-29.
- G-66 Garner, F. A., Gilbert, E. R., Gelles, D. S. and Foster, J. P., "The Effect of Temperature Changes on Swelling and Creep of AISI 316," in *Proceedings, ASTM 10th International Symposium on Effects of Radiation on Materials*, ASTM STP 725, Savannah, GA, (June 3-5, 1980), pp. 698-712.
- G-67 Yang, W. J. S. and Garner, F. A., "Relationship Between Phase Development and Swelling of AISI 316 During Temperature Changes, "Effects of Radiation on Materials: Eleventh Conference, ASTM STP 782, H. R. Brager and J.S. Perrin, Eds., American Society for Testing and Materials, 1982, pp. 186-206.
- G-68 Agarwal, S. C., Ayrault, G., Potter, D. I., Taylor, A. and Nolfi, F. V., Jr., *J. Nuclear Materials*, 85-86 (1979) 653.
- G-69 Kohyama, A., Loomis, B. A., Ayrault, G. and Igata, N., in "Effects of Radiation on Materials: Twelfth International Symposium," ASTM STP 870, F. A. Garner and J. S. Perrin, Eds, 1985, pp. 277-296.
- G-70 Brager, H. R. and Garner, F. A., "Microstructural and Microchemical Comparisons of AISI 316 Irradiated in HFIR and EBR-II," *Journal of Nuclear Materials*, 117, (1983), pp. 159-176.
- G-71 Balachov, I. I., Garner, F. A., Isobe, Y., Sagisaka, M. and Tang, H. T., "NDT Measurements of Irradiation Induced Void Swelling," *10th International Conference on Environmental Degradation of Materials in Nuclear Power Systems – Water Reactors*, 2003, pp. 640-646.
- G-72 Balachov, I. I., Shcherbakov, E. N., A. V. Kozlov, A. V., Portnykh, I. A. and Garner, F. A., "Influence of Irradiation-Induced Voids and Bubbles on Physical Properties of Austenitic Structural alloys," *Journal of Nuclear Materials*, 329-333 (2004) 617-620.

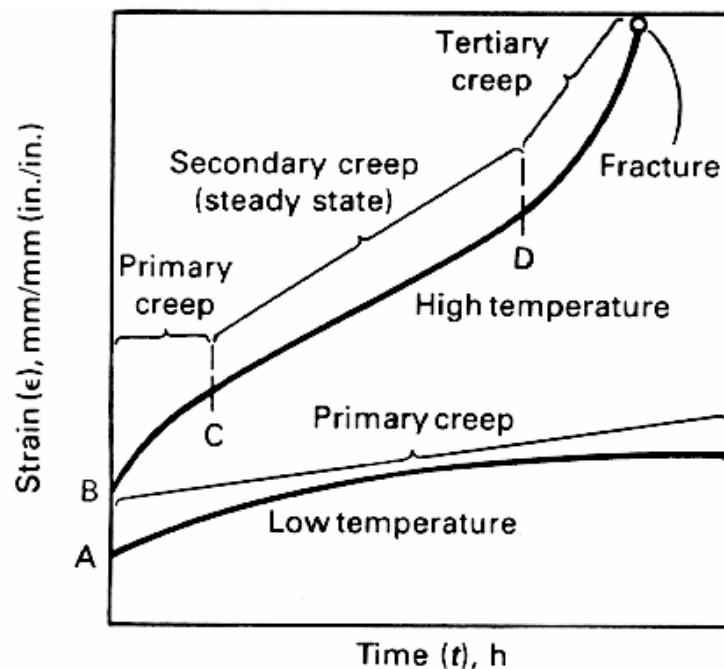
- G-73 “Materials Reliability Program, Hot Cell Testing of Baffle/Former Bolts Removed from Two Lead PWR Plants (MRP-51),” 1003069, Final Report, November 2001, EPRI, Palo Alto, CA.
- G-74 “Characterization of Neutron-Irradiated 300-Series Stainless Steels to Assess Mechanisms of Corrosion Cracking, Volume 2: Core Components,” 1001497, Final Report, August 2001, EPRI.

H

APPENDIX H: STRESS RELAXATION AND IRRADIATION CREEP

H.1 General Description of Stress Relaxation and Irradiation Creep

The general mechanisms of stress relaxation (SR) and creep are discussed in this section. Both of these mechanisms are affected by temperature and neutron irradiation. Much of the confusion in discussion of stress relaxation and creep phenomena comes from overlapping use of mechanisms, behavior, and terminology. For instance, most engineers are familiar with the terms primary, secondary, and tertiary creep. These terms do not refer to mechanisms or even different types of deformation; they are more properly described as regions of a creep curve, and then only under constant load conditions (Figure H-1). The mechanisms operative during secondary creep are also operative during primary creep, but not vice versa.



(A and B denote the elastic strain on loading; C denotes transition from primary-to-secondary creep; D denotes transition from secondary-to-tertiary creep)

Figure H-1
Schematic Representation of Creep Curves Under Constant Load.^[H-3]

Some authors go further in narrowing the definition of creep to that of a constant load test where a steady stage deformation rate (secondary creep) is attained. This is usually at temperatures above half the absolute melting point ($> 0.5 T_m$); thus, materials creep above $0.5 T_m$, and relax below $0.5 T_m$. It becomes exasperating when one learns that relaxation is in reality primary creep at a temperature where, by definition, creep does not exist. Excellent discussions of these phenomena are contained in References H-1 and H-2.

The real issue is permanent deformation of the material below the yield point. Thus, stress relaxation refers to any plastic deformation under constant strain that occurs below the yield point of a material, and creep is any time-dependent plastic deformation that occurs below the yield point of a material under constant load.

A flux of high energy neutrons strongly accelerates the microscopic deformation of metal under stress much like that resulting from thermal creep at elevated temperatures. Irradiation-enhanced creep, usually referred to as irradiation creep, will also act to relax any loads resulting from either externally applied loads or from internal stresses arising from gradients in void swelling. Of particular importance is that the irradiation creep rate accelerates in direct proportion to the local swelling rate, thereby limiting the local stress to be well below the yield stress and also significantly flattening local stress gradients.

Of importance to aging degradation of PWR internals, especially for bolting and springs where maintenance of load is required for functionality, is the stress relaxation process arising from the action of either thermal stress relaxation (primary creep) or irradiation creep.

The RI-ITG sponsored a project in 2001 to evaluate the available data on these two creep relaxation processes. This effort is compiled in an MRP technical basis document (MRP-50)^[H-3] and only a brief review of the data are reproduced herein.

MRP-50 includes thermal effects and irradiation effects, as well as the interrelationship between thermal and irradiation-enhanced stress relaxation and creep. It includes available data for the following materials:

- Wrought austenitic stainless steels – Type 304/304L and Type 316/316L; including cold-worked versus solution-annealed material
- Age-hardenable alloys –Alloy X-750

Data are provided to the extent available for use in the assessment of temperature (and temperature history), dose rate, applied stress or strain, material orientation, material chemical composition, and irradiation hardening.

H.1.1 Thermal Stress Relaxation

For PWR internals, concern over thermal stress relaxation (primary creep) has been associated with bolted joints, coil and leaf springs. Pertinent data are presented and discussed in MRP-50. Only a few thermal stress relaxation tests were identified in the literature for austenitic stainless steels at PWR internals temperatures. Of these, Manjoine's 1973 stress relaxation test data of

Type 304 stainless steel are the most detailed and relevant results.^[H-4] Stress relaxation results of this study are shown in Figures H-2 through H-5 for solution-annealed, 10% cold-worked, and 20% cold-worked materials tested at temperatures between 500 and 775°F (260 and 413°C).

Based on these short-term (< 1000 hours) test data, the following general conclusions can be made about thermal SR for austenitic stainless steels:

- The percentage of stress relaxation increases with increasing initial load and levels off at about
- Under monotonic loading at operating temperatures characteristic of PWR internals, stress relaxation saturates within 100 hours with a maximum reduction of 10 to 20% of initial preload stress depending on the material's thermal-mechanical history.
- The thermal stress relaxation of coil springs in general appears to relax to a much larger extent and is believed to be dependent on the coil design geometry.

However, as noted above, this degree of thermal stress relaxation is deduced from short-term (< 1000 hours) tests. These tests have not taken into account the accumulated steady-state creep strain over long operating lives (nor the effects of cyclic loading) of the PWR internals. Extrapolation based on deformation-mechanism maps indicates that even a very small steady-state strain rate could accumulate a significant creep strain over many years. If this is the case, there could be additional thermal stress relaxation above the saturation level observed from short-term tests.

H.1.2 Irradiation-Enhanced Stress Relaxation and Creep

Irradiation creep manifests itself in two roles that impact PWR component functionality. In the first case, irradiation creep operates to mitigate potential problems caused by void swelling; especially problems that might be caused by gradients in swelling within a given component item. In the second case, however, it is important to note that creep exists even in the absence of void swelling and can have potential consequences arising primarily from relaxation of preloaded components or from sustained pressure differences across a component such as a plate. Irradiation creep, especially when compared to thermal creep, is an inherently non-damaging process on the microstructural level, and its deleterious effects arise primarily from component distortions that might interfere with fluid flow or heat transfer.

In the absence of neutron irradiation, the steady-state region of thermal creep does not occur at temperatures of PWR internals for austenitic stainless steels and nickel-base alloys. Neutron irradiation, however, greatly increases the rate of the primary and steady-state creep regions at temperatures below $0.5 T_m$.

Figure H-6 shows a comparison of thermal creep and irradiation-enhanced creep of a 20% cold-worked Type 316 stainless steel under a constant uniaxial tensile stress of 138 MPa (20 ksi) at 454°C (850°F), with neutron irradiation occurring in the EBR-II fast reactor.^[H-5] Under this irradiation condition void swelling has not yet occurred.

Figure H-2
Thermal Stress Relaxation (Without Irradiation) of a 10% Cold-Worked and Solution-Annealed Type 304 Bar^[H-4]

Figure H-3
Thermal Stress Relaxation (Without Irradiation) of Mill Annealed, Straightened, and 50% Cold-Worked & Solution-Annealed Type 304 Bar.^[H-4]

Figure H-4
Thermal Stress Relaxation (Without Irradiation) of 10% Cold-Worked Type 304 Bar^[H-4]

Figure H-5
Thermal Stress Relaxation (Without Irradiation) of 20% Cold-Worked Type 304 Bar^[H-4]

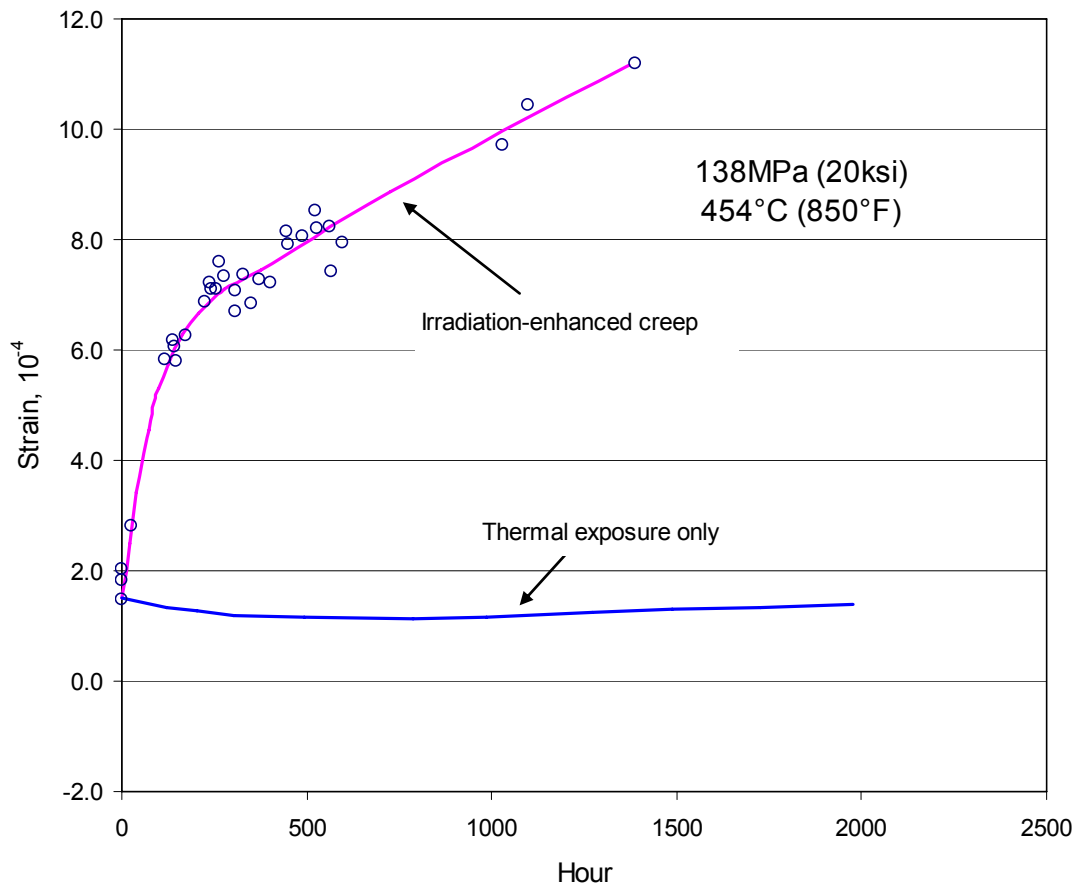


Figure H-6
Comparison of Thermal Creep and Irradiation-Enhanced Creep of a 20% Cold-Worked Type 316 Stainless Steel Irradiated in EBR-II^[H-5]

Note that thermal creep was nearly imperceptible at this temperature and stress level, with slightly negative strains developing initially that arise from densification associated with carbide precipitation. In contrast, irradiation-enhanced creep exhibited a short but significant transient creep region, followed by the steady-state creep regime that persists until void swelling begins.

The important general aspects of irradiation creep in constant load tests are that both the magnitude of the transient and the steady-state creep rate are directly proportional to the equivalent stress level. The transient is usually complete in one dpa or less. While the magnitude of the transient is highly dependent on the fabrication history, material texture, orientation of the texture to the applied stress level, irradiation temperature, etc., the steady-state creep rate appears to be independent of these variables.^[H-6]

These characteristics are also exhibited (but are somewhat harder to observe) in stress relaxation tests where the stress level is constantly relaxing at a rate proportional to the current stress level. The data scatter observed in stress relaxation tests is usually larger than seen in constant load

tests, especially as the relaxation progresses toward the lowest levels of retained stress. This scatter reflects the action of various interference processes associated with test fixture constraints and grain-to-grain interactions.

Studies of irradiation-enhanced stress relaxation of 300-series stainless steels have been performed in fast reactors.^[H-7 – H-10] Empirical equations were derived by regression fitting to the observed stress relaxation results as a function of initial stress and irradiation dose. The regression coefficients are usually dependant on dose rate, stress state, and material type and condition.

The general form of these stress relaxation equations is shown below in Eq. H-1.

$$\frac{\sigma}{\sigma_0} = \exp\{-E[A_1(1 - \exp(-A_2f)) + A_3f]\} \quad (\text{H-1})$$

σ_0 – initial stress

σ – remaining stress

E – elastic modulus

f – neutron exposure in fluence or dpa

The first term $A_1(1 - \exp(-A_2f))$ models stress relaxation due to the irradiation-enhanced transient creep and the second term A_3f represents stress relaxation due to the irradiation-enhanced steady-state creep rate.

Based on fast and thermal reactor studies as well as charged particle irradiation studies, the steady state creep rate can be reliably estimated to be $1 \times 10^{-6} (\text{MPa dpa})^{-1}$. However the transient uncertainty will dominate the uncertainty of any prediction. Assuming this creep rate with no transient therefore defines the least amount of relaxation to be expected.

Even within the fast reactor database there is significant variation in the results, usually manifested most strongly in the magnitude of the transient regime. When considering the differences between fast reactor and PWR conditions the potential uncertainty in the magnitude of the transient regime becomes even more pronounced. Therefore, regression coefficients for irradiation-enhanced stress relaxation in PWR internals cannot reliably be obtained from studies performed in fast reactor conditions. Hence, these equations are of limited value in predicting irradiation-enhanced stress relaxation in PWR internals materials and relevant conditions. Only the minimum relaxation level can be estimated.

H.2 SR/IC Summary and Discussion

The following paragraphs summarize the current knowledge on both thermal- and irradiation-enhanced stress relaxation and creep.

H.2.1 Summary of Thermal Stress Relaxation and Creep

At typical PWR internals temperatures, thermal stress relaxation is limited to the primary (transient) creep region, which is considered insignificant as far as component item geometry or distortion is concerned. The available data show that thermal stress relaxation appears to reach saturation in a short time (< 100 hours) with a maximum reduction of 10 to 20% of initial bolt preloads at PWR internals temperatures. However, this is based on tests that lasted 1000 hours or less and additional SR could feasibly occur over the decades of operation anticipated for PWR internals.

H.2.2 Summary of Irradiation-Enhanced Stress Relaxation and Creep

Despite the amount of research work in the field of irradiation-enhanced stress relaxation and creep over the past three decades, data obtained in a PWR internals environment are rather limited. Adequate data to forecast the overall effect of irradiation creep on stress relaxation for PWR components based on tests in a PWR flux spectrum environment currently do not exist. It is possible to estimate only the lowest level of relaxation to be expected.

In Reference B-15, the JOBB program investigation on irradiation creep was summarized. By testing irradiation creep in pressurised tubes of representative materials (solution annealed 304L, cold-worked 316, 308L) welded in a fast reactor environment (BOR-60) to 80 to 120 dpa), laws predicting irradiation creep for austenitic stainless steels irradiated in PWR conditions were proposed. There is good agreement between the results obtained in fast breeder reactors (BOR-60) and those from light-water reactors (Osiris) in the low dose region. The creep rate values appear slightly higher for irradiation in a light-water reactor.

H.3 SR/IC Threshold and Screening Criteria

Based on the above literature review of thermal stress relaxation tests and irradiation-enhanced stress relaxation or creep tests, the following conclusions have been reached:

- Stress relaxation of austenitic stainless steels and nickel-base alloys due to thermal exposure alone in PWR internals is limited to between 10 and 20% within the first 1000 hours of operation. Additional stress relaxation may occur over the decades of operation anticipated for PWR internals.
- Irradiation-enhanced stress relaxation and creep is a function of fabrication history and texture-stress orientation relationship, especially in the transient regime, as well as stress and irradiation dose. However, adequate data at PWR relevant conditions do not currently exist and the only possibility is to predict the minimum creep relaxation to occur.

It is concluded that no reliable quantifiable threshold criteria can be developed for SR/IC in PWR internals materials and conditions with the available literature data.

Suggested screening criteria are developed herein based on a conservative evaluation of the irradiation-enhanced stress relaxation test data presented in Section H.1.2. Figure H-7 contains a

plot of all available irradiation-enhanced stress relaxation data from these studies. Equation H-2 below represents an irradiation-enhanced screening trend curve based on the work of Foster et al.^[H-9] This trend curve conservatively bounds all available irradiation-enhanced stress relaxation data points. Due to the limited test data available for solution-annealed Type 304, 20% cold-worked Type 316, or Alloy X-750 materials, it was decided that separate trend curves for these materials cannot be established.

Figure H-7
Trend Line for Screening Irradiation-Enhanced Stress Relaxation Based on Available Test Data.

(H-2)

f – Accumulated fluence in units of dpa

The suggested screening fluence for irradiation-enhanced stress relaxation is 0.2 dpa (1.3×10^{20} n/cm², $E > 1.0$ MeV), which corresponds to approximately 40% of the remaining initial preload stress in Figure H-7.

Therefore, it is concluded that relative to long-term thermal stress relaxation, all bolted PWR internals locations or spring component items that require preload for functionality be screened in for further evaluation. It is further concluded that all bolted PWR internals locations or spring component items that reach 0.2 dpa (1.3×10^{20} n/cm², $E > 1.0$ MeV) or higher be identified for initial irradiation-enhanced SR/IC screening purposes and further evaluated for functionality concerns.

H.4 SR/IC References

- H-1 Manjoine, M. J., and Voorhees, H. R., "Compilation of Stress-Relaxation Data for Engineering Alloys," ASTM Data Series Publication DS 60, 1982, ASTM Philadelphia, PA.
- H-2 Reed-Hill, R.E., Physical Metallurgy Principles, D. Van Nostrand, New York, New York, 1973.
- H-3 MRP, Technical Basis Document Concerning Irradiation Induced Stress Relaxation and Void Swelling in PWR RV Internals Components (MRP-50), EPRI 1000970, 2001.
- H-4 M. J. Manjoine, "Stress Relaxation Characteristics of Type 304 Stainless Steel," Conference Publication C165/73 in Institution of Mechanical Engineer, 1973.
- H-5 Gilbert, E. R., et al., "Fast Reactor Induced Creep in 20% Cold Worked Type 316 Stainless Steel," Proc. Conf. on Irradiation Embrittlement and Creep in Fuel Cladding and Core Components, 1972, British Nuclear Energy Society, London pp. 239 – 251d.
- H-6 Garner, F. A., Chapter 6: "Irradiation Performance of Cladding and Structural Steels in Liquid Metal Reactors," Vol. 10A of Materials Science and Technology: A Comprehensive Treatment, VCH Publishers, 1994, pp. 419-543.
- H-7 Joseph, Jr., J. W., "Stress Relaxation in Stainless Steel During Irradiation," USAEC Report DP-369, Savannah River Laboratory, I.E. Dupont de Nemours & Co., Inc., 1959.
- H-8 Kenfield, T. A., Busboom, H. J. and Appleby, W. K., "In-Reactor Stress Relaxation in Bending of 20% Cold-Worked 316 Stainless Steel," Journal of Nuclear Materials, Vol. 66, 1977, pp. 238-243.

- H-9 Causey, A. R., Carpenter, G. J. C., and MacEwen, S. R., “In-Reactor Stress Relaxation of Selected Metals and Alloys at Low Temperature,” *Journal of Nuclear Materials*, Vol. 90, 1980, pp. 216 – 223.
- H-10 Foster, J. P., Gilbert, E. R., Bunde, K., and Porter, D. L. “Relationship Between In-reactor Stress Relaxation and Irradiation Creep,” *Journal of Nuclear Materials*, Vol. 252, 1998, pp. 89 – 97.